

POWER QUALITY ASSESSMENT OF HIGH PENETRATION
RENEWABLE SOURCE IN DISTRIBUTION GRIDS

BY

ATTA UR RAHMAN

A Thesis Presented to the
DEANSHIP OF GRADUATE STUDIES

KING FAHD UNIVERSITY OF PETROLEUM & MINERALS

DHAHRAN, SAUDI ARABIA

In Partial Fulfillment of the
Requirements for the Degree of

MASTER OF SCIENCE

In

ELECTRICAL ENGINEERING

August 2014

KING FAHD UNIVERSITY OF PETROLEUM AND MINERALS

DHAHRAN 31261, SAUDI ARABIA

DEANSHIP OF GRADUATE STUDIES

This thesis is written by **ATTA UR RAHMAN** under the direction of his thesis advisor and approved by his thesis committee members, has been presented to and accepted by the Dean of Graduate Studies, in partial fulfillment of the requirements of degree of **MASTER OF SCIENCE IN ELECTRICAL ENGINEERING**

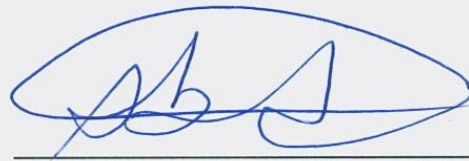
Thesis Committee



Dr. Ibrahim M. El-Amin (Advisor)
Professor, EE Dept.



Dr. Ali Ahmad Al-Shaikhi
Department Chairman



Dr. Mohammad A. Abido (Member)
Professor, EE Dept.



Dr. Salam A. Zummo
Dean of Graduate Studies



Dr. A.H.M. Abdur-Rahim (Member)
Professor, EE Dept.

24/8/14

Date

© Atta Ur Rahman

2014



Dedicated to

My Mother, Father

And

My Brothers and sister

And

My Fiancée Hafsa

Acknowledgement

In the name of ALLAH, the Most Gracious and the Most Merciful

“Read! In the name of your Lord who created. He has created man from a clot. Read! And your lord is the most generous. Who has taught (the writing) by the pen. He has taught man that which he knew not.”[Al Quran 96 Ayah 1-5].

All praise and glory be to Almighty Allah Subhanaho wa Taala; we praise Him; we worship Him alone without associating any partners and seek forgiveness from Him. Peace and blessings be upon his last messenger Muhammad sallallahu alaihi wa-sallam, his family, his companions, and all those who followed him until day of judgement.

Acknowledgement is due to King Fahd university of Petroleum & Minerals for providing support that has led my way through this point of undertaking my research work.

My deep appreciation and heartfelt gratitude goes to my thesis advisor Dr. Ibrahim-El-Amin for his valuable time, suggestions and enormous effort that has spent for me. I am grateful for his guidance, encouragement and constant support that he provided throughout my master’s program. I would like to express my deepest appreciation towards him.

I would like to express my grateful thanks to my committee members for their care, cooperation, support and for their suggestions in the improvements in my thesis.

Adil Humayun Khan for their support, company and positive criticism throughout my master's which will be memorable for lifetime.

Finally, from the bottom of my heart, I thank my mother and father, my brothers {Sana Ur Rehman and Jamshed Ali}, my younger sister and my beloved fiancée Hafsa for their continuous love, encouragement, prayers, emotional and moral support throughout my life. Words fall short in conveying my gratitude towards them. A prayer is the simplest way I can repay them – May Allah give them good health and give me ample opportunities to be of service to them throughout my life.

Table of Contents

Acknowledgement	v
Table of Contents	vii
List of Figures	x
THESIS ABSTRACT	xii
ملخص الأطروحة	xiv
CHAPTER 1	1
1.1 Introduction to Renewable Energy	1
1.2 Problem Statement	1
1.3 Thesis Motivation	2
1.4 Thesis Objective	2
1.5 Thesis Organization	4
CHAPTER 2	5
2.1 Power Quality of Grid Connected Systems	5
2.2 Harmonic Issues of Grid Connected System	8
2.3 Power Quality Standards	10
2.4 Different Studies related to Power Quality	11
2.4.1 Studies Related to Grid Integration Issues of PV Systems	15
2.4.2 Studies Related to Grid Integration Issues of Wind Systems	15
CHAPTER 3	17

3.1	PV System	17
3.1.1	PV Cell.....	17
3.1.2	Bypass and blocking Diode	22
3.1.3	Photovoltaic Module and Array.....	22
3.1.4	Power Conditioning Unit	23
A.	DC/DC converter model	23
B.	Maximum Power Point Tracking.....	25
C.	DC-link capacitor model.....	28
D.	Inverter Model	29
E.	Active Filter Model.....	34
3.2	Components of Wind System.....	36
3.3	Wind System Modeling.....	38
3.3.1	Wind turbine model	39
3.3.2	PMSG Model	40
3.3.3	Full Converter Configuration.....	42
A.	Generator (or machine) side converter	44
B.	Grid side converter:.....	45
C.	Active Filter Model.....	47
CHAPTER 4	49
4.1	Design of a Grid Connected PV system.....	49

4.2	Simulation Results of Grid Connected PV Systems	53
4.3	Correlation functions for PV system.....	60
CHAPTER 5		64
5.1	Design of Grid Connected Wind System	64
5.2	Simulation Results of Grid Connected Wind Systems.....	67
5.3	Correlation functions for wind system.....	75
CHAPTER 6		77
6.1	Design of PV and Wind System Combined.....	77
6.2	Simulation Results of PV and Wind System Combined.....	77
CHAPTER 7		82
7.1	Conclusion.....	82
7.2	Future Work	83
APPENDIX A.....		84
APPENDIX B		86
REFERENCES		87
Vitae.....		96

List of Figures

FIGURE 3-1 PV CELL.....	18
FIGURE 3-2 SIMULINK MODEL OF SOLAR CELL	19
FIGURE 3-3 SIMULINK MODEL OF DIODE	21
FIGURE 3-4 SIMULINK DIAGRAM OF A BOOST CONVERTER.....	24
FIGURE 3-5 FLOW CHART OF INCREMENTAL CONDUCTANCE METHOD	27
FIGURE 3-6 SIMULINK BLOCK DIAGRAM OF INCREMENTAL CONDUCTANCE	27
FIGURE 3-7 PWM PULSE IS GENERATION.....	28
FIGURE 3-8 CENTRAL AND STRING INVERTER	30
FIGURE 3-9 MODULE INVERTER	31
FIGURE 3-10 MULTI-STRING INVERTER.....	31
FIGURE 3-11 INVERTER MODEL ALONG WITH CONTROL.....	32
FIGURE 3-12 INVERTER CONTROL MODEL.....	33
FIGURE 3-13 MEASUREMENT AND TRANSFORMATION BLOCK	34
FIGURE 3-14 ACTIVE FILTER MODEL	35
FIGURE 3-15 WIND TURBINE MODEL IN SIMULINK.....	39
FIGURE 3-16 EQUIVALENT CIRCUIT OF PMSG.....	41
FIGURE 3-17 BACK TO BACK CONVERTERS.....	42
FIGURE 3-18 GENERATOR SIDE CONVERTER.....	44
FIGURE 3-19 CONTROL OF GENERATOR SIDE CONVERTER.....	45
FIGURE 3-20 GRID SIDE CONVERTER ALONG WITH CONTROL SYSTEM	45
FIGURE 3-21 GRID SIDE CONVERTER CONTROL MODEL.....	46
FIGURE 3-22 MEASUREMENT AND TRANSFORMATION BLOCK	47
FIGURE 3-23 ACTIVE FILTER MODEL.....	48
FIGURE 4-1 GRID CONNECTED PV SYSTEM.....	50
FIGURE 4-2 PV SYSTEM SIMULINK BLOCK	51
FIGURE 4-3 UTILITY GRID SIMULINK BLOCK	51
FIGURE 4-4 TEMPERATURE AT KFUPM ON 9TH OF JULY, 2010.....	52
FIGURE 4-5 SOLAR IRRADIANCE AT KFUPM ON 9TH OF JULY, 2010	52
FIGURE 4-6 RELATION BETWEEN SOLAR IRRADIANCE AND CURRENT & VOLTAGE RMS.....	53
FIGURE 4-7 RELATION BETWEEN SOLAR IRRADIANCE AND CURRENT & VOLTAGE THD.....	54
FIGURE 4-8 RELATION BETWEEN NUMBER OF PV SYSTEMS AND VOLTAGE RMS.....	55
FIGURE 4-9 RELATION BETWEEN NUMBER OF PV SYSTEMS AND CURRENT RMS.....	55
FIGURE 4-10 RELATION BETWEEN NUMBER OF PV SYSTEMS AND VOLTAGE THD	56
FIGURE 4-11 RELATION BETWEEN NUMBER OF PV SYSTEMS AND CURRENT THD.....	56
FIGURE 4-12 RELATION BETWEEN CURRENT RMS AND SOLAR IRRADIANCE	57
FIGURE 4-13 RELATION BETWEEN CURRENT THD AND SOLAR IRRADIANCE	57
FIGURE 4-14 INDIVIDUAL VOLTAGE HARMONICS OF GRID CONNECTED SOLAR SYSTEMS.....	58
FIGURE 4-15 INDIVIDUAL CURRENT HARMONICS OF GRID CONNECTED SOLAR SYSTEMS	58
FIGURE 4-16 INDIVIDUAL VOLTAGE HARMONICS BEFORE AND AFTER THE FILTER.....	59
FIGURE 4-17 INDIVIDUAL CURRENT HARMONICS BEFORE AND AFTER THE FILTER	59
FIGURE 4-18 SIMULATED CURRENT RMS AND CURRENT RMS FROM EQUATION	62
FIGURE 4-19 SIMULATED CURRENT THD AND CURRENT THD FROM EQUATION	62

FIGURE 5-1 GRID CONNECTED WIND SYSTEM.....	65
FIGURE 5-2 WIND SYSTEM SIMULINK BLOCK	65
FIGURE 5-3 UTILITY GRID SIMULINK BLOCK	66
FIGURE 5-4 WIND SPEED ON 5TH OF FEB, 2011	66
FIGURE 5-5 RELATION BETWEEN WIND SPEED AND CURRENT & VOLTAGE RMS.....	67
FIGURE 5-6 RELATION BETWEEN WIND SPEED AND CURRENT & VOLTAGE THD.....	68
FIGURE 5-7 RELATION BETWEEN NUMBER OF WIND SYSTEMS AND VOLTAGE RMS.....	69
FIGURE 5-8 RELATION BETWEEN NUMBER OF WIND SYSTEMS AND CURRENT RMS	69
FIGURE 5-9 RELATION BETWEEN NUMBER OF WIND SYSTEMS AND VOLTAGE THD	70
FIGURE 5-10 RELATION BETWEEN NUMBER OF WIND SYSTEMS AND CURRENT THD.....	70
FIGURE 5-11 RELATION BETWEEN CURRENT RMS AND WIND SPEED	71
FIGURE 5-12 RELATION BETWEEN CURRENT THD AND WIND SPEED	71
FIGURE 5-13 INDIVIDUAL VOLTAGE HARMONICS OF GRID CONNECTED WIND SYSTEMS	72
FIGURE 5-14 INDIVIDUAL CURRENT HARMONICS OF GRID CONNECTED WIND SYSTEMS.....	73
FIGURE 5-15 INDIVIDUAL VOLTAGE HARMONICS BEFORE AND AFTER THE FILTER.....	74
FIGURE 5-16 INDIVIDUAL CURRENT HARMONICS BEFORE AND AFTER THE FILTER	74
FIGURE 5-17 APPLYING CURVE FITTING TOOL ON CURRENT RMS AND WIND SPEED.....	76
FIGURE 6-1 GRID CONNECTED RENEWABLE SYSTEM	77
FIGURE 6-2 RELATION BETWEEN NUMBER OF RENEWABLE SYSTEMS AND VOLTAGE RMS.....	78
FIGURE 6-3 RELATION BETWEEN NUMBER OF RENEWABLE SYSTEMS AND CURRENT RMS.....	78
FIGURE 6-4 RELATION BETWEEN NUMBER OF RENEWABLE SYSTEMS AND VOLTAGE THD	79
FIGURE 6-5 RELATION BETWEEN NUMBER OF RENEWABLE SYSTEMS AND CURRENT THD.....	79

THESIS ABSTRACT

Name: ATTA UR RAHMAN

Title: Power Quality Assessment of High Penetration Renewable Source in Distribution Grids

Degree: MASTER OF SCIENCE

Major Field: ELECTRICAL ENGINEERING

Date of Degree: August, 2014.

The increasing penetration of renewable resources in distribution systems poses many challenges in terms of voltage variations and fluctuations because of reverse power into the grid. Renewable resource indices (e.g. solar irradiance and wind speed) are random in nature. This variation in renewable resource indices may lead to power quality issues because of variation in current level. The impact of variation in renewable resource indices on power quality is highly depended on location and size of grid connected renewable system. It is necessary that grid interconnection of renewable resources should be properly checked to ensure the proper flow of electric power.

Direct measurement method might be expensive and time consuming. Therefore, simulation method is being used here because it may offer a reasonable assessment of the power quality indices. SimPower-Systems in Matlab Simulink is being used for simulations. For simulations 1.5 MW grid connected PV system and 1.5 MW grid connected wind system are designed in Simulink SimPower-Systems. In designing of renewable systems central type inverters are being used. This work attempts to find the relationship between harmonic levels and renewable resource indices using simulation

method. The results show that there is a strong relation between renewable energy parameters and power quality indices.

ملخص الأطروحة

الاسم: عطا الرحمن.

عنوان الأطروحة: تقييم الجودة في شبكات توزيع الطاقة بعد ارتفاع اختراق مصدر متجدد.

الدرجة: ماجستير في العلوم الهندسية.

التخصص: الهندسة الكهربائية.

سنة التخرج: 2014

الاختراق المتزايد للموارد المتجددة في أنظمة التوزيع يطرح العديد من التحديات من حيث اختلافات الجهد والتقلبات بسبب القوة العكسية في شبكة التوزيع. مؤشرات الموارد المتجددة (مثل الإشعاع الشمسي وسرعة الرياح) توجد بشكل عشوائي في الطبيعة. هذا الاختلاف في مؤشرات الموارد المتجددة قد يسبب مشاكل في جودة الطاقة بسبب الاختلاف في مستوى التيار. هذا التأثير يعتمد بشكل كبير على موقع وحجم نظام الطاقة المتجددة. فمن الضروري أن الربط بين الموارد المتجددة مع شبكة الكهرباء يجب أن يتم التحقق منه بشكل صحيح لضمان التدفق السليم للطاقة الكهربائية.

طريقة القياس المباشر قد تكون مكلفة وتستغرق وقتاً طويلاً. لذلك، يتم استخدام طريقة المحاكاة هنا لأنه قد تقدم تقييماً معقولاً من مؤشرات نوعية الطاقة. يتم استخدام ماتلاب لمحاكاة. أولاً، صممت 1.5 ميغاواط نظام الضوئية ثم 1.5 ميغاواط نظام الرياح في ماتلاب. يحاول هذا العمل لإيجاد العلاقة بين مستويات التوافقية ومؤشرات الموارد المتجددة باستخدام طريقة المحاكاة. أظهرت النتائج أن هناك علاقة قوية بين العوامل الطاقة المتجددة ومؤشرات نوعية الطاقة.

CHAPTER 1

INTRODUCTION

1.1 Introduction to Renewable Energy

The introduction of renewable energy systems (RES) at distribution level presents utilities with new problems related to the quality of the supply at or near the point of common coupling (PCC). Solar and wind energy systems are two of the most popular forms of renewable sources. The integration of solar/wind into the grid is achieved by the use of electric rectifiers, inverters and dc-dc choppers. These devices generate harmonics causing voltage and current distortion at the PCC. Thus utilities and regulators setup standards for connection of RES into the systems. The main concern is propagation of harmonics into the network. Several utilities conduct studies prior to the connection of RES. This is especially required as the penetration levels of the RES have increased. Moreover the connection of the distributed generators (DG) at distribution network poses new problems and challenges regarding power quality indices & levels.

1.2 Problem Statement

With the widespread introduction of renewable resources into the grid, there is an urgent need to carry out an assessment of power quality indices of renewable resources. This can be achieved through direct measurement at or near the PCC. However, as the penetration of renewable resources increases, the direct measurement may be expensive and time consuming. This is especially true as the power output level of both solar and wind is intermittent depending on solar radiation and wind speed respectively.

Simulation methods may offer a reasonable assessment of the power quality indices as compared to direct measurement method. The objective of this work is to find the relationship between harmonic levels and renewable resource indices.

1.3 Thesis Motivation

In kingdom of Saudi Arabia renewables are the best candidate among future power resources. Saudi Arabia has announced a 16 GW PV and 9 GW wind energy target by 2032. Saudi Arabia is planning to invest hundred billion dollar worth investment in renewable energy. The country seeks to generate one-third of its energy demand through renewable which would be about 41 GW by the end of 2032 to meet rising demand from a rapidly growing population. So the Kingdom of Saudi Arabia is emerging as a new hot spot in the Middle East and Africa region for renewable energy. To reach this ambitious target the kingdom's grid is expected to connect some 3 GW from renewable plants in the next five years and up to 17 GW would be added by 2023. The kingdom has already completed its new biggest PV plant till date with a 3-5MW capacity in January 2013[1][2].

This application of renewable resources would present the power operators with new problems. There is a need to understand the impact of grid integration of renewable resources on power quality at PCC and how the grid will react.

1.4 Thesis Objective

Non-renewable world energy resources are depleting rapidly so the integration of renewable energy resources into the current electrical power systems is inevitable. The

integration of renewable sources into electric networks presents power system planners and operators with new challenging issues. These are related to the intermittent nature of the renewable sources and their integration via power semiconductor devices. The integration of these sources may result in the new problems related to power quality issues. Variation in solar irradiance and wind speed may lead to adverse power quality issues. On the other hand, increasing penetration of renewable sources may lead to power quality issues related to voltage levels.

The general objective of the thesis is to identify and study the relationship between the input indices of renewable resources and levels of harmonics at PCC. The purpose of this thesis is to achieve the following objectives:

- ✓ Carryout and document literature related to the correlation between harmonics and the parameters of renewable sources.
- ✓ Study the behavior of harmonics at low and high solar irradiance by using actual irradiance data. Then study the behavior of harmonics at low and high wind speed by using actual wind data. This will help to develop a correlation.
- ✓ Study the behavior of harmonics for different penetration levels of renewable sources.
- ✓ Find a correlation between the parameters of renewable sources and power quality indices through simulation results and comprehensive study of related work done in this field.

1.5 Thesis Organization

This thesis is organized as follows:

Chapter 2 presents a literature survey of power quality, power quality standards, harmonic issues and grid integration issues. The recent studies on power quality of grid connected RES are included in this section.

Chapter 3 presents the detailed Matlab Simulink based models of photovoltaic and wind systems. Complete models of inverter, converter and their control circuit along with grid interface through LC filter are described in this section.

Chapter 4 presents the detailed simulation results of grid connected PV systems.

Chapter 5 presents the detailed simulation results of grid connected wind systems.

Chapter 6 presents the simulation results of grid connected PV system and wind systems combined.

Chapter 7 presents conclusions and future work of this study.

CHAPTER 2

LITERATURE REVIEW

The literature review on this subject is divided into the four sections. In the first section, the introduction of power quality of RES is documented. In the second section, harmonics issues of grid connected RES are discussed. In third section various power quality standard related to RES are discussed. In the last section, different studies related to power quality of RES have been discussed.

2.1 Power Quality of Grid Connected Systems

Power quality at any point of the network is the aggregate impact of all different elements at that point of network. All these network equipment and elements act in a very complex way to create an aggregate impact. RES connected to the distribution grid can have significant effects on the aggregated impact.

A swing or change in voltage is called voltage fluctuation and if it moves out of a specified limit then it could cause series power quality problems. If the voltage changes above or below 10% of its rated value then it may affect the loads, can change network operation or can damage network equipment. Extended under-voltage can cause damage of sensitive equipment. It may decrease life of equipment and can cause the light dimming or inability in operation of some components of loads.

Grid connected inverters usually are designed to follow grid voltage. If grid voltage moves outside the set parameters, then inverters are supposed to disconnect from grid to protect itself and other network equipment [3].

The introduction of distributed generation causes the power flow in both direction and that changes the dynamics of the network. Now voltage and power flow are determined by the aggregate effect of both the distributed and centralized generators as well as location and size of loads. Adding distributed generation, the voltage level at load side may rise higher than the load side voltage. In some cases even over-voltages can occur at load side and this may result in reverse power flow [4]. The situation may become worse if local load demand is at its lowest and distributed generation is at its peak [5].

The frequency, which is an important factor of power quality, is controlled by keeping a balance between loads and generation. It rises when demand falls and it falls when demand rises [6]. Frequency control in distribution networks is becoming more difficult because of increasing penetration of RES. The current size of grid connected PV systems is very small as compared to grid connected wind systems. Current contribution of frequency fluctuation of grid connected RES are not so high but as the penetration of grid connected RES would increase, the situation may become worse [7].

Increasing 10% penetration requires 2.5% increase in frequency control while if penetration goes up to 30% then the increase in frequency control would be 10% [8]. Inverters may be used for frequency control providing control in milliseconds which is faster than conventional control [6]. But inverters control would only be helpful if RES constitute a reasonable amount of generation. RES can only control frequency if they inject power to the network so PV inverters will not be able to provide frequency control at night time [9]. Similarly wind inverters will not be able to support frequency control in the absence of wind.

There are two types of control schemes in grid connected RES. Voltage source type or current source type. Most of the RES are current source type. In this type inverter follow the grid voltage. Voltage remains constant while current varies as the environmental conditions (irradiance or wind) changes.

If the power factor of inverter is unity then it means that it will provide in-phase component of load while grid will have to supply out of phase current and harmonics. There are two methods to eliminate harmonics (1) through inverter control (2) through filtering.

Filtering method is being used to eliminate harmonics because it is cheaper. There are two type of filtering (1) passive filtering (2) active filtering. Harmonics are eliminated through capacitor and reactors in passive filtering which absorb the harmonics. Passive filters are further divided into two categories (1) High order (2) and tuned filters.

High order passive filter can absorb an entire range of higher order harmonics. Tuned filters on the other hand are used to eliminate specific low order harmonics. The working of active filters is based on the principal of generating the harmonics of opposite sequence to the existing harmonics. Active filters are smaller, quieter, and better than passive filters. They can eliminate several harmonics at a time and even if a change in grid occurs, active filter do not require system setting change for their working.

The deployment of DG is increasing rapidly. It can reduce losses by reducing network flow. Some of its drawback include harmonics, fault currents, frequency regulation, voltage regulation, power fluctuation and reverse power flow, grounding issues, power factor changing issues and unintentional islanding. Grid connected small

scale wind is very rare so it has very little impact on distribution network as compared to grid connected small scale PV.

Solar PV is a source of energy that fluctuates very rapidly over time scale based on solar irradiance. Solar irradiance changes throughout the day. There is no irradiance at night while irradiance is at peak at noon time. A PV power is highly dependent on irradiation, temperature and also time of the day[10].

Also in grid connected PV systems, the harmonic distortion is highly depended on solar irradiance and number of PV systems while in grid connected wind systems the harmonic distortion is highly depended on wind speed and number of wind systems.

2.2 Harmonic Issues of Grid Connected System

Harmonics are components of voltage or current whose frequency are integer multiple of fundamental frequency. The fundamental frequency is 60 Hz in this study. Thus harmonics would have frequencies of 120, 180, 240, and 300 and so on. If harmonics have high values, they can cause flickering of light and TV monitors, Vibration of elevators, malfunction of protection devices, and poor quality of sound devices and even can cause fires[7]. Different power quality standards impose limitation on converters to produce lesser amount of harmonics than a specified limit. These limitations could be on total harmonic distortion (THD) or even on individual harmonics.

Harmonics distortions are not desirable in any distribution system because they cause many problems including malfunction of power systems protection devices distortion and degradation of voltage waveforms, heating and life reduction of induction motors and transformers, and unsafe currents in power factor correction capacitors [11][12].

It is necessary to investigate the individual harmonics before deciding the penetration level of PV inside the distribution grid [13]. The angle of each individual current harmonic is described with reference to the fundamental angle of current at each bus. A change of 180 degree means that harmonics current are being changed from absorbing to injecting or vice versa. It is observed that current harmonic phasors have a strong correlation with environmental conditions. In order to get a better comparison with standard EN 50160, simulations were performed for each time to get the percentage of time measurement and results were analyzed based on the requirements of EN 50160 [10].

RES are connected to grid via converters and converters are the main source of distortion. The most widely used are pulse width modulation (PWM) inverters. An inverter in voltage following mode has usually unity power factor. Theoretically these inverters only produce high order harmonics which are attenuated easily by the system.

Most grid connected inverters are unlikely to cause high harmonic even at high penetration level because they produce very low level of harmonic current [14][15][16]. If a grid is weak or distorted then integration of the inverter can cause low order harmonics. It will behave like external disturbance which will distort the inverter's current output. Deficiencies in the control loop of inverter are the main reason for low order current harmonics.

Another problem in supplying the reliable and quality power supply is the background harmonic distortion. Variable speed drivers, power electronic devices, electronic ballasts and computers are the examples of the some of the devices which produce power quality problems [10].

Different non-linear load (e.g. arc furnace, 6 and 12 pulse rectifiers) generate background harmonics. THD_v becomes worse in the presence of background harmonics and level of THD_v rises when there is background harmonics. Thus installation of high concentration of RES, on a bus where there are background harmonics present, may degrade the power quality to an extent that it may violate the power quality standards.

Background harmonics may play its role and effect the power quality when RES is installed as a DG [17]. Harmonic currents in linear loads, extra losses and change in related characteristics of load are some of the outcomes of harmonic voltage distortion in distribution grids [18]-[20].

2.3 Power Quality Standards

To ensure the safety of end user equipment and infrastructure and for the efficiency of electric power the electricity utility grid must operate at standard conditions. These standard conditions are often referred as power quality requirement or power quality standards. Power quality standards are defined by international professional societies or by power supply authorities. Most commonly these standards are related to harmonics, frequency and voltage regulation and power factor correction. There are many different reasons for the degradation of power quality. Some reasons are related to network equipment and lines. Some are related to end users operation and non-linear loads. Some reasons arise because of technical characteristic or weather conditions.

There are many different power quality standards. Different utilities have adopted different power quality standards. Most common in use are IEEE-519, EN 50160 [21] and IEC 60001-4-30 [22]. In case of grid connected PV the most relevant standard is IEC 61727 standard [11][23]. International power standard regarding wind systems is IEC

61400 while IEC standard 61400-21 is related to power quality of grid connected wind systems [24]. It recommends limits for flicker emissions and only focus on harmonic issues so IEEE-519 or EN 50160 are far comprehensive as they discuss the power quality issues in more details [25].

Standard EN 50160, not only provides limits for different power quality parameters, but also provides time based percentage during which the limits should not be violated. IEC standard 61000-4, not only provides measurement formulas and accuracy limits, but also describes the measuring methods of voltage and currents as well as aggregation periods. Current power quality standards have shortfalls and validation of these standards is a serious issue during grid integration. Investigation about these concerns have started to emerge in literature [26]-[30]. According to EN 50160, which is adopted by most of the European utilities, THD limit up to 40th harmonic is 8%. According to IEEE standard 519-1992, the THD limit is 5% and the limit for individual harmonics up to 69 Kv is 3%. According to European standard IEC-61727 limits for current THD is 5% and limits for even harmonics should be 25% lower than limits of odd harmonics [23]. THD_v should not exceed 5% at PCC according to IEEE standard 519-1992 while IEC standard 61727 does not address THD_v and does not give any guidelines regarding this issue.

2.4 Different Studies related to Power Quality

The environmental effects on voltage quality were studied in [13] and [17]. Using ampacity of cables as reference, the limits in installing high penetration of DG in urban areas is studied in [31]. Under the framework of EU project POLYCITY, the study of electrical impact is done for rural and urban networks in [32]. Economic losses of poor

power quality in both rural and urban network are analyzed in [33]. In [34] a new control scheme is proposed to control the inverter by taking input from inverter side of the load as well as grid side of the load. Traditionally an inverter is controlled by only taking input from the inverter side of the load. So in this case voltage becomes more stable in case of a sudden change in system conditions.

Integration of small RES to grid may not degrade the power quality much but large penetration of RES may result in violation of power quality standards. Level of voltage THD at high penetration grid connected RES, may become excessive in the presence of background harmonics distortion. Therefore utilities should carry out several constraint checks before integration of RES to grid to avoid power quality problems from RES. To find the optimal size and place of DG there are many techniques based on deterministic approach [35]-[37]. Since power output from RES is changing depending on environmental conditions(e.g. solar irradiance and temperature in case of grid connected system and wind speed in case of grid connected system), so voltage regulation is more complicated [38]-[41]. Many authors have proposed design of optimum grid connected RES but they have not considered power quality constraints. One such design is proposed in [42]. In their vision paper, Electrical Power Research Institute (EPRI) has described a complete outline for future power quality research in 2007. Their target is to define the objective power quality research and fill in the critical gap as well as to specify the role of power quality in minimizing the economic loss of electric power suppliers and other related key organizations.

If linear loads are connected in DG then clustered RES do not cause extensive voltage distortion [43]. Also if certain number of non-linear loads is used in simulations

then voltage distortions may violate the limits proposed by international power quality standards. High penetration of renewable systems has already been built in different locations of the world. Gumma village in Japan, Solarsiedlung Freiburg Germany, Holidaypark Bronsbergen Netherlands, Heerhugoward Suncity Netherlands and Soleil Marguerite France are some of such examples. Results obtained from 200 installed systems out of 553 in Gumma village revealed that at low load conditions over-voltage phenomena is causing substantial power loss. Voltage measurements have not shown any significant distortion during the operation of RES. It is observed that different type of inverters show different distortion levels so selection of inverter could play a vital role in minimizing the power loss. Some of the methods to minimize the over-voltage are reactive power control, voltage control strategies, curtailment of produced power, and storage of extra power. These are some of many different methods to minimize the over-voltage and to improve the voltage profile during the variation of produced power of renewable source when RES with high penetration is connection to grid [10].

A study which is done on 29 houses in Denmark in a location having 1 kWp grid connected RES shows no series impact of RES installation on grid voltage distortion. Although the installed capacity was exceeding 30% of transformer's rated capacity but still the highest voltage distortion was being caused by external sources [10].

Another study on RES, located at the Sydney Olympic site in Australia, reveals that voltage harmonic distortions were far below the limits imposed by IEEE standard 519-1992. This was true even when all the inverters of 665 homes having 1kWp were operating under the same feeder [44]. A real network is under construction in Bavaria Germany which will be used for field tests and actual power quality analysis [45]. The

highest RES installed capacity was 3.9kWp in early 2010 and was expected to increase by 60% in near future [45]. According to simulations results shown in [46], it was demonstrated that more than 30% saturation of installed RES capacity is required to exceed the voltage distortion limits imposed by IEEE standards. A study in [47] shows that resonance seems unlikely at frequencies below 1 kHz so attention should be given to higher frequencies but capacitance at the interface of DG may shift the resonance to lower values.

It was demonstrated in [48] that introduction of RES into grid after proper planning reduces the capital and maintenance costs as it eliminates the need of phase balance and voltage regulators. In a measurement campaign [49], using different penetration level of RES inside distribution grid, it is demonstrated that most of the power quality standards are met, while limits are violated only in a few cases. On the other hand if proper planning is not done then interconnected RES with grid may lead to violation of international power quality standards [50].

The annual report of international energy agency (IEA) in 2010 revealed that appropriate modeling is required to unveil all the possible unwanted outcomes of the large grid integration of RES. Promoting the use of high penetration grid connected RES is one of the main objective of IEA- Task 14. Their purpose is to achieve high RES penetration by reducing the technical barriers and by proposing appropriate grid integration configuration as was depicted in [51] and [52].

2.4.1 Studies Related to Grid Integration Issues of PV Systems

The resonance phenomenon between existing network and PV inverters which occurs typically between 5th and 40th harmonic is discussed in [53]. This phenomenon is responsible for higher than expected distortion level in voltage and current in grid connected PV systems.

Different control schemes suggested in literature have different impact on harmonic distortion and if solar irradiance increases for a given temperature then current THD would decrease [54][55]. Similarly increasing the PV penetration will shift the RMS voltage to a higher level [55][56]. Using different power quality standards, adopted within a certain utility, many researchers have tried to find the maximum penetration level of PV inside the distribution network for different type of utilities and network configuration [11][15].

Minas Patsalides has attempted to predict maximum PV integration allowed in low voltage networks based on systematic measurements of power quality indices for a period of two weeks. According to this study, solar irradiance has a strong correlation with power quality indices. High solar irradiance case presents the worst case in case of voltage harmonics. Using this worst case the effect of different PV penetration on power quality was determined [10].

2.4.2 Studies Related to Grid Integration Issues of Wind Systems

Three level converters allow conversion in megawatt range for wind energy conversion [57] so these converters has become a promising power converter interface [58] for wind turbines. A survey on control strategies, network interface topologies and

different applications for three level converters has been discussed in [59]. Some of the drawbacks of these three level inverters in grid connected wind system include increased control complexity and voltage unbalance [60]. DC link capacitor unbalance is a critical issue in three level converters in grid connected wind systems and it may lead to control malfunctions. This issue has been discussed in [61] and a contribution has been made in order to mitigate this critical issue in grid connected wind systems.

Different advantages of three level converter over two level converter for a grid connected wind system have been discussed in [62]. In three level inverters THD is lower because of increased number of voltage levels which lead to the production of higher power quality waveforms [63]. In [64] the technique of active power filters to reduce current harmonics has been discussed in grid connected wind system.

It is important to look into the different component of grid connected renewable energy system to understand the power quality issue. To understand how these components interact with each other and with the power grid, the complete design of grid connected renewable energy system is given in next chapter. Active power filter is used in design of grid connected RES for harmonic reduction of both grid connected PV and wind systems.

CHAPTER 3

MODELING OF RENEWABLE SYSTEMS

The dynamic models of grid connected renewable energy systems are developed in this chapter. These models of grid connected renewable energy systems are designed in Matlab Simulink. The design of grid connected PV system is presented first along with complete description of subsystem. Extra details could be found in Appendix A. The design of grid connected wind system is presented in second half of the chapter. Complete description of subsystems is presented along with extra detail in Appendix B. In designing of PV systems incremental conductance technique is being used for maximum power point tracking. In designing of wind system PMSG is being used. The technique of active power filtering is being used for harmonic reduction along with voltage controlled converter.

3.1 PV System

3.1.1 PV Cell

Photovoltaic cell behaves as current source when light is thrown upon it so it generates electricity. It is actually a semiconductor device which behaves as diode in dark. If light is thrown upon it in reverse biased condition it absorbs the photon of energy. If energy of photon is greater than band gap then an electron jumps from valance band to conduction band and moves toward positive terminal leaving behind a deficiency of electron called hole. These electron hole pairs are created throughout the semiconductor under light and move in opposite directions.

The general equivalent model consists of a photo current, a diode, a shunt resistor representing a leakage current and a series resistance expressing an internal resistance to the current flow [65].

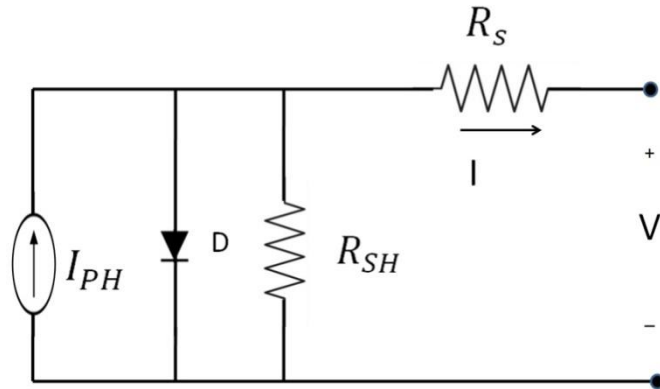


Figure 3-1 PV cell

The net output current from the PV cell is given in equation 3.1. It is the difference of photovoltaic current and the sum of normal diode current and leakage current in the shunt resistance.

$$i_{pv} = I_{ph} - I_D - \frac{V_D}{R_{sh}} \quad (3.1)$$

$$V_D = V_{pv} + R_S i_{pv} \quad (3.2)$$

Where

I_{ph} = photovoltaic current

I_D = diode current

R_{sh} = shunt resistance

i_{pv} = cell current

V_{pv} = cell voltage

R_s = series resistor

R_{sh} = shunt resistance

A Simulink model of a solar cell, which is the basic building block of photovoltaic array, is described in the figure 3.2.

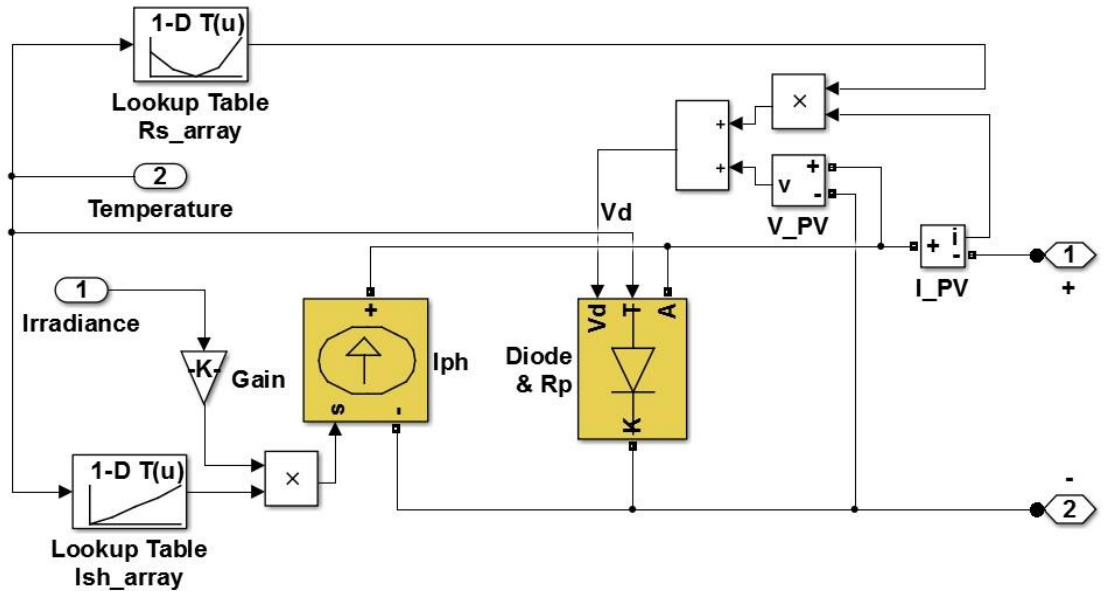


Figure 3-2 Simulink model of solar cell

In this figure temperature dependent PV array parameters (I_{ph} and R_s) are implemented in look-up tables. The light generated current (I_{ph}) mainly depends on the cell's working temperature and solar irradiation. The operation of PV is greatly determined by the irradiation, array short circuit current, array open circuit voltage, cell temperature and the load connected to the array [66]. The PV output current has very little effect on the temperature variation. By increasing the temperature, PV cell produces a slightly higher output current but this increase in the cell temperature forces the PV cell to conduct at a lower voltage thus greatly reducing the power output of PV [67]. The diode current I_D is given as:

$$I_D = I_s \left(e^{\frac{V_D}{nV_T}} - 1 \right) \quad (3.3)$$

Where

I_D = diode current (A)

V_D = diode voltage (V)

I_s = diode saturation current (A)

V_T = temperature voltage = $\frac{kT}{q} \times Qd$

n = $N_{cell} \times N_{ser}$

T = cell temperature (K),

k = Boltzman constant = 1.3807×10^{-19} J/K

q = electron charge = 1.6022×10^{-19} C

Qd = diode quality factor

N_{cell} = number of series-connected cells per module

N_{ser} = number of series-connected modules per string

The Simulink model of diode is shown in figure 3.3 where temperature-dependent PV array parameters (I_s , V_T and R_{sh}) are implemented in look-up tables.

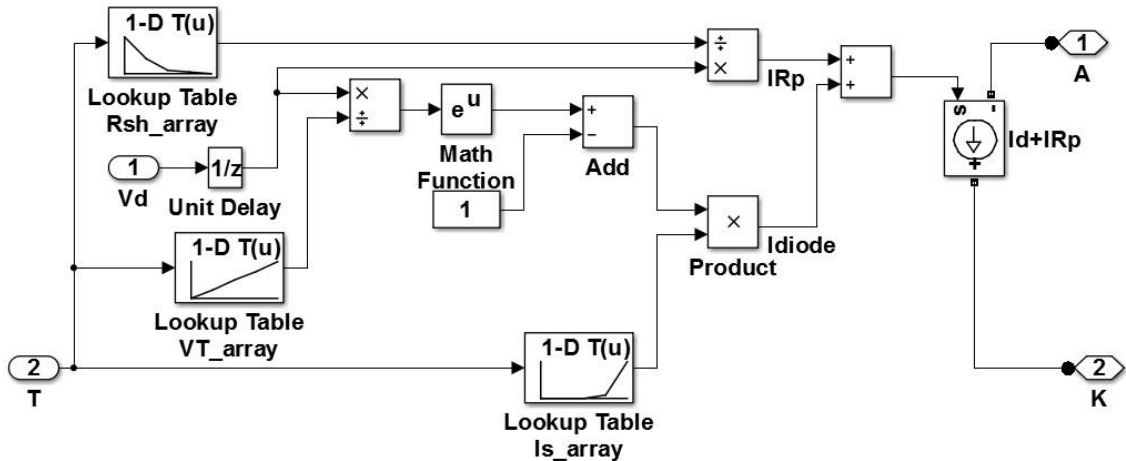


Figure 3-3 Simulink model of diode

Energy produced by PV cell is less than 2 watt at 0.5 volts approximately. When cells are connected in series the current remain same while voltage increases as a multiple of number of cells and if we connect the cells is parallel then voltage remain the same while current increases as a multiple of number of cells. Therefore cells are connected in series parallel configurations to generate the required amount of power. Voltage of a typical photovoltaic array is low. A high voltage gain is necessary, if we want to put the extra generated voltage to grid. For example, the household appliances are designed to work on a specific rated voltage and power so first of all this voltage requirement is met. The PV cells are connected in series of 36 or 72 in a module to get the required amount of voltage. These module can then be connected in a combination of series and parallel to get the required voltage and current [68].

The voltage across parallel connected modules or string of modules should be same otherwise the module or string of modules having highest voltage would not be able to work at maximum power. This is because the voltage across parallel connection should be same which would be less than highest voltage. Bypass diodes are used to solve this problem.

3.1.2 Bypass and blocking Diode

The purpose of bypass diode is to ensure the maximum voltage across module. When some cells are in shade, covered with some dirt etc. or are dead because of some issue then it may not produce the required amount of voltage, so bypass diodes are used in parallel with each cell. If a solar cell is unable to work, to produce the required amount of voltage, then the bypass diode becomes forward biased. It behaves as short circuit for current but keep the required voltage difference across cell.

Since a PV cell behaves as diode in dark so at night or in absence of light, these cell may act as diode and draw power from storage device or grid. In this case, they will act as load instead of generator. To prevent this, isolation diodes are used on positive terminal of each string of module. These are also called blocking diodes.

3.1.3 Photovoltaic Module and Array

The purpose of module is not only to join cells in series along with bypass diodes to get the required amount of voltage but isolation diodes are also added to ensure the safely and block the reverse current [69]. All cells are placed in encapsulated flat glass to protect from water, dust etc. Most of manufacturers produce cells in form of solar modules. A variety of modules are available in market with different combinations of solar cells. To position the module relative to sun module mounts may also be used.

A photovoltaic array consists of series and parallel combinations of modules. The voltage requirement decides the number of module connected in series while power requirement decides the number of module connected in parallel.

3.1.4 Power Conditioning Unit

It provides interface between PV array and power grid. It consists of DC-AC inverter, maximum power point tracking (MPPT) unit, charge controller, DC-DC convertor, rectifier, other control switches and protection devices. The purpose of power electronic converter in power conditioning unit is to change the voltage level to a suitable form at high efficiency.

A. DC/DC converter model

The voltage of a typical photovoltaic array is low so high voltage gain is necessary to if we want to put the extra generated voltage to grid. Purpose of the DC-DC converter is to change DC voltage from one level to another. It consists of five basic components: diode, inductor, capacitor, PWM controller and a power switch [70]. Switching control the transfer of power from input to output dynamically. It does this through varying the duty cycle. Duty cycle is the ratio of “on” time to the switching time. It has two main types. One is called buck and the other is called boost converter. A boost type converter is used in PV system. It steps up the voltage to a higher level. Simulink diagram of a boost converter is given in figure 3.4.

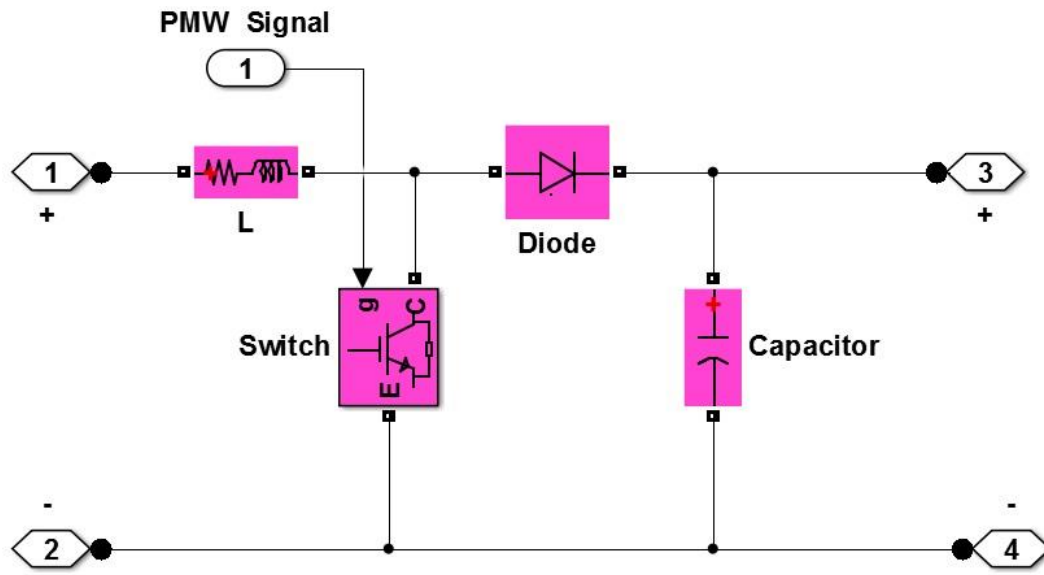


Figure 3-4 Simulink diagram of a boost converter

Capacitor is used to smooth the output. Dynamics of the DC/DC converter can be easily obtained by applying as

$$V_{pv} = L \frac{di_{pv}}{dt} + (1 - D)V_{cap} \quad (3.4)$$

This can be written as,

$$\frac{di_{pv}}{dt} = \frac{1}{L}(V_{pv} - (1 - D)V_{cap}) \quad (3.5)$$

Here L is the inductance of the DC/DC converter. The variable D is called duty ratio of switch. When switch is on, the PV current flows through the inductor and then it flows back to source through switch. The diode act as reverse biased in this case and conducts no current. The energy is stored in the inductor and the voltage across inductor has a value of V_{in} . Current flows through diode when switch is off. Now capacitor starts charging and when it is fully charged, all the energy of inductor is transferred to capacitor. The capacitor has a voltage V_{cap} across it in this case.

A DC/DC converter can operate in continuous conduction mode (CCM) or discontinuous conduction mode (DCM). In CCM, current fluctuates but never goes down to zero. In DCM, the current fluctuates and goes down to zero before or at the end of switching period. In this work, continuous conductor mode of operation is employed as the photovoltaic array has to feed power into the grid without any interruption.

B. Maximum Power Point Tracking

For a given PV system either value of current or value of voltage can be fixed. The value of other would depend upon the value of first. For different values of voltage and current the power output would be different for a given system and there would be only one point at which power output would be the maximum. The process of finding this point is called MPPT. I-V curve of typical PV module also show this behavior [71]. To run the PV system efficiently, MPPT is necessary. There are several complex and efficient techniques to find MPPT but some famous MPPT algorithms are [71]:

1. Perturb and observe

2. Incremental conductance
3. Current Sweep Method
4. Constant voltage

Among these algorithms perturb and observe, and incremental conductance can provide a true maximum power point. The incremental conductance method has the advantage over perturb and observe method because it can perform maximum power point tracking under rapidly varying irradiation conditions with more accuracy than the perturb and observe method [71].

The most efficient MPPT algorithm is incremental conductance method [68]. Many others have used this method in simulations [72]. This method is used in simulations in this study. In this method maximum power point is obtained when;

$$\frac{dP}{dV} = 0 \quad (3.6)$$

Where $P = VI$

Thus:

$$\frac{d(VI)}{dV} = 0 \quad (3.7)$$

$$I + V \frac{dI}{dV} = 0 \quad (3.8)$$

$$\frac{dI}{dV} = \frac{-I}{V} \quad (3.9)$$

$$\frac{dI}{dV} + \frac{I}{V} = 0 \quad (3.10)$$

So according to equation 3.10, this algorithm tries to minimize the error $(\frac{dI}{dV} + \frac{I}{V})$

A flow chart of incremental conductance method is shown in figure 3.5 while Simulink block diagram of incremental conductance is shown in figure 3.6.

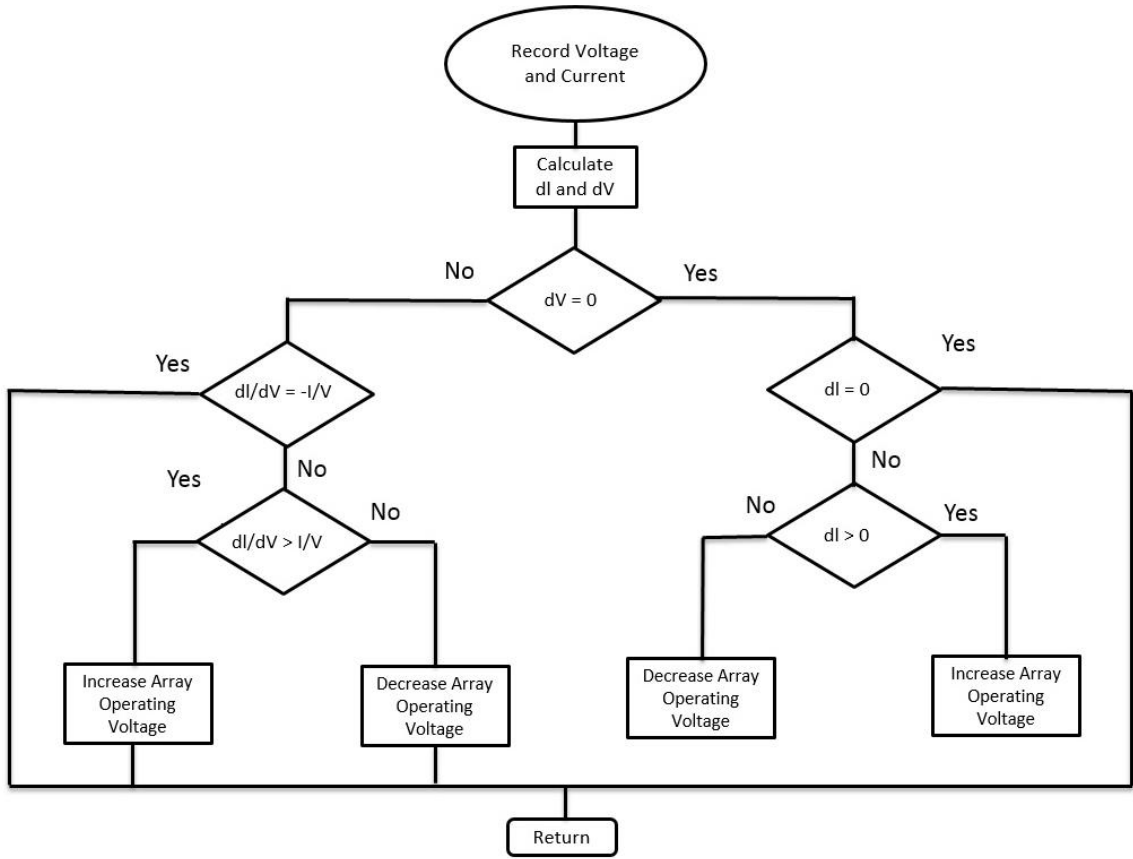


Figure 3-5 Flow chart of incremental conductance method

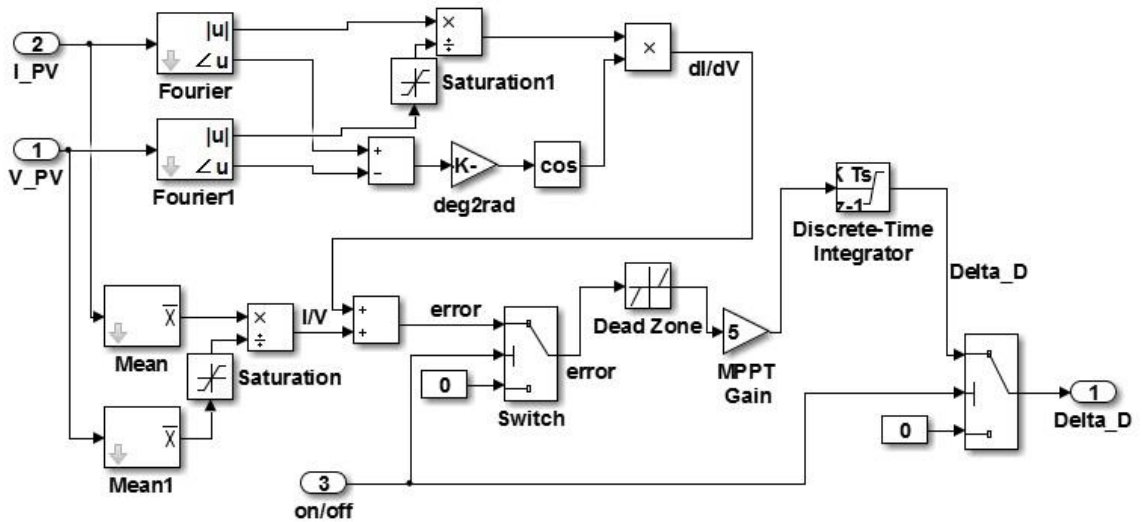


Figure 3-6 Simulink block diagram of incremental conductance

Using the output of incremental conductance PWM pulse is generated as shown in figure 3.7 which controls the switching of boost converter. The PWM generator block is further described in more detail in appendix A.

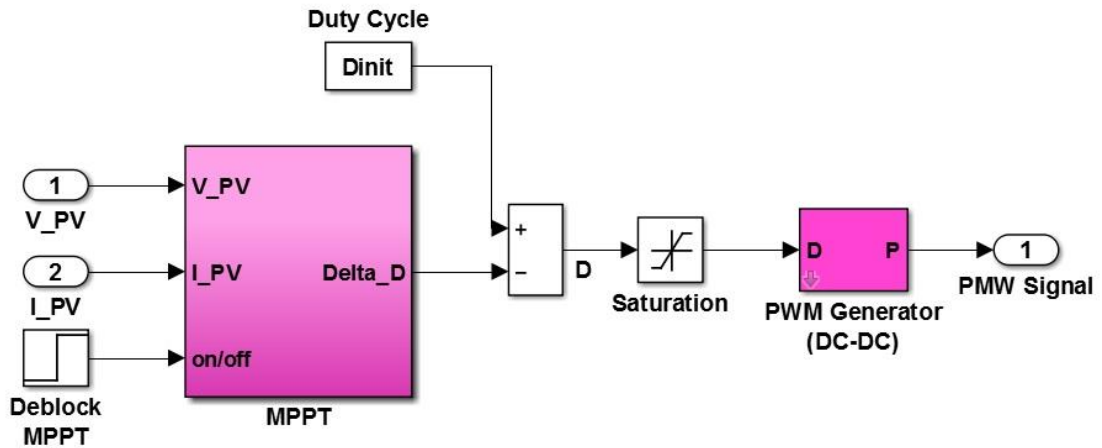


Figure 3-7 PWM pulse is generation

Maximum power point tracking (MPPT) plays an important role in minimizing the overall system cost and maximizing array efficiency by maximizing overall power output.

C. DC-link capacitor model

The DC-link capacitor is a storage device used to maintain constant DC voltage for DC side of inverter. This DC voltage is regulated by DC/DC converter irrespective of the inverter operation. On the other hand the inverter provides the proper current to the grid using this voltage variation feature of capacitor on DC side of inverter. No current will flow through DC-link capacitor, if inverter input is equal to converter output current. This will reduce the size of DC-link capacitor considerably [73].

D. Inverter Model

The purpose of inverter is to convert direct current to alternating current. The resultant AC current may be single phase or multi-phase and there are many different techniques for designing the single phase or multi-phase inverters. A very short interval of time called “blanking time” is inserted between turning of one switch and turning the other switch on to avoid short circuit condition. The inverter converts the PV array DC output and feeds the grid at the proper frequency. In this study, the voltage gain model of the voltage source inverter (VSI) operating in the PWM mode is adopted.

Types of inverters based on PV system connection design are given in the following.

Central Inverter

In PV systems, which are large than 10 kilowatt and have parallel strings, if all strings are connected to one common inverter, then such common inverter is called central inverter as shown in figure 3.7. Although it is cheap but it has certain disadvantages: power is lost due to common MPPT and due to module and string mismatch, high DC voltage cable is required between inverter and panels and the reliability of whole system depend upon only single inverter [34].

String Inverter

In this design a separate inverter is used for each string of modules and then all the inverters are connected to grid in parallel fashion as shown in figure 3.8. In this case there would be a separate MPPT for each string so overall yield would be improved. There would no string diode so losses would decrease. If string voltage is high enough

then voltage boosting may not be required but if voltage of string is not high enough then voltage boosting would be required [34].

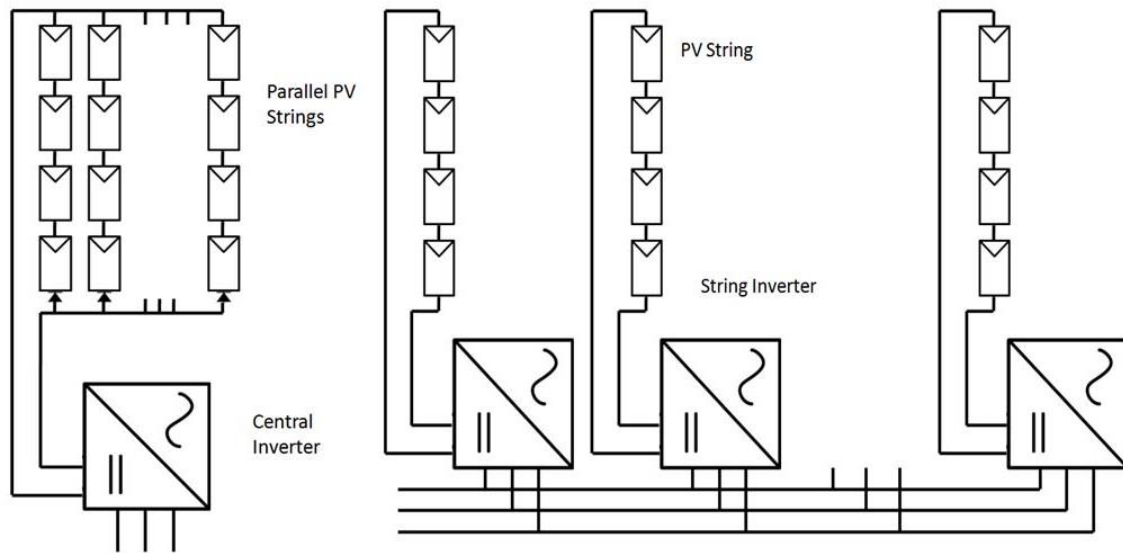


Figure 3-8 Central and String Inverter

Module Inverter

In this case each module has its own inverter and all inverters are connected to grid directly as shown in figure 3.9. There would be no mismatch losses and each module would have its own MPPT. The overall power production would increase. The efficiency of module inverter would be better than string inverter but high voltage amplification is required which may lead to lower efficiency. This design is more costly than previous one [34].

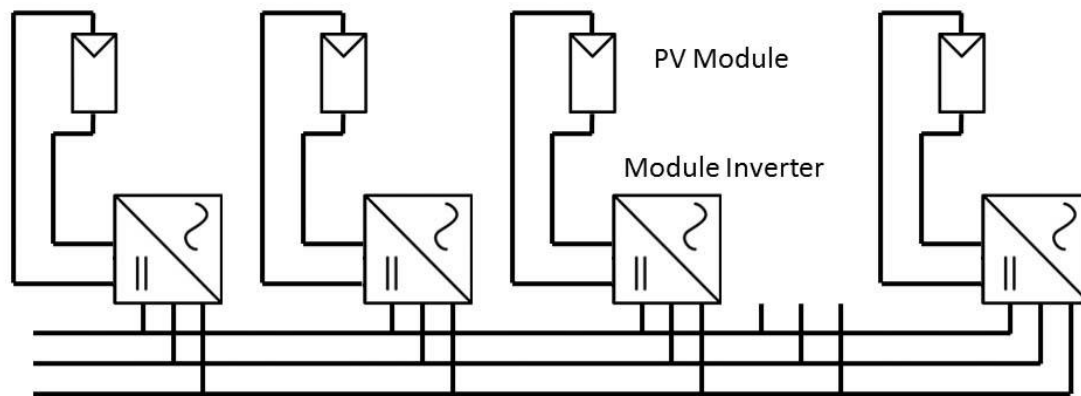


Figure 3-9 Module Inverter

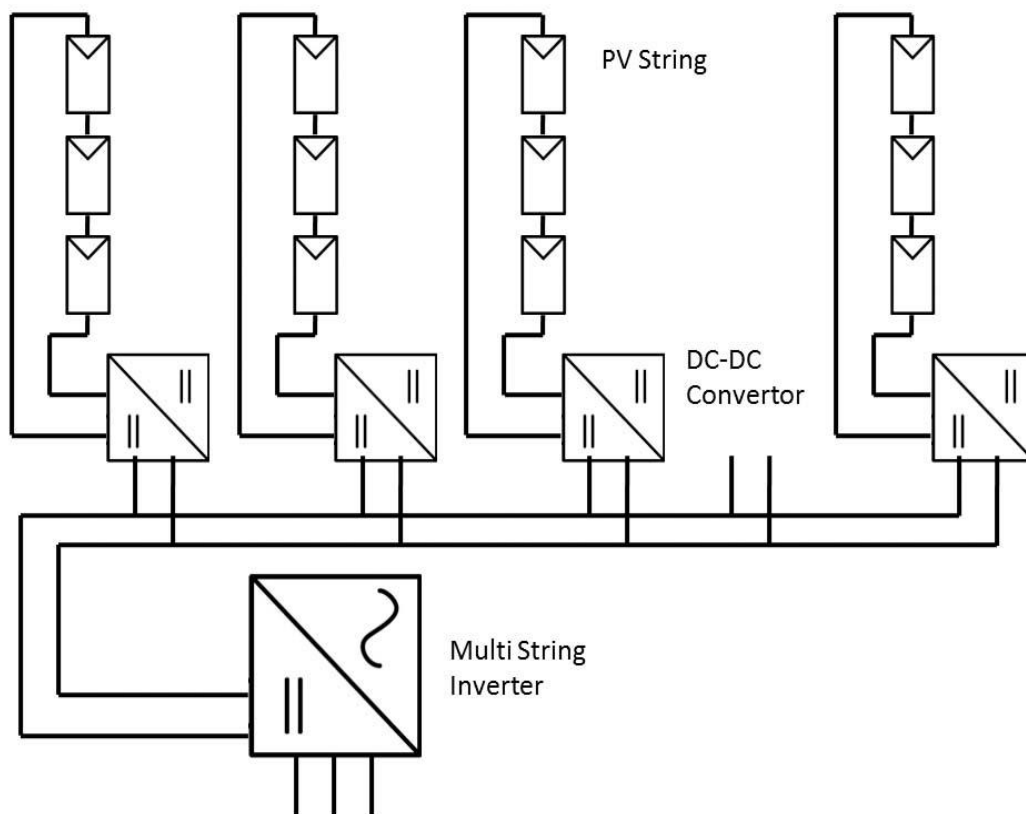


Figure 3-10 Multi-String Inverter

Multi-String Inverter

This design combines the advantages of string inverter and module inverter as shown in figure 3.10. A DC-DC converter is used for each string of module and each string of module has its own MPPT. These converters are then connected one common DC-AC inverter. Overall efficiency increases in this case as compared to string or module inverters [34]. Simulink block diagram of inverter along with control system is shown in figure 3.11.

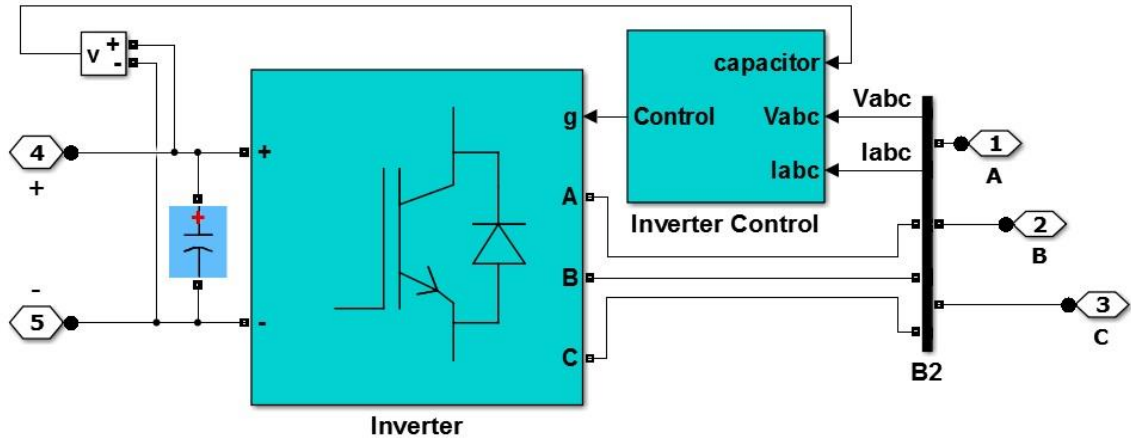


Figure 3-11 Inverter Model along with Control

The instantaneous active power on the AC side of the inverter is given as

$$P_{ac} = V_{pd}I_{pfd} + V_{pq}I_{pfq} \quad (3.11)$$

Where,

V_{pd}, V_{pq} = inverter output voltages in terms of d-q axes.

I_{pfd}, I_{pfq} = inverter output currents in terms of d-q axes.

While power on the DC side of the inverter is given as

$$P_{dc} = V_{dcp} I_{dc} \quad (3.12)$$

Where,

V_{dcp} = voltage on the DC side of the inverter.

I_{dc} = current on the DC side of the inverter.

Inverter control model is described in figure 3.12. It has measurement and transformation block, grid side control block and 3 phase PWM generator block. Measurement and transformation block is further described in figure 3.13 while the detail on other two blocks could be find in appendix A.

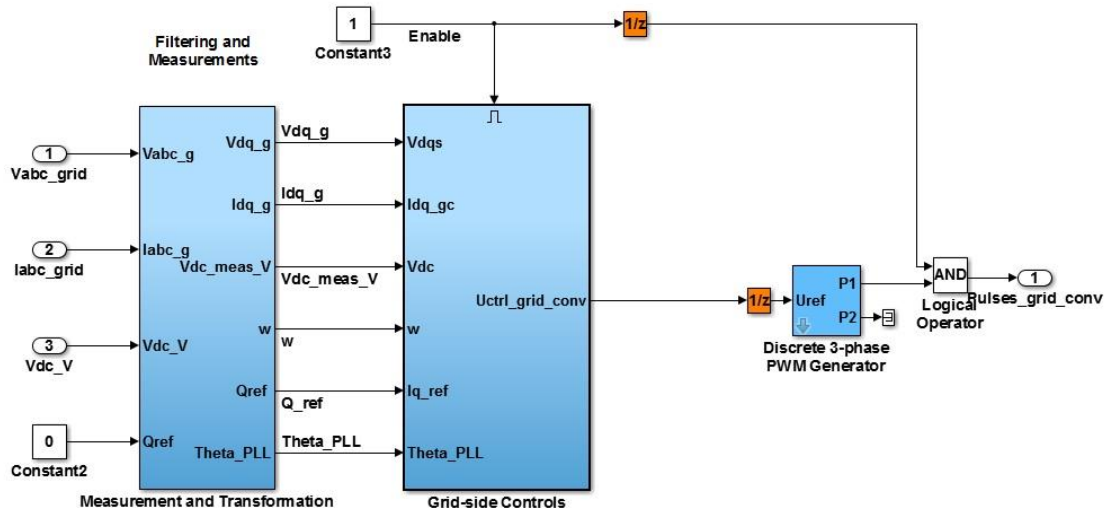


Figure 3-12 Inverter control model

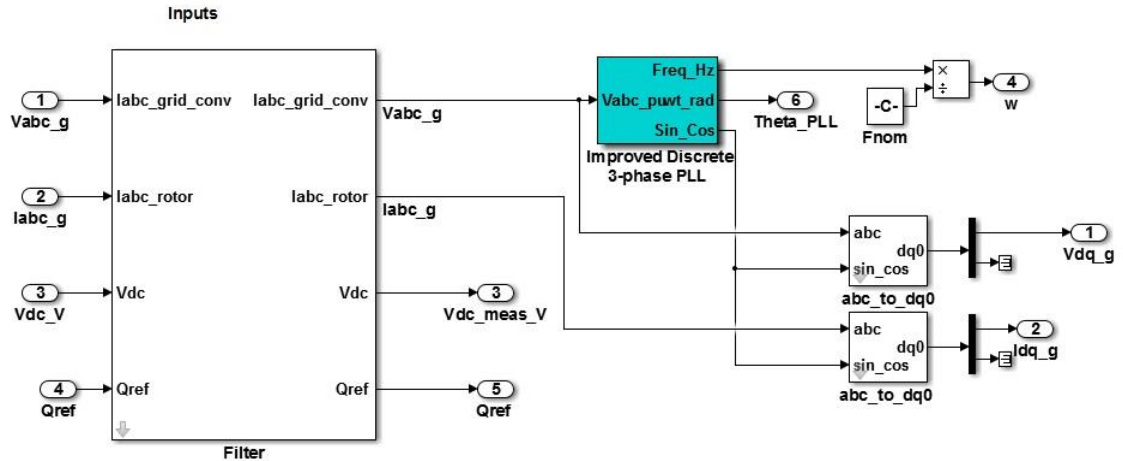


Figure 3-13 Measurement and transformation block

First block in figure 3.13 is a simple low pass filter while the detail on other blocks could be find in appendix A.

E. Active Filter Model

For smoothing the output current, a passive low-pass LC filter is commonly employed between the PV system and utility network. The resistance R_{damp} in series with the filter capacitor is used to avoid the resonance between the filter capacitor and the coupling inductance.

The inductor blocks the high frequency harmonics and passes the low frequencies, while the capacitor allows high frequencies and blocks low frequencies. So these reactive devices can block most of the harmonics and reduce the switching frequency ripple of the inverter output[74]. To avoid the resonance that may arise with the coupling inductance and the filter capacitor, a passive damping circuit is added to the filter such as damping resistor.

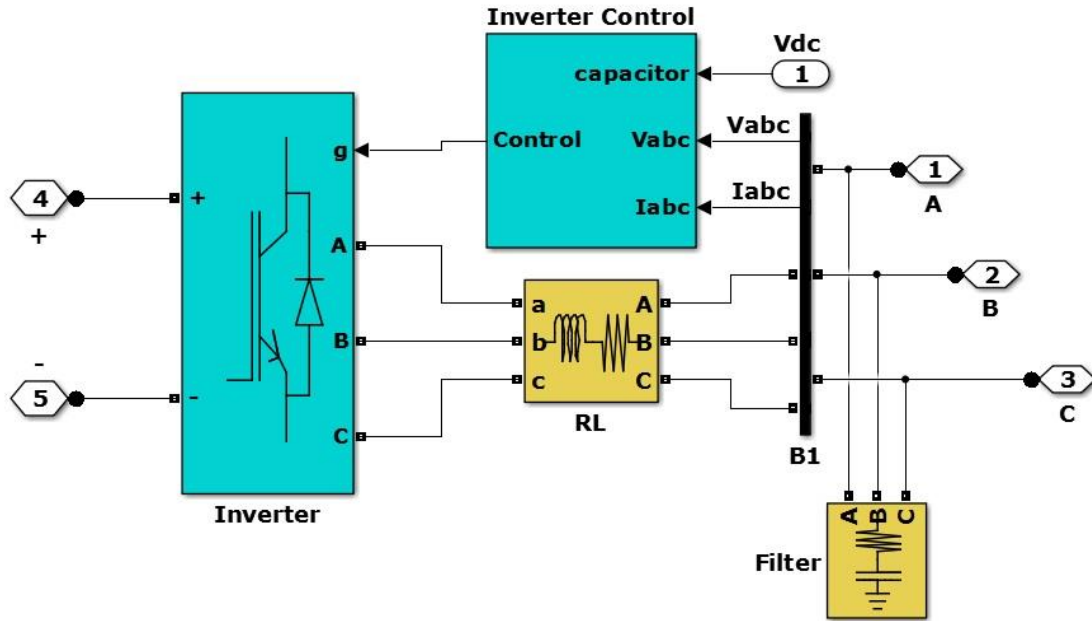


Figure 3-14 Active Filter Model

Applying KVL around the PV inverter and on left side of filter capacitor gives a non-linear differential equation as

$$V = i_{filter}R_{filter} + L_{filter} \frac{di_{filter}}{dt} + V_{cap} + (i_{filter} - i)R_{damp} \quad (3.13)$$

Where, R_{filter} is the filter resistance, L_{filter} is the filter inductance, R_{damp} is the damping resistance, V_{cap} is the capacitor voltage.

Similarly, equation from the right leg of capacitor is,

$$V_{cap} = iR + L \frac{di}{dt} + V - (i_{filter} - i)R_{damp} \quad (3.14)$$

The voltage across the filter capacitor is given as

$$C_{filter} \frac{dV_{cap}}{dt} = (i_{filter} - i) \quad (3.15)$$

Where C_{filter} is the capacitance of the filter.

3.2 Components of Wind System

Since last 10 years, the wind turbine is the world's fastest expanding power generation technology. In a wind system, energy is converted into rotational mechanical energy through blades (rotor) then a generator converts this mechanical energy into electrical energy. A gear-box connects the low speed shaft of the rotor to the high speed shaft of generator [75]. Early wind farms had fixed speed wind turbines and they were based on squirrel cage induction generators. There was no control method so fluctuations were passed through system causing mechanical stress on wind turbine rotor [76]. Those systems were not so efficient therefore variable speed wind turbines (VSWT) took over. VSWT cause less stress on the blades and shaft on mechanical component of the wind turbine system. VSWT can adjust its rotational speed according to wind speed. In this way it achieves optimum efficiency over a wide range of wind speeds. Therefore these system are 10-15% more efficient than old systems [77]. Now a day VSWT are available both in kW as well as in MW size range.

There are many kinds of wind generators. Modern large scale VSWT are either based on doubly fed induction generators (DFIGs) or permanent magnet synchronous generators (PMSGs). PMSGs do not have to be installed with a gear box [78]-[87], while other generators including DFIGs do have to be connected with a gear-box.

DFIG has several advantages over PMSG in terms of reactive power control and size [88][89]. The maximum size available of PMSGs is 2MW while DFIG come in size as large as 10 MW. A permanent magnet (PM) provides magnetization in PMSGs so it has the property of self-excitation. Rotor of PMSGs needs no external excitation so this

allows PMSGs to work at higher power factors and efficiencies. PMSGs have several advantages over other type of generators some of them are listed below:

- Maintenance of PMSGs is easy
- Have longer lifetime
- No external power supply is required
- No rotor winding or copper losses
- More reliable because no slip ring or brushes needed
- Lighter in weight so higher ratio of power to weight

VSWT has two types of control:

- Mechanical Control
- Electrical Control

The purpose of VSWT control is to operate the wind system at maximum power point tracking to extract the maximum wind power. Blade pitch angle is controlled in mechanical control. Power delivered to the generator can be maximized at a particular wind speed by controlling the pitch angle carefully [90]. Electrical control covers the control of the power converters and the load side control. The stator in PMSGs is not directly connected to grid unlike the DFIGs where stator is directly connected to the grid. The PMSG is connected to the grid through full scale voltage source converters. These converters are called back to back converters and are connected between PMSGs and grid. Back to back converters are actually consist of two converters:

- Generator side converter
- Grid side converter

The converter on the generator side converts from AC to DC while grid side converter is a general PWM voltage inverter which converts from DC to AC. Integration of wind generation with the power grid brings many challenges. The fluctuations of power output in wind energy conversion system may cause some problems for the grid especially in a weak grid [91][92]. The inverter terminal is connected to the transmission grid through a step-up transformer. The system model consists of PMSG, wind turbine, the converters, loads, generator and the transmission line.

An issue with PMSGs that is needed to be considered is the risk of demagnetization of magnets due to the temperature rise. The magnets can be partially or fully demagnetized. In partial demagnetization the magnetic properties are weakened. In full demagnetization magnetic properties are completely lost and they require re-magnetization which is a tedious task and in some cases impossible and a new rotor is required. Thus a thermal study is suggested to guarantee that the magnet working temperature is, in any conditions, preserved low. Additionally, the partial demagnetization is usually a case during a short circuit where some parts of the magnets are exposed to high opposing magnetic fields [93]-[95]. The complete block diagram of grid connected PV system used for simulations is given in chapter 4.

3.3 Wind System Modeling

Permanent magnet synchronous generator (PMSG) type wind system is considered in this work. The model consists of a two mass drive-train, a synchronous generator, full-scale converter and filter circuit. The wind turbine connects to the rotor of the synchronous generator through a gearless drive train. The permanent magnets are mounted on the generator rotor, providing a fixed excitation to the generator. The 3-phase

stator windings of the generator feed power to the full frequency converter which converts variable frequency of the wind generator to the constant grid frequency.

3.3.1 Wind turbine model

The wind turbine extracts power from wind and converts it into mechanical power. The power output of the wind turbine depends on wind speed and rotor size.

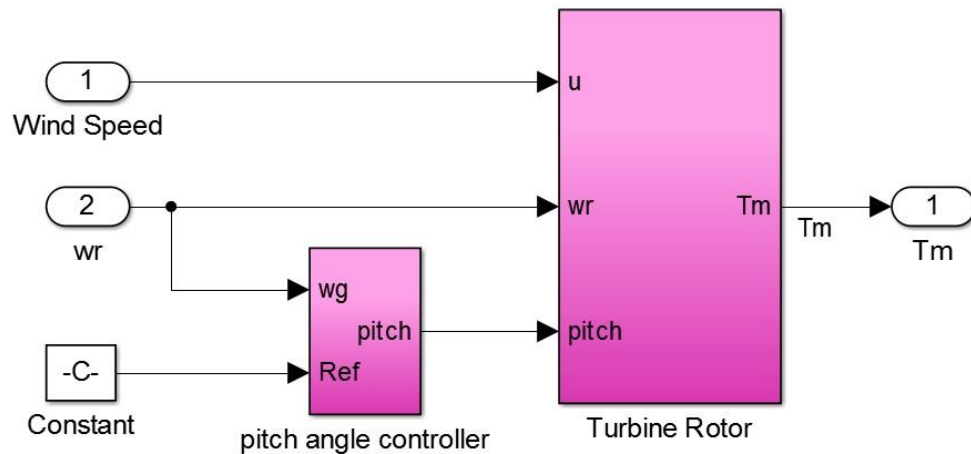


Figure 3-15 Wind Turbine Model in Simulink

The mechanical power developed is proportional to the cubic power of wind speed hence a small increase in speed causes larger increase in the wind power. In addition, the power output of the turbine also increases with increase in blade area by allowing turbine to intercept more wind and energy capture. But the size of the blades in wind turbine has a limitation put by the technical and economic aspects. The amount of aerodynamic power produced by the wind turbine is given as follows

$$P_w = \frac{1}{2} C_p A \rho V^3 \quad (3.16)$$

Where:

ρ = Density of the air (kg/m^3),

S = area swept by the turbine (m^2),

C_p = Power coefficient of the wind turbine rotor

Power coefficient defines the aerodynamic efficiency of the wind turbine rotor, and is a function of the tip speed ratio λ and blade pitch angle β . The tip speed is defined as the ratio between the peripheral speed of the blades and the wind speed. Power coefficient changes with the different values of β , but the wind turbine is most efficient for $\beta=0$.

The theoretical upper limit of C_p is 0.59 but in practical its value lies in range of 0.2-0.4.

3.3.2 PMSG Model

The equivalent circuit of a three phase permanent magnet synchronous generator considering sinusoidal flux distribution is as [96],

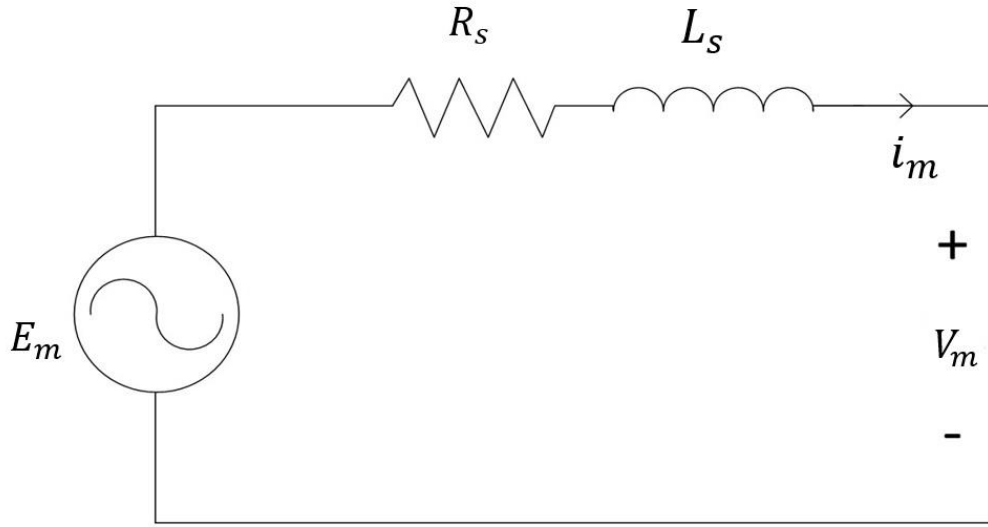


Figure 3-16 Equivalent circuit of PMSG

The voltage current relations of the stator circuit is,

$$E_m = L_s \frac{di_m}{dt} + R_s i_m + V_m \quad (3.17)$$

Where, R_s and L_s armature resistance and inductance, V_m is the PMSG terminal voltage, E_m is the emf generated by the permanent magnet developed field.

The electromechanical torque generated by the machine is given as

$$T_e = E_{fd} \times i_{mq} + (x_q - x_d) \times i_{md} \times i_{mq} \quad (3.11)$$

Here i_{md} and i_{mq} are the d-q axes PMSG currents, x_d and x_q are the stator reactance in d-q axes, E_{fd} is the field voltage along d-axis, The electrical power output of the generator is the product of torque and rotor speed, and is expressed as,

$$P_{ew} = \omega \times T_e \quad (3.18)$$

ω is the generator rotor speed. The electromechanical dynamics of the rotor can be expressed through the second order model,

$$\frac{d\delta}{dt} = \omega_0(\omega_w - 1) \quad (3.19)$$

$$\frac{d\omega_w}{dt} = \frac{1}{2H_m}(K_s\theta_s - P_{ew}) \quad (3.20)$$

Where δ is the rotor angle of the PMSG, H_m is the PMSG inertia constant, θ_s is the torsional angle and K_s is the stiffness of shaft. A two mass model representation of the drive train is employed in this work. Higher inertia turbine rotor is connected to the lower inertia generator rotor through a flexible shaft having a stiffness of K_s . The high speed shaft is assumed to be stiff. No gear box is employed in this concept.

3.3.3 Full Converter Configuration

Full converter composed of a force commutated machine side converter and grid side converter connected with a common DC-link as shown in figure 3.17. The advantage of such a system is that the DC-link capacitor decouples the two converters and hence a separate control on each converter can be employed.

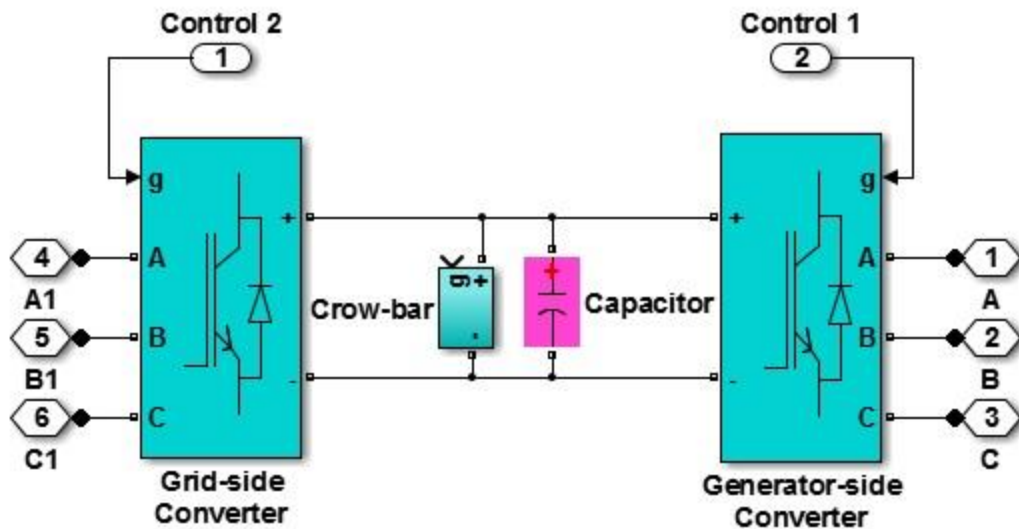


Figure 3-17 Back to Back Converters

Back to back convertors and power control system are required for a typical grid connected wind system in addition to blades and generator. Frequency and voltage output of a wind system have fluctuations so back to back convertors are required. Back to back convertors along with power control system convert the variable frequency and voltage into constant voltage and frequency to meet the power quality standards [82].

The machine side converter acts as rectifier which converts the generator's low frequency alternating current to direct current. The rectifier operates on the pulse width modulated technique. The main advantage of using PWM is that it reduces the losses in the switching devices.

The DC link capacitor provides an intermediate energy storage, which isolates the generator side synchronous system from grid side synchronous system. The transfer of real power from the generator into the grid can be realized through this DC-link by keeping its voltage constant. The current in the DC-link is discontinuous as it is switched on or off with respect to the switching frequency of the converter. This process induces voltage ripples in the DC-link capacitor which can be made small to the extent that the voltage appears virtually constant during switching period by selecting a large value of capacitor. On the other hand a small capacitor enables fast control of the DC-link voltage. Hence the selection of the size of the capacitor has to be a trade-off between the voltage ripples and fast changes in DC voltage.

The grid side converter acts as an inverter, which converts the DC power to fixed frequency AC power. The grid side converter also operates on the PWM technique. The magnitude of the inverter output voltage depends upon the modulation index m and DC link voltage.

A. Generator (or machine) side converter

The terminal voltage of the synchronous generator can be expressed in terms of the modulation index of the rectifier, dc-link voltage and the rotor angle of the generator in d-q axes as.

$$V_m = m_r V_{dc} (\sin\delta + j\cos\delta) \quad (3.21)$$

The power on the AC side of the converter is given as

$$P_m = V_{md} i_{md} + V_{mq} i_{mq} \quad (3.22)$$

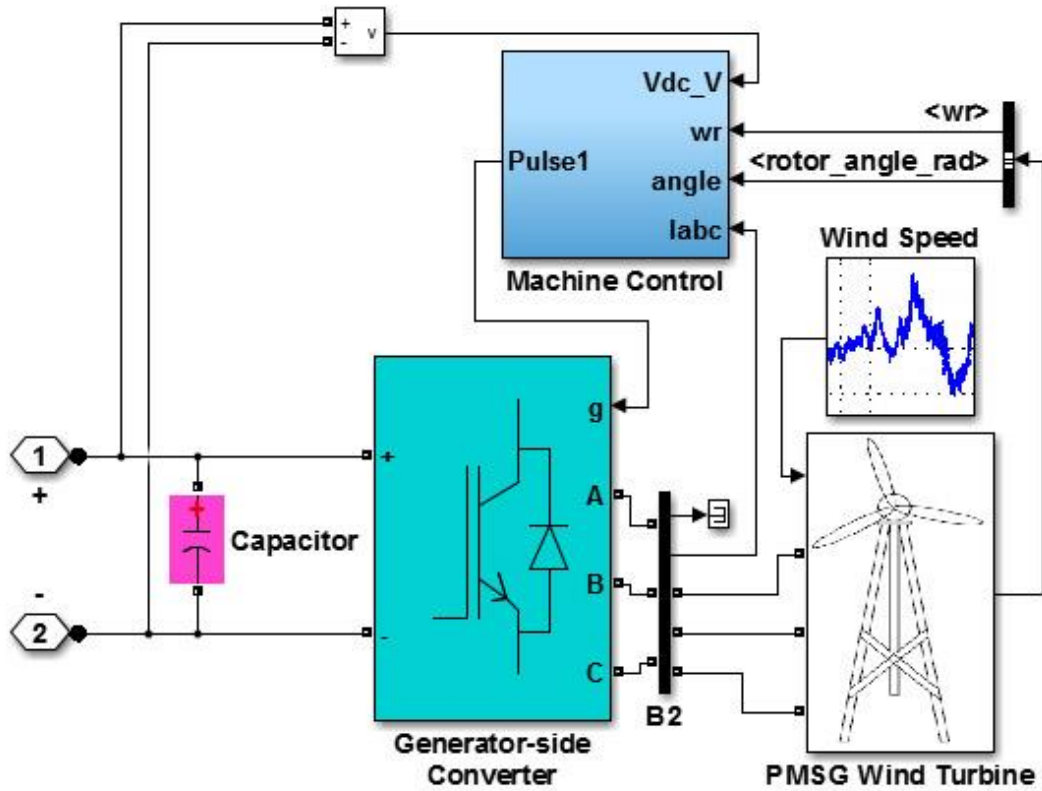


Figure 3-18 Generator Side Converter

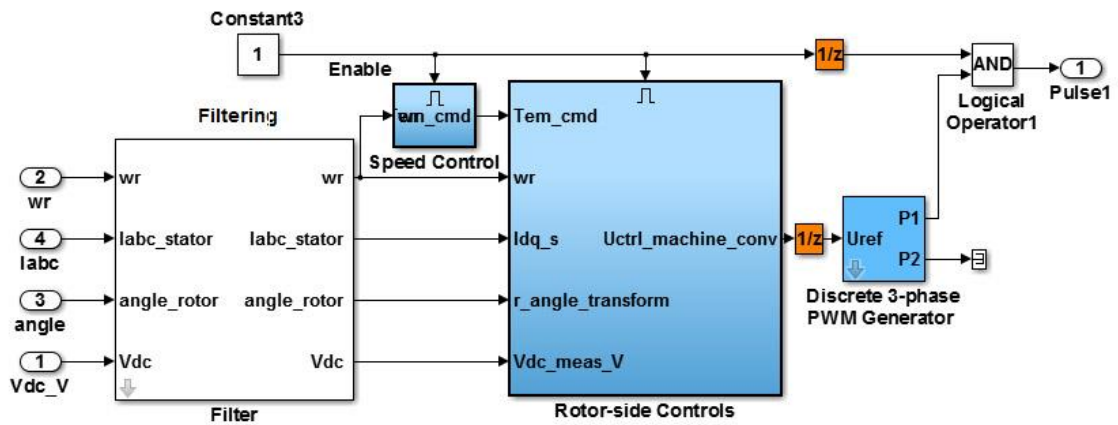


Figure 3-19 Control of Generator Side Converter

First block in figure 3.19 is a simple low pass filter while other blocks are described in more detail in appendix B.

B. Grid side converter:

A Simulink block diagram of grid side converter along with control system is shown in figure 3.20.

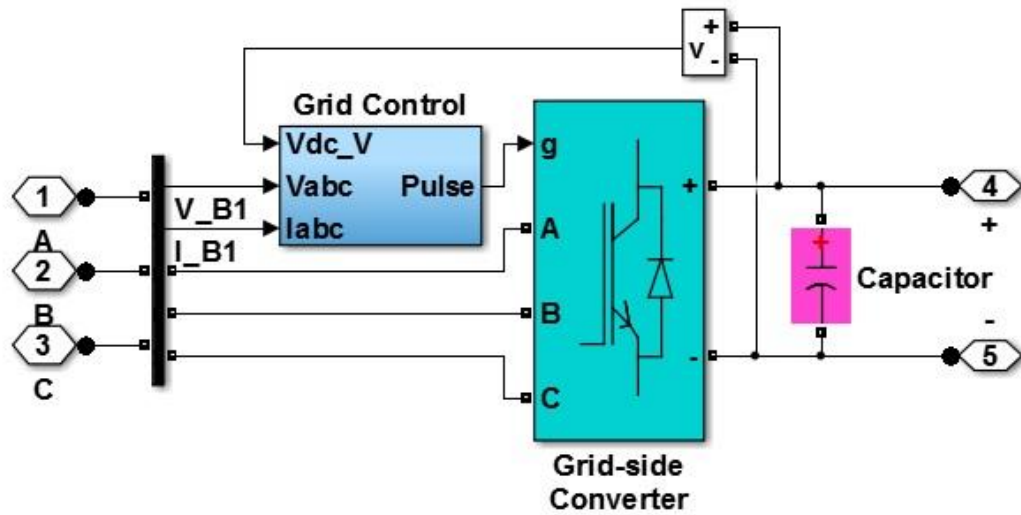


Figure 3-20 Grid Side Converter along with Control System

The output voltage of the converter in terms of the d-q axes is given as

$$V = m_i V_{dc} [\cos(\psi_i + \theta) + j \sin(\psi_i + \theta)]$$

Here, θ is the phase angle of the grid voltage, V_{dc} is the voltage across the dc-link, V is the inverter output voltage.

The power on the AC side of the inverter is given as

$$P = V_d i_{fd} + V_q i_{fq} \quad (3.23)$$

i_{fd} and i_{fq} are the d- q axes component of the inverter output current i_f .

The grid side converter control model is described in figure 3.21. It has measurement and transformation block, grid side control block and 3 phase PWM generator block. The measurement and transformation block is further described in figure 3.22 while detail on other two blocks could be find in appendix B.

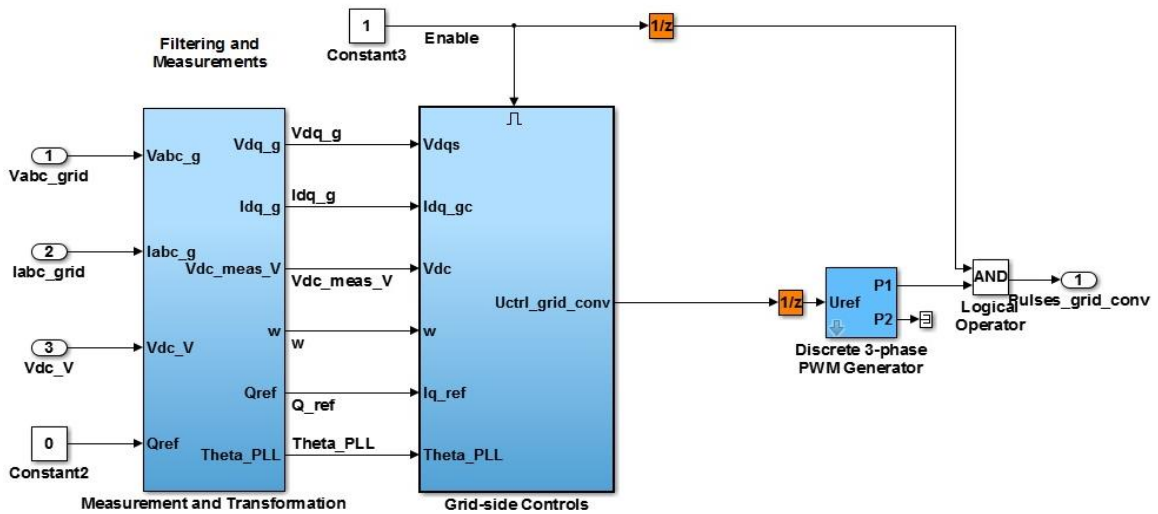


Figure 3-21 Grid Side Converter Control Model

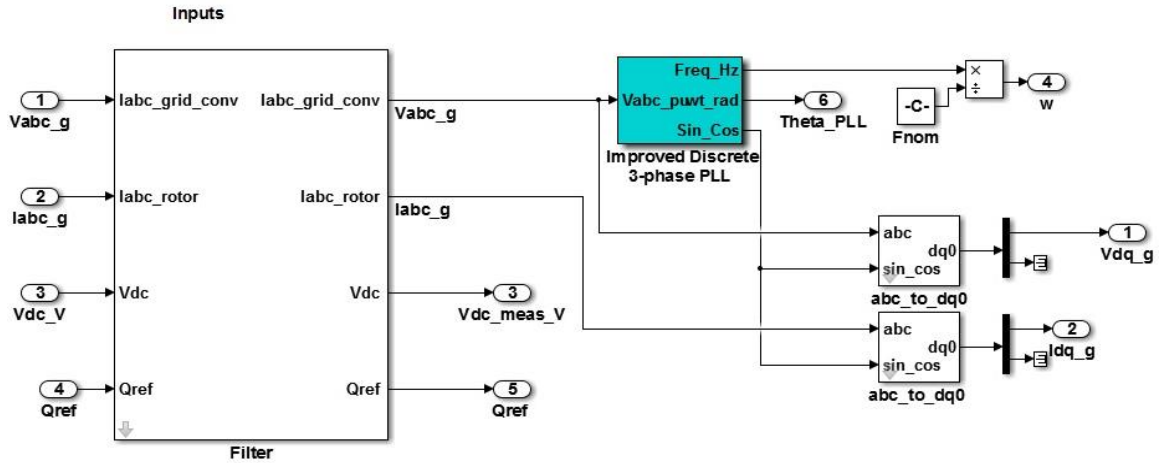


Figure 3-22 Measurement and transformation block

First block in figure 3.22 is a simple low pass filter while details of other blocks are presented in appendix B.

C. Active Filter Model

For smoothing the output current, an LC filter is employed between the wind system and common bus. This filter model is similar to the model used for PV system.

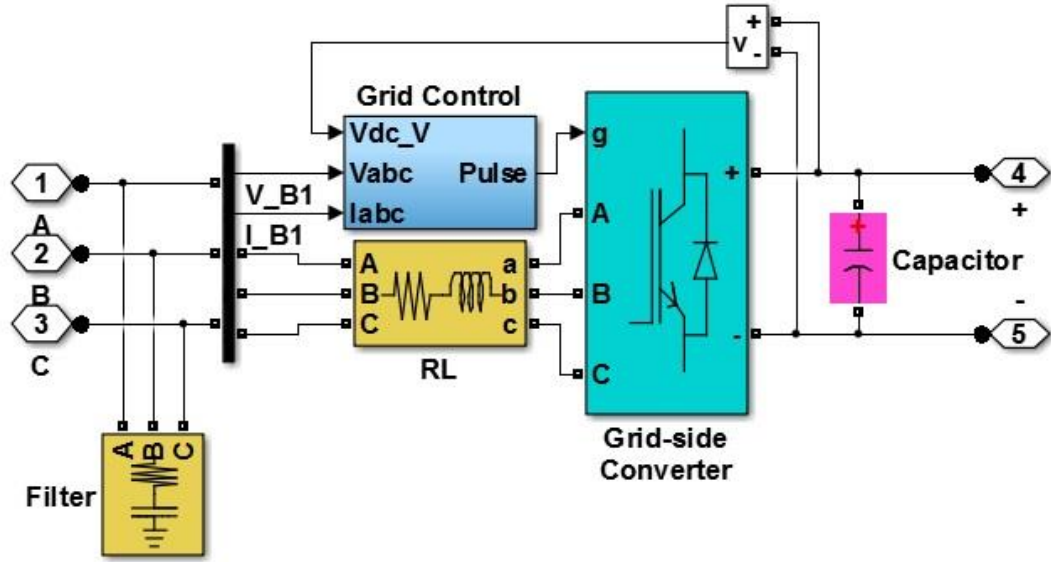


Figure 3-23 Active filter Model

Applying KVL and KCL on the right side of the filter section give the equations,

$$V = i_{filter}R_{filter} + L_{filter} \frac{di_{filter}}{dt} + V_{cap} + (i_{filter} - i)R_{damp} \quad (3.24)$$

Where, R_{filter} is the filter resistance, L_{filter} is the filter inductance, R_{damp} is the damping resistance, V_{cap} is the filter capacitor voltage.

Similarly, equation from the left leg of capacitor is,

$$V_{cap} = iR + L \frac{di}{dt} + V - (i_{filter} - i)R_{damp} \quad (3.25)$$

The voltage across the filter capacitor is given as

$$C_{filter} \frac{dV_{cap}}{dt} = (i_{filter} - i) \quad (3.26)$$

Here, C_{filter} is the capacitance of filter after grid converter of grid connected wind system.

CHAPTER 4

SIMULATION RESULTS OF GRID CONNECTED PV SYSTEMS

In this study, it is assumed that PV systems are located close to each other therefore PV systems are exposed to the same solar irradiance behaving in the same manner in term of power quality. PV systems will usually experience different solar irradiance based on their location. However in order to find correlation it is necessary that all PV systems should behave the same way so that a model should be developed. The assumptions considered in this work are given in the following.

1. PV systems have no reactive support
2. All loads are linear
3. All PV systems are installed on the same feeder
4. Transient response is not considered
5. Utility substation is a strong bus

4.1 Design of a Grid Connected PV system

The block diagram of the grid connected PV system is shown in figure 4.1. Here a step up transformer is used for grid integration. Voltage and current measurement blocks are located between RES and transformer.

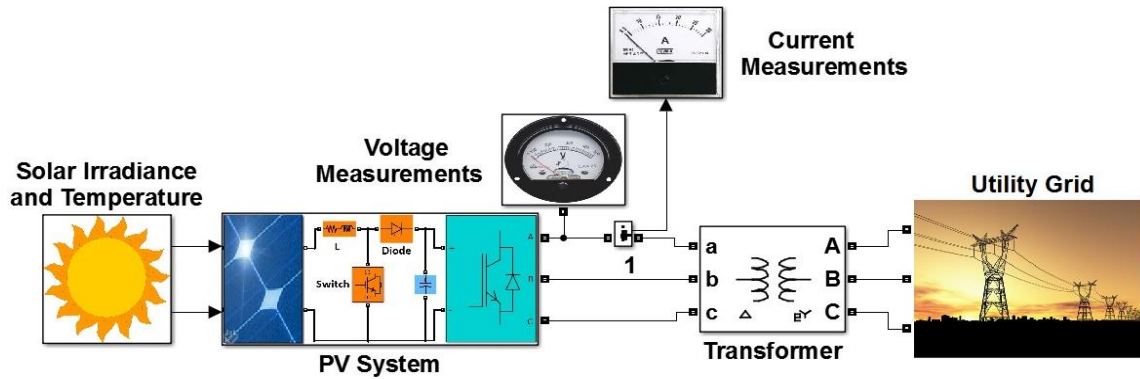


Figure 4-1 Grid Connected PV System

The PV system block is described in more details in figure 4.2. Here 1.5 MW PV system is connected to the grid via converter and inverter. The PV array is modeled based on the design of 305 WP SunPower PV modules (SunPower SPR-305) manufactured by SunPower. The rated power is peak power at 1000 W/m^2 irradiance. If solar irradiance is 1000 W per meter square at $25 \text{ }^\circ\text{C}$ then output of one module is 305 W . The numbers of series connected modules per string are 15 while 330 such strings are used. The total power would be $305 \times 330 \times 15 = 1.51 \text{ MWp}$ @ 1000 W/m^2 and $25 \text{ }^\circ\text{C}$ temperature. The PV module use incremental conductance method as maximum power point tracking (MPPT) technique. Details of utility grid block are shown in figure 4.3.

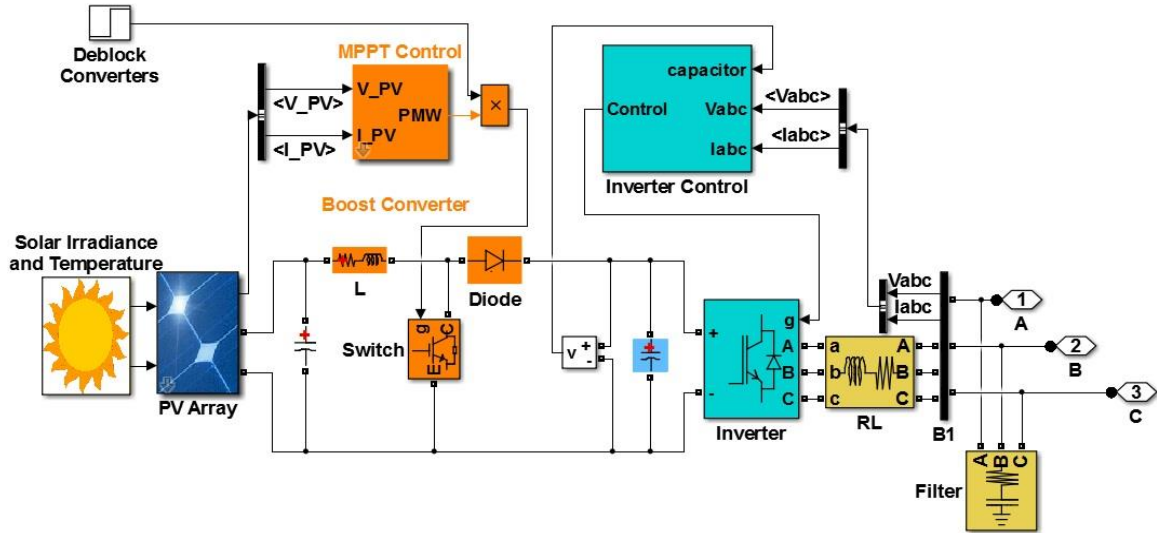


Figure 4-2 PV System Simulink Block

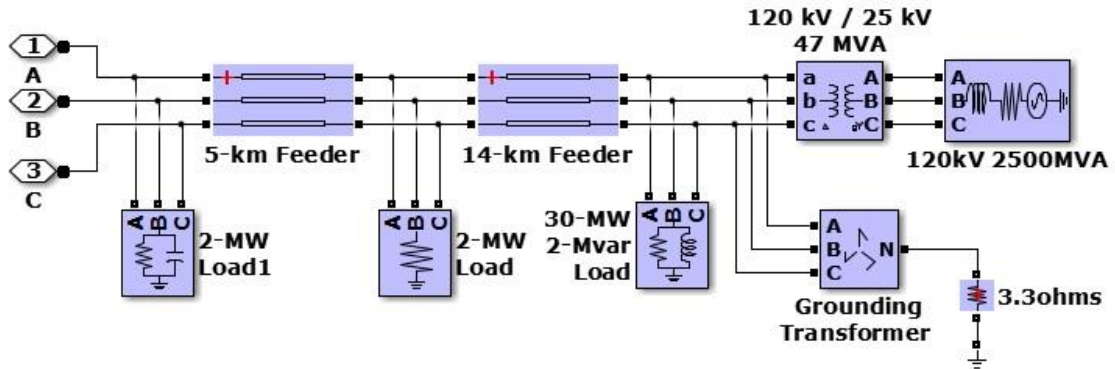


Figure 4-3 Utility Grid Simulink Block

Solar irradiance and temperature, taken at KFUPM Dhahran (26.18°35' N, 50.08°24' E) on 9th of July 2010, are used as inputs for grid connected PV system. Irradiance curve, and temperature used in simulations are shown in figure 4.4 and 4.5.

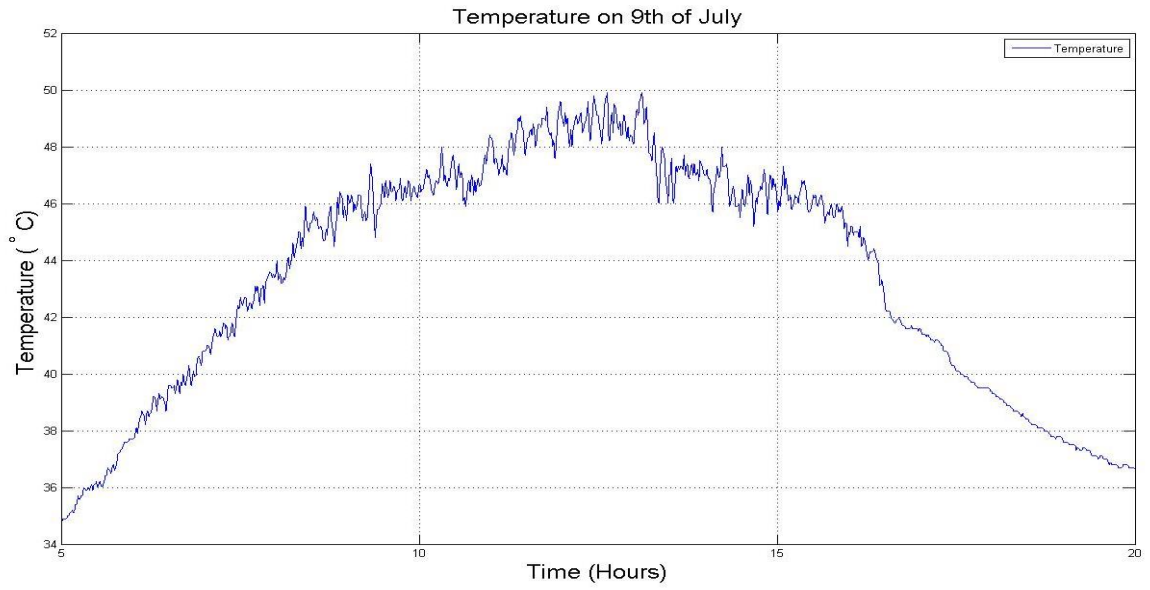


Figure 4-4 Temperature at KFUPM on 9th of July, 2010

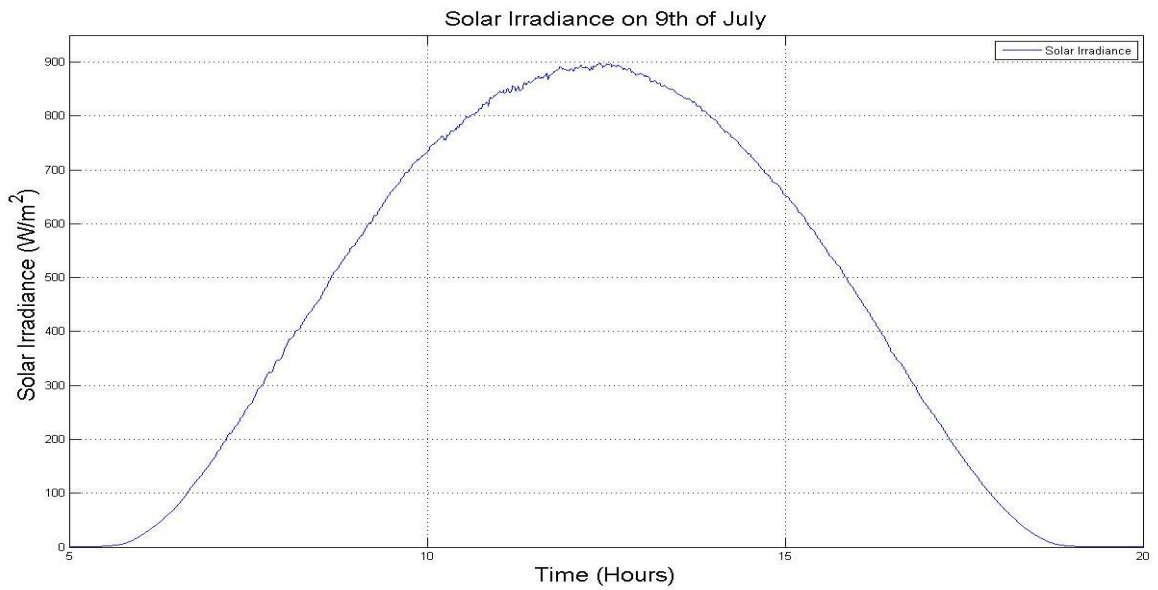


Figure 4-5 Solar Irradiance at KFUPM on 9th of July, 2010

4.2 Simulation Results of Grid Connected PV Systems

A grid connected PV system is used to verify the relation between PV system parameters and power quality indices. By designing voltage measurement block and current measurement block as shown in figure 4.1 the following relation were found between current/voltage RMS of a grid connected PV system and solar irradiance as shown in figure 4.6.

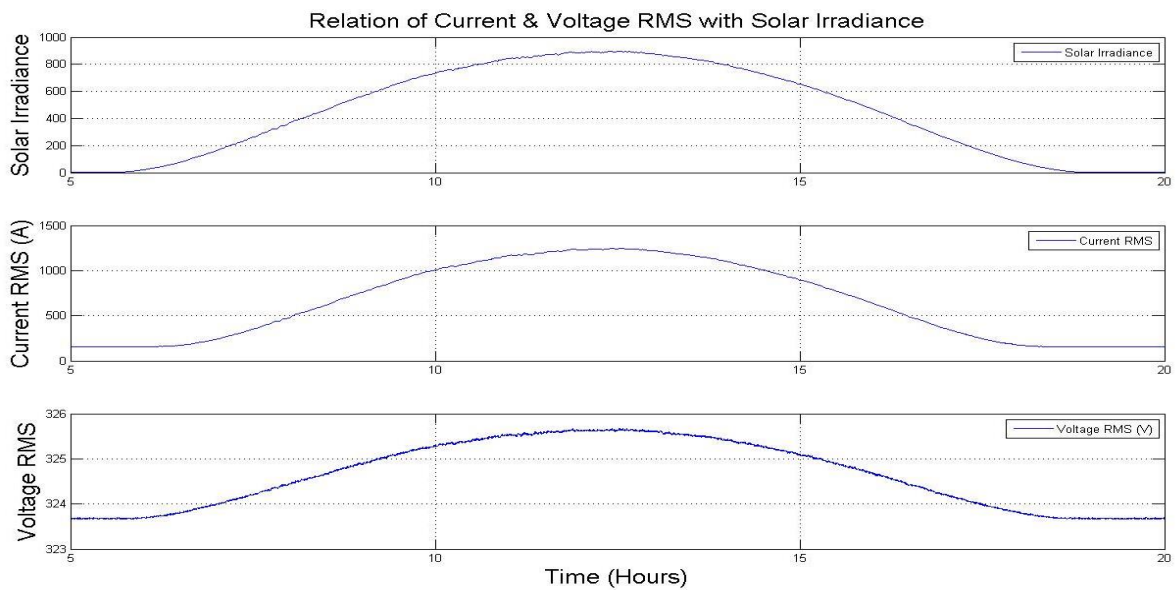


Figure 4-6 Relation between Solar Irradiance and current & voltage RMS

First curve is the irradiance from 5 AM to 8 PM. Second curve shows current RMS from 5 AM to 8 PM at given irradiance. Third curve is the voltage RMS from 5 AM to 8 PM at given irradiance. A direct relation exists between current & voltage RMS and solar irradiance. This is the simplest scenario as not any other kind of harmonic distortions are present there in the system. We have to consider other factors too when system will become more complex.

The relation between current & voltage THD and solar irradiance is shown in figure 4.7.

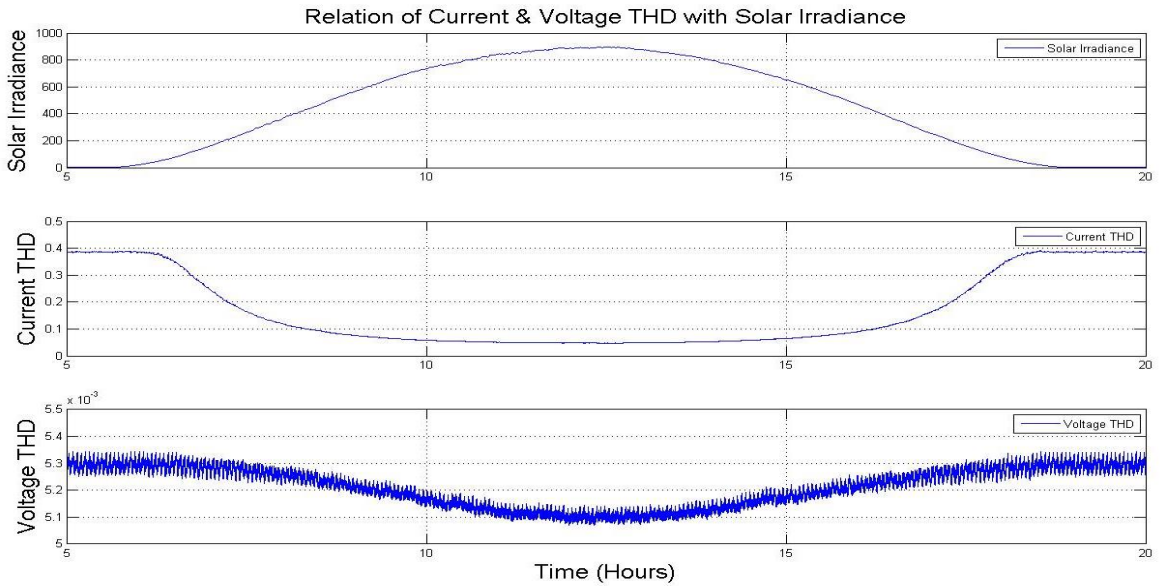


Figure 4-7 Relation between Solar Irradiance and current & voltage THD

First curve is the irradiance from 5 AM to 8 PM. Second curve shows current THD from 5 AM to 8 PM at given irradiance. Third curve is the voltage THD from 5 AM to 8 PM at given irradiance. An inverse relation exists between voltage & current THD and solar irradiance.

The relation of voltage RMS curve with the different number of PV systems, from 5 AM to 8 PM, is shown in figure 4.8 while the relation of current RMS curve with the different number of PV systems, from 5 AM to 8 PM, is shown in figure 4.9. These results clearly show that as the number of grid connected PV system is increased both the voltage & current RMS are shifted to a higher level.

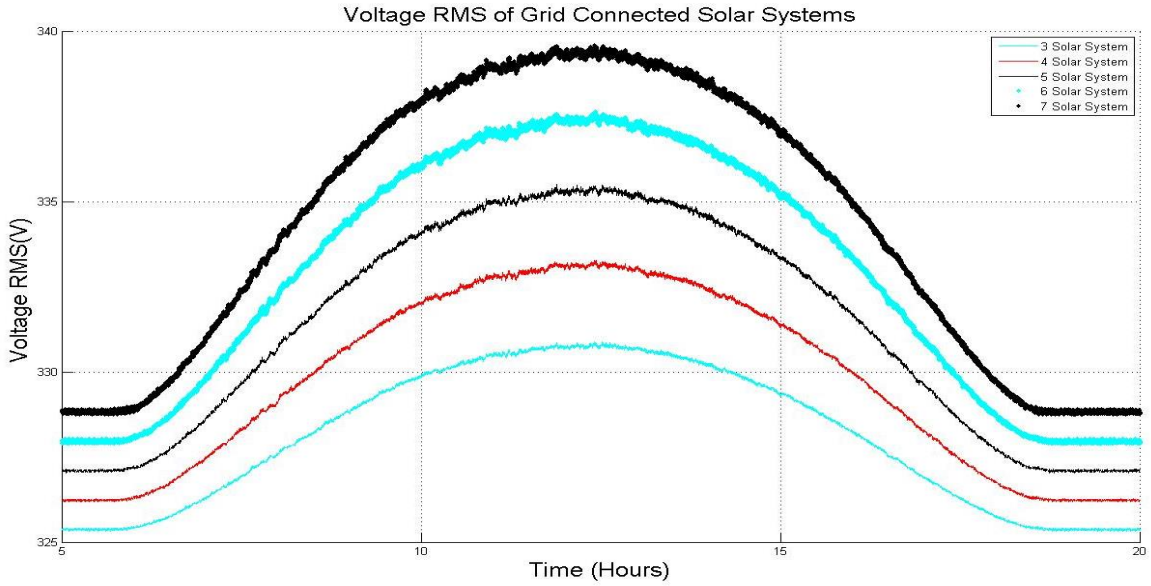


Figure 4-8 Relation between number of PV systems and voltage RMS

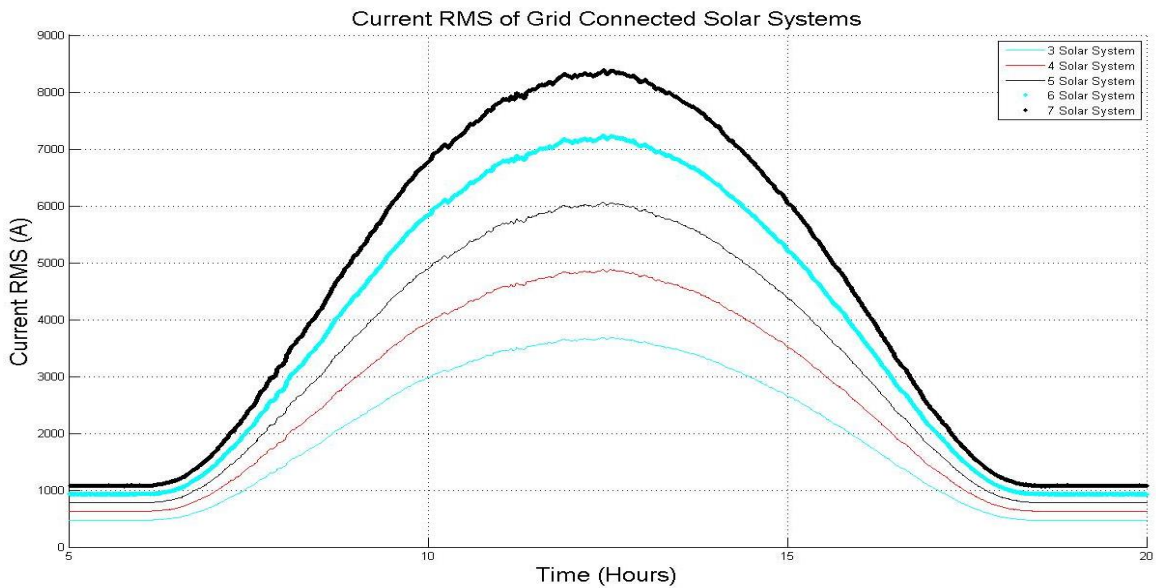


Figure 4-9 Relation between number of PV systems and current RMS

The relation of voltage THD with the different number of PV systems, from 5 AM to 8 PM, is shown in figure 4.10 while the relation of current THD with the different number of PV system, from 5 AM to 8 PM, is shown in figure 4.11.

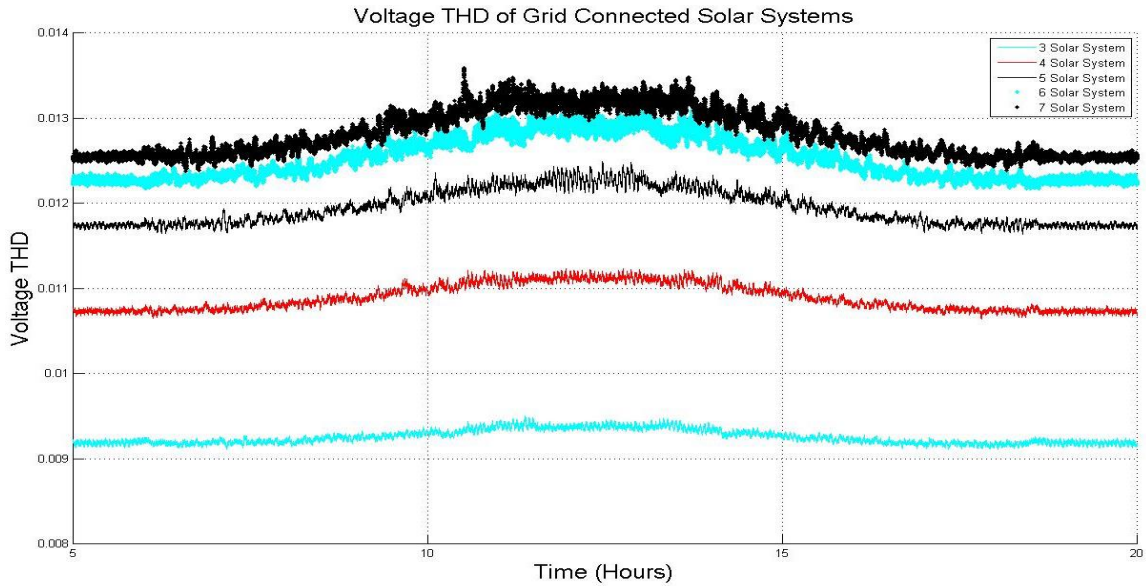


Figure 4-10 Relation between number of PV systems and voltage THD

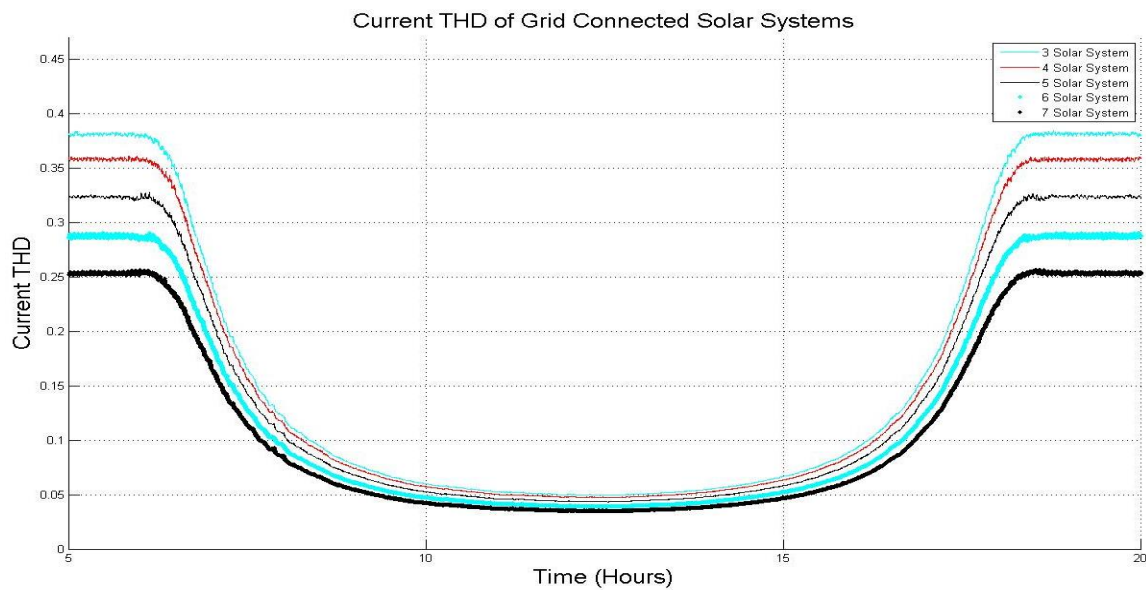


Figure 4-11 Relation between number of PV systems and current THD

These results show that as the number of grid connected PV system is increased the voltage THD is shifted to a higher level while current THD is shifted to a lower level e.g. current THD for 4 PV systems would be lower than current THD for 3 PV systems. It

means that current THD would be highest when only one PV system is connected to the grid. The relation between solar irradiance and current RMS is shown in figure 4.12 while the relation between solar irradiance and current THD is shown in figure 4.13.

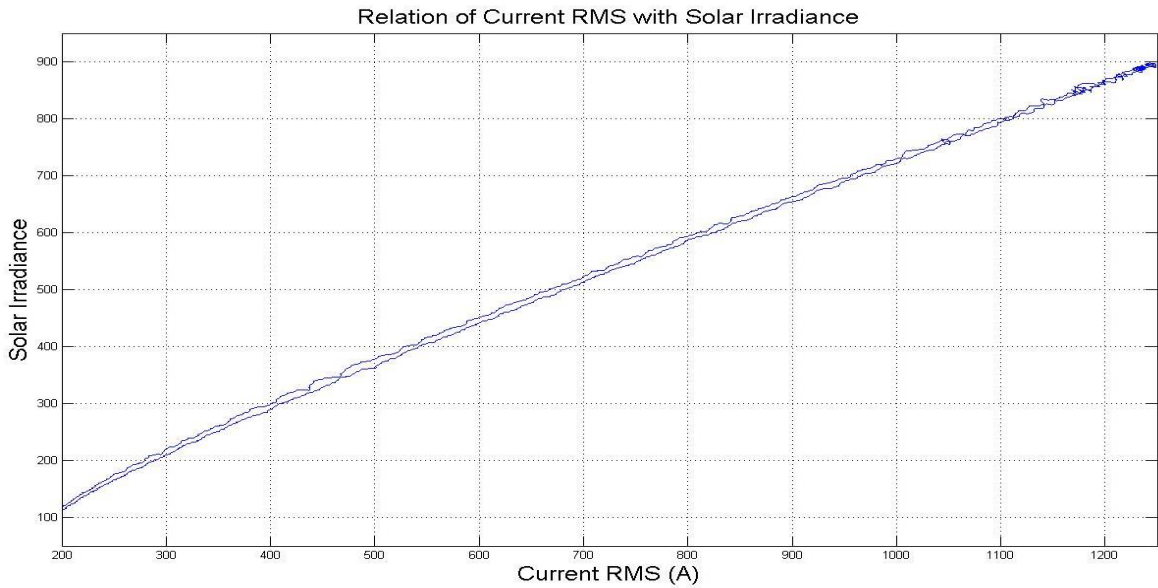


Figure 4-12 Relation between Current RMS and Solar Irradiance

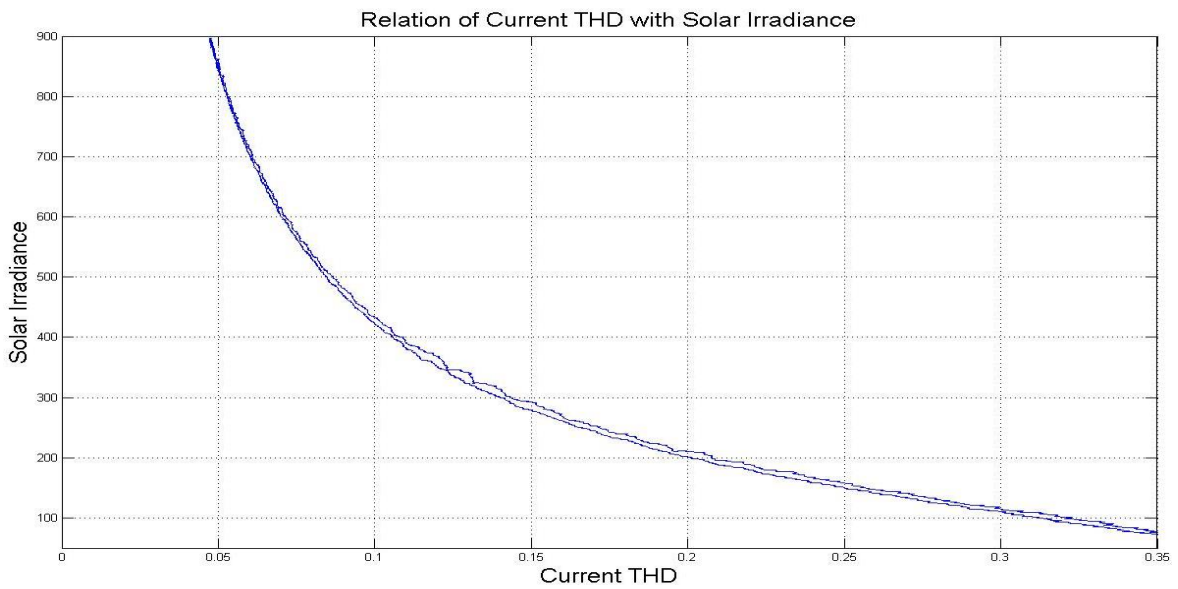


Figure 4-13 Relation between Current THD and Solar Irradiance

If solar irradiance is increased, current RMS increases but current THD decreases. Both current RMS and THD in a PV system are almost the same for both increasing irradiance and decreasing irradiance.

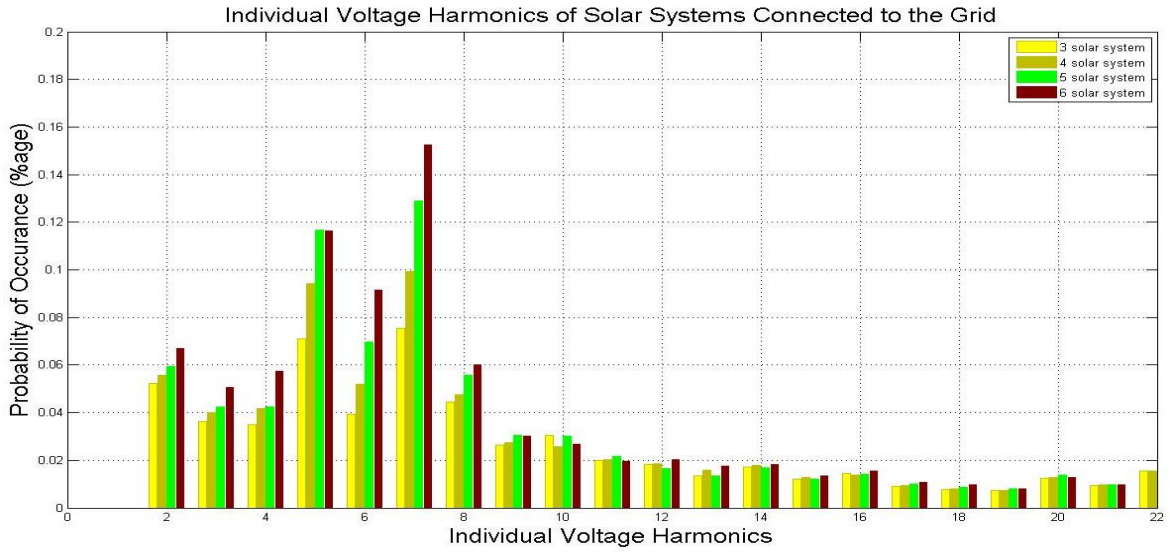


Figure 4-14 Individual voltage harmonics of grid connected solar systems

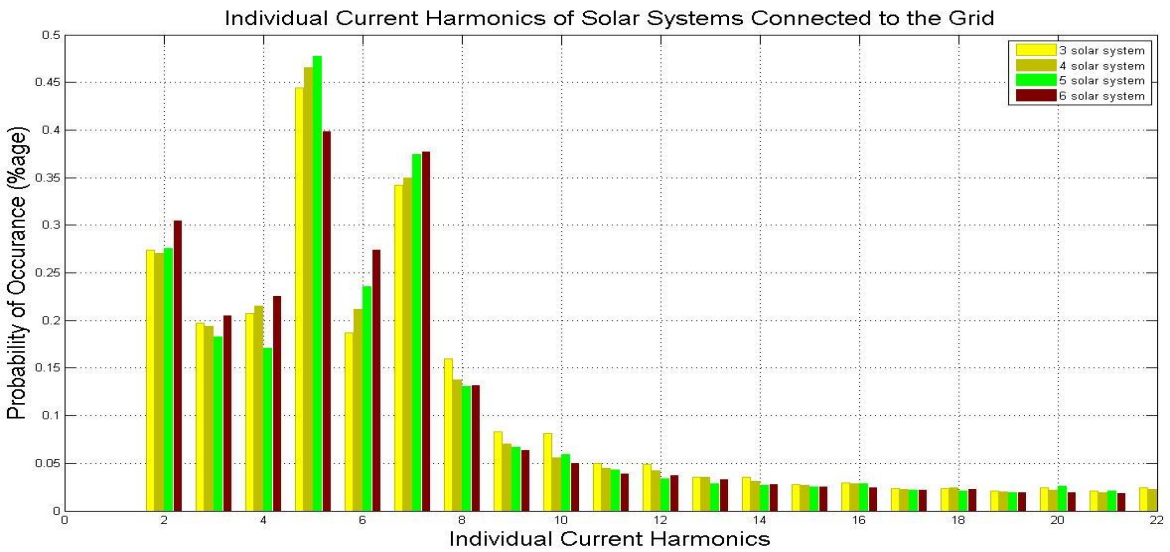


Figure 4-15 Individual current harmonics of grid connected solar systems

Individual voltage harmonics of different grid connected solar systems are shown in figure 4.14 and individual current harmonics of different grid connected solar systems are shown in figure 4.15. As the number of solar system increases, individual voltage harmonics also increases but individual current harmonic do not show any clear pattern.

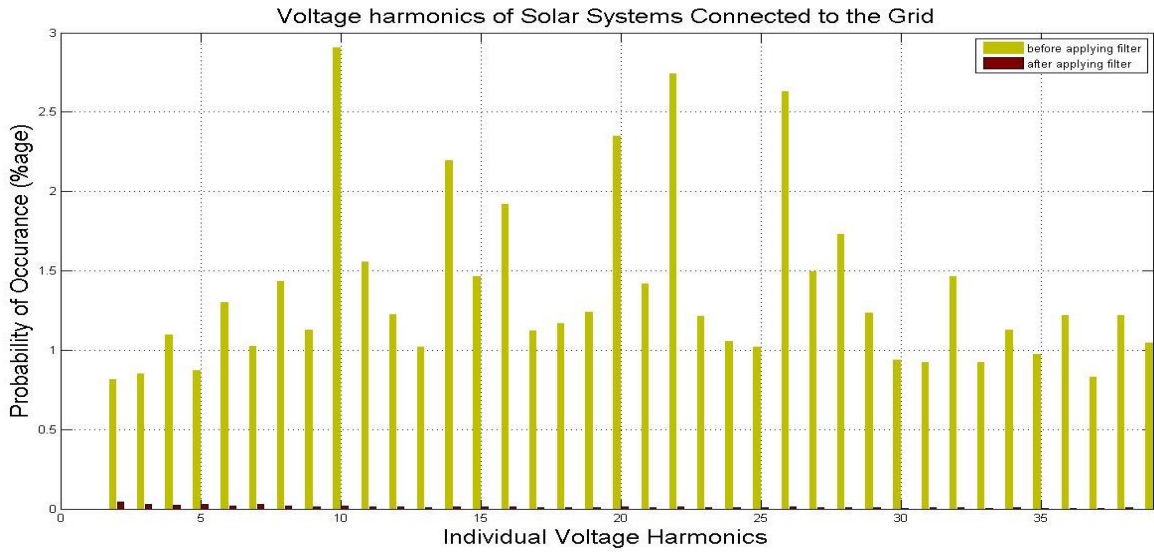


Figure 4-16 Individual voltage harmonics before and after the filter

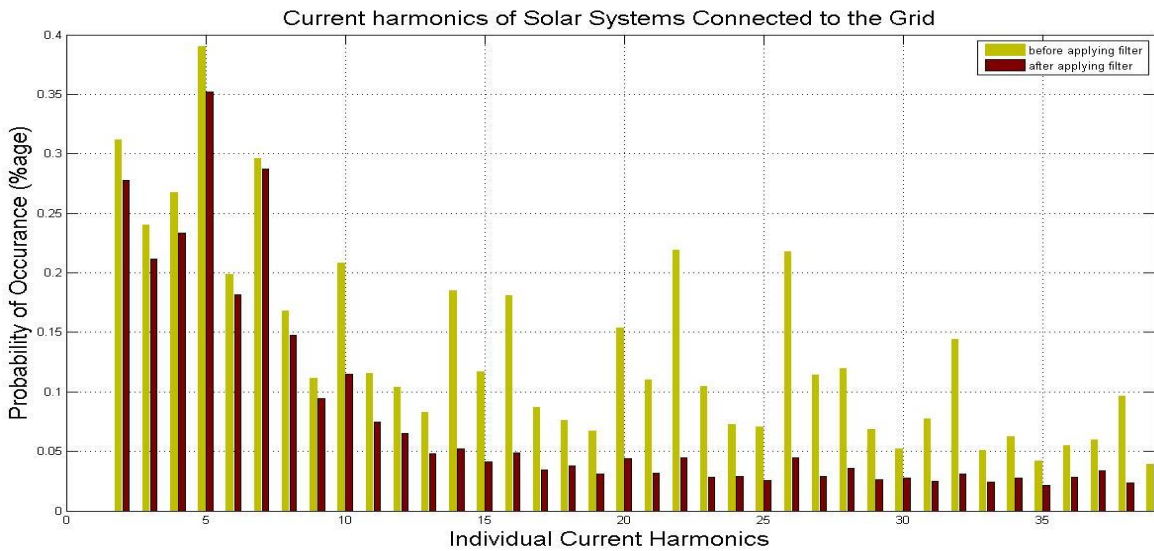


Figure 4-17 Individual current harmonics before and after the filter

According to figure 4.11, the worst case for the current harmonics is when only one PV system is connected to the grid. Individual voltage & current harmonics before and after the filter for one PV system are shown in figure 4.16 and 4.17. Harmonics are reduced considerably after applying the filter.

The control circuit and sensors are unable to measure and maintain the sinusoidal shape of the waveform at low power so high current distortions are observed. There are many factors which play vital roles in non-linearity of the inverter. Delays in tuning on or tuning off of the switches or in circuits of gate drive could be one of the reasons. Zero current clumping could be another reason. One reason of non-linearity could be parasitic capacitance effects. Some other reasons could be “voltage drop in switching devices” or “short pulse dropping” [97].

4.3 Correlation functions for PV system

It is clear from these simulations, that results verify some of the relation mentioned in [29] in case of grid connected PV system. Results of THD shows that solar irradiance plays the main role in distorting the current waveform and these results verify the results presented in [10]. But according to results presented in [10] voltage THD is not strongly correlated to fluctuations of solar irradiance and current harmonics are very sensitive and correlated to variation of solar irradiance. But these results clearly show that both voltage & current THD are strongly related to solar irradiance.

The above results, after putting into curve-fitting tool, show the following correlation function between current RMS/THD and solar irradiance for one PV system:

$$I_{rms_pv} = k_{i_rms_pv} S_{Ir} + I_{rms_pv0} \quad (4.1)$$

$$I_{thd_pv} = k_{i_thd_pv} S_{Ir}^{b_{i_thd_pv}} + I_{thd_pv0} \quad (4.2)$$

Where

S_{Ir} = Solar Irradiance (W/m^2)

I_{rms_pv} = RMS Current at grid side of inverter (A)

I_{rms_pv0} = RMS Current constant for given PV system (A)

$k_{i_rms_pv}$ = Scalar Multiple for RMS Current

I_{thd_pv} = THD Current at grid side of inverter

$I_{thd_pv0}, k_{i_thd_pv}, b_{i_thd_pv}$ = THD Current constants for given PV system

Similarly the relation of voltage RMS and THD with solar irradiance is given by:

$$V_{rms_pv} = k_{v_rms_pv} S_{Ir} + V_{rms_pv0} \quad (4.3)$$

$$V_{thd_pv} = k_{v_thd_pv} S_{Ir} + V_{thd_pv0} \quad (4.4)$$

Where

V_{rms_pv} = RMS Voltage at grid side of inverter (V)

V_{rms_pv0} = RMS Voltage constant for given PV system (V)

$k_{v_rms_pv}$ = Scalar Multiple for RMS Voltage

V_{thd_pv} = THD Voltage at grid side of inverter

V_{thd_pv0} = THD Voltage constant for given PV system

$k_{v_thd_pv}$ = Scalar Multiple for THD Voltage

Using these equations current RMS output and current THD are shown in figure 4.18 and figure 4.19.

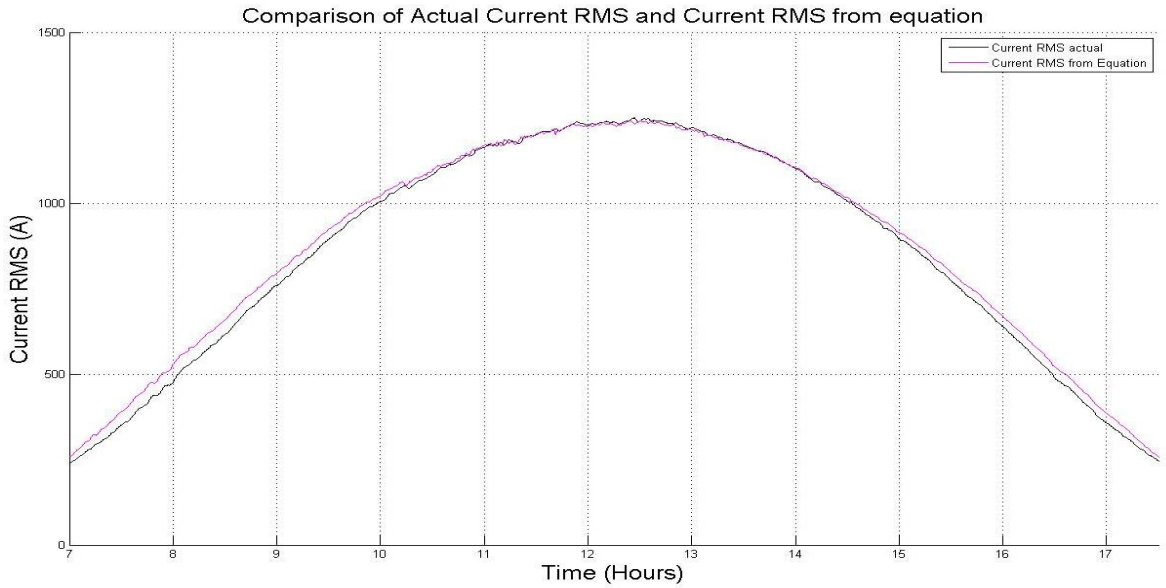


Figure 4-18 Simulated Current RMS and Current RMS from equation

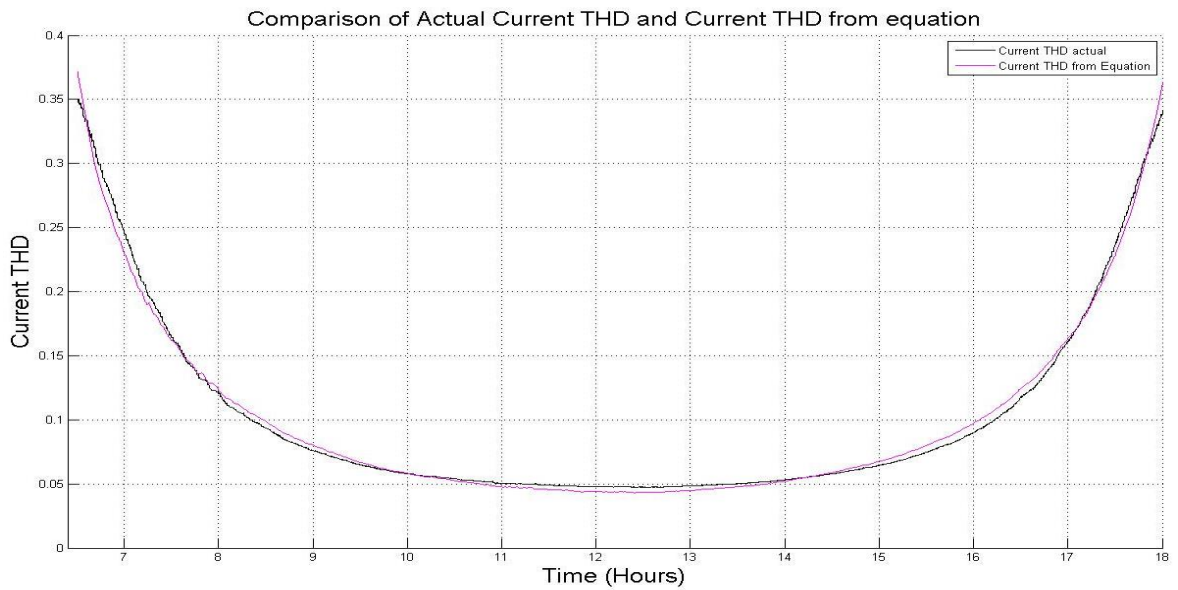


Figure 4-19 Simulated Current THD and Current THD from equation

Following values are used for different parameters

$$S_{Ir} > 100 \text{ (W/m}^2\text{)}$$

$$I_{rms_pv0} = 40.8358 \text{ (A)}$$

$$k_{i_rms_pv} = 1.3376$$

$$b_{i_thd_pv} = -0.4581$$

$$k_{i_thd_pv} = 3.523$$

$$I_{thd_pv0} = -0.1132$$

The voltage RMS and voltage THD would also show similar relations.

CHAPTER 5

SIMULATION RESULTS OF GRID CONNECTED WIND SYSTEMS

In this study it is assumed that wind systems are also located close to each other therefore wind systems are exposed to same wind speed behaving in the same manner in term of power quality. Wind systems will usually experience different wind speed based on their location. However in order to find correlation it is necessary that all wind systems should behave the same way so that a model should be developed. The assumption considered in this work are same as considered for PV systems and are given in the following.

1. Wind systems have no reactive support
2. All loads are linear
3. All wind systems are installed on the same feeder
4. Transient response is not considered
5. Utility substation is a strong bus

5.1 Design of Grid Connected Wind System

The block diagram of the grid connected wind system is shown in figure 5.1. Here also a step up transformer is used for grid integration. Voltage and current measurement blocks are located between wind system and the transformer.

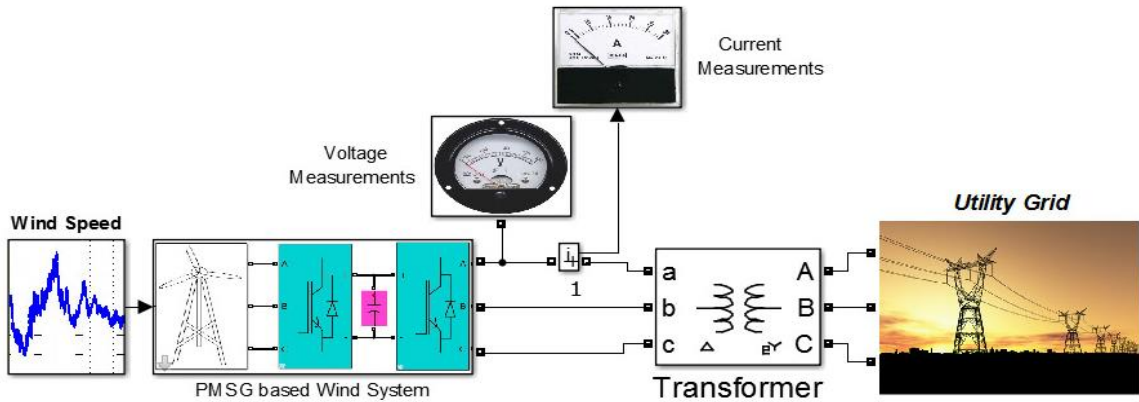


Figure 5-1 Grid Connected Wind System

Inside of PMSG based wind system block shown in figure 5.1 is described in more detail in figure 5.2. Here 1.5 MW PMSG based wind system is connected to the grid via back to back converters. Details of all individual blocks are given in chapter 3.

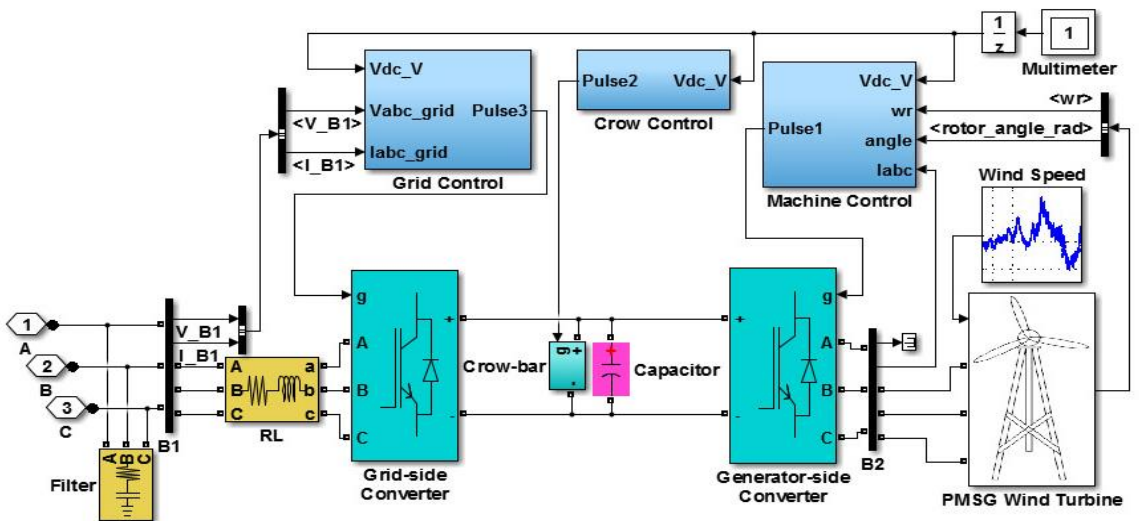


Figure 5-2 Wind System Simulink Block

Inside of utility grid block shown in figure 5.1 is described in more detail in figure 5.3.

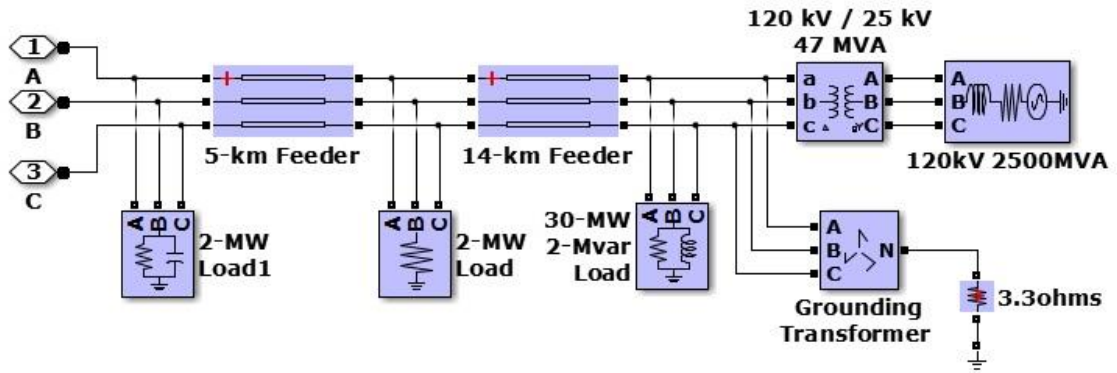


Figure 5-3 Utility Grid Simulink Block

Wind speed, taken at KFUPM Dhahran (26.18°35 N, 50.08°24 E) on 5th of Feb. 2011, is used as input for grid connected PMSG based wind system. Wind speed used in simulations is shown in figure 5.4.

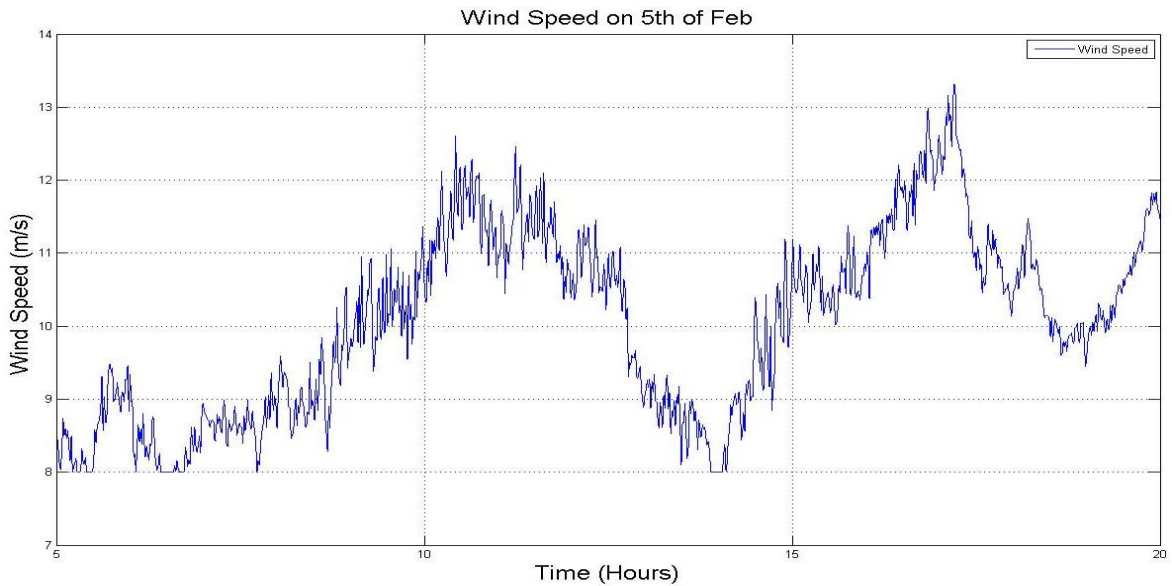


Figure 5-4 Wind Speed on 5th of Feb, 2011

5.2 Simulation Results of Grid Connected Wind Systems

In simulations grid connected wind system is used to verify the relation between wind system parameters and power quality indices. By designing voltage measurement block and current measurement block as shown in figure 5.1 following relation were found between current & voltage RMS of a grid connected wind system and wind speed as shown in figure 5.5. It is clear from the figure 5.5 that a direct relation exists between current & voltage RMS and wind speed.

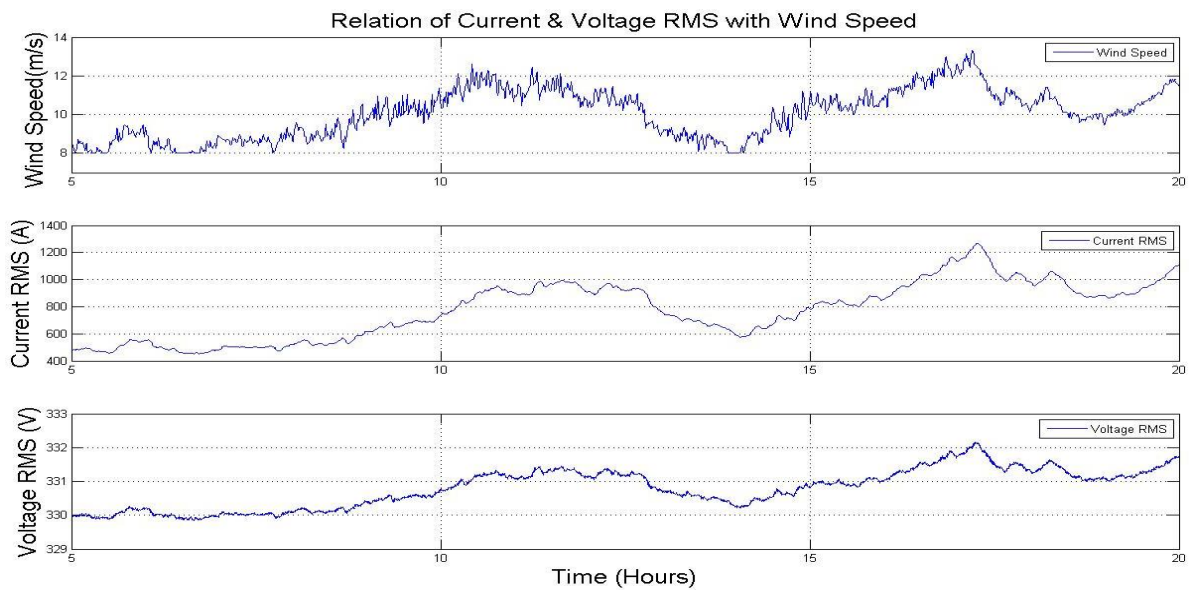


Figure 5-5 Relation between Wind Speed and current & voltage RMS

The relation between current & voltage THD and wind speed is shown in figure 5.6. First curve is the wind speed from 5 AM to 8 PM. Second curve shows current RMS from 5 AM to 8 PM at given wind speed. Third curve is the voltage RMS from 5 AM to 8 PM at given wind speed. A direct relation exists between voltage THD and wind speed while inverse relation exists between current THD and wind speed.

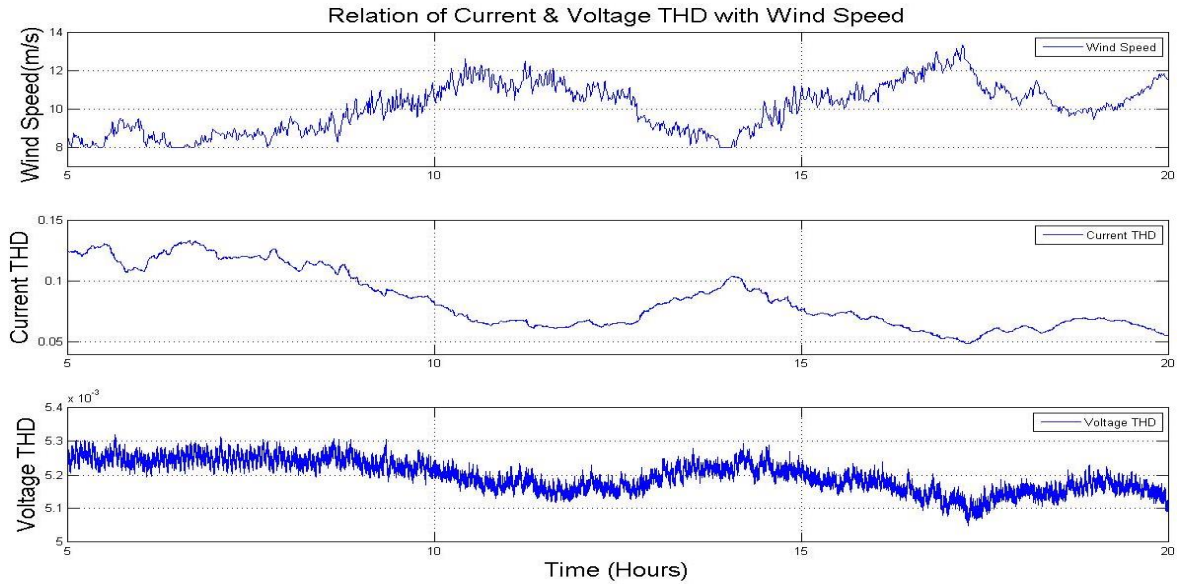


Figure 5-6 Relation between Wind Speed and current & voltage THD

The relation of voltage RMS with the number of wind systems, from 5 AM to 8 PM, is shown in figure 5.7 while the relation of current RMS with the number of wind systems, from 5 AM to 8 PM, is shown in figure 5.8. These results also clearly show that both the voltage & current RMS increase as the number of grid connected wind system is increased.

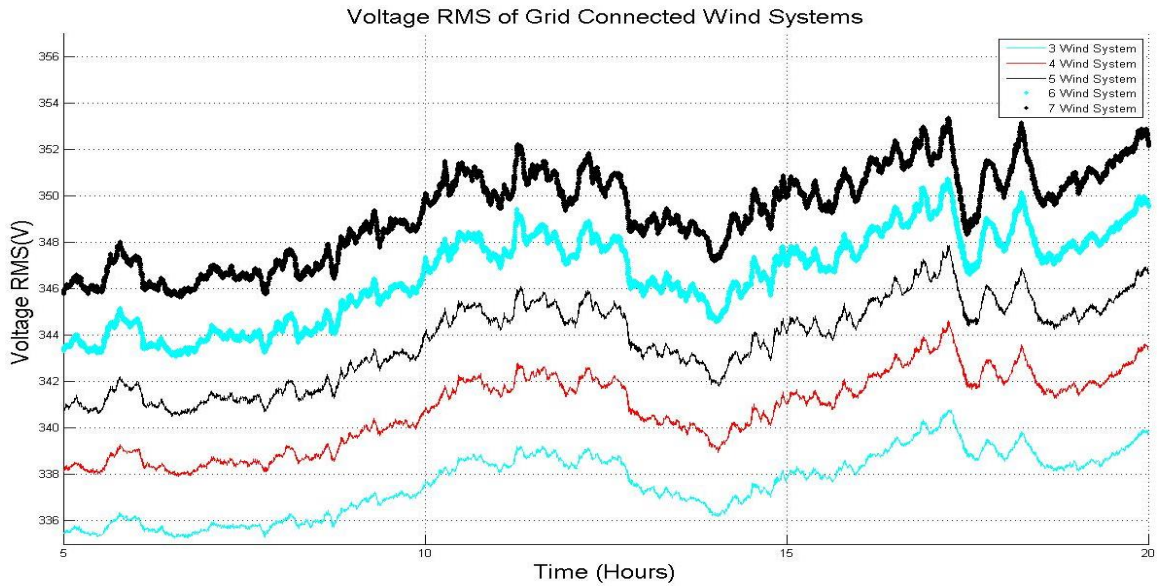


Figure 5-7 Relation between number of wind systems and voltage RMS

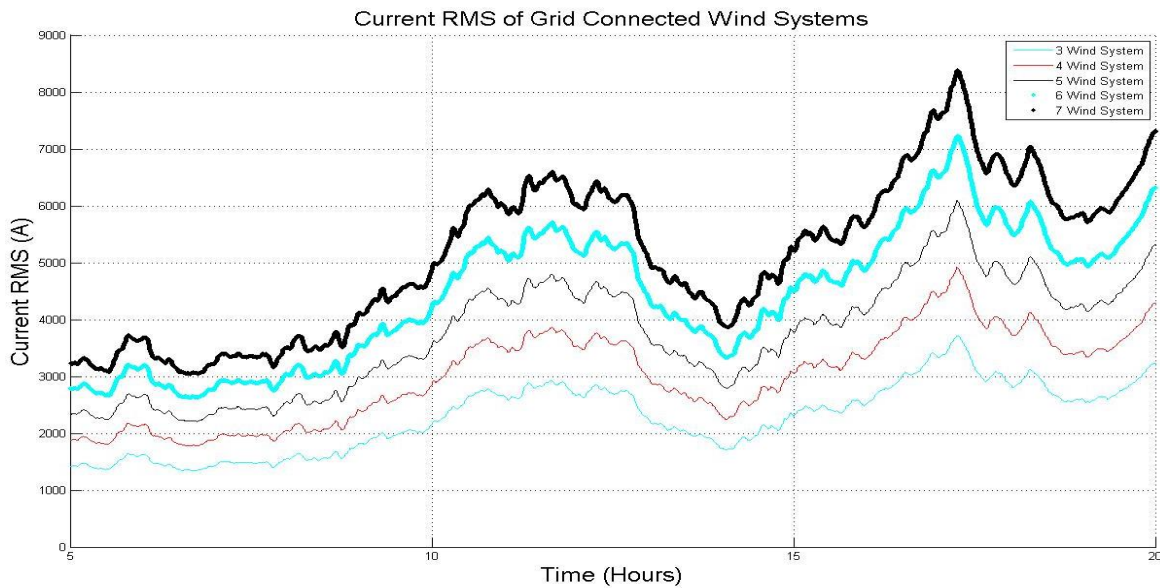


Figure 5-8 Relation between number of wind systems and current RMS

The relation between number of wind systems and voltage THD is shown in figure 5.9 while the relation between the number of wind system and current THD is shown in figure 5.10. These results show that voltage THD increases while current THD decreases

as the number of grid connected wind system is increased. Figure 5.10 shows that current THD curve would be at highest level when only one wind system is connected to the grid.

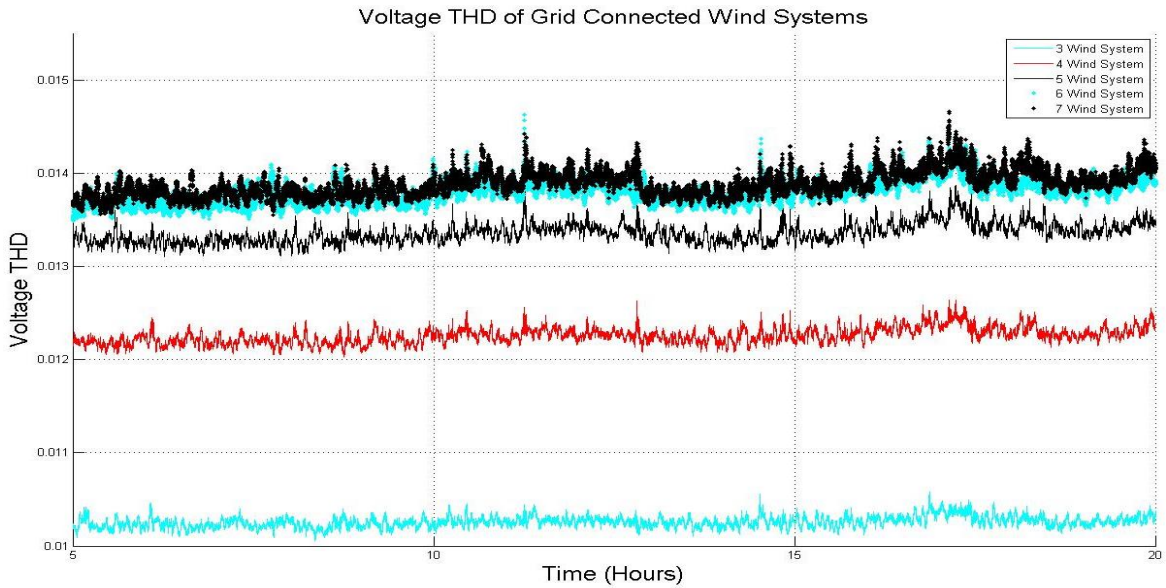


Figure 5-9 Relation between number of wind systems and voltage THD

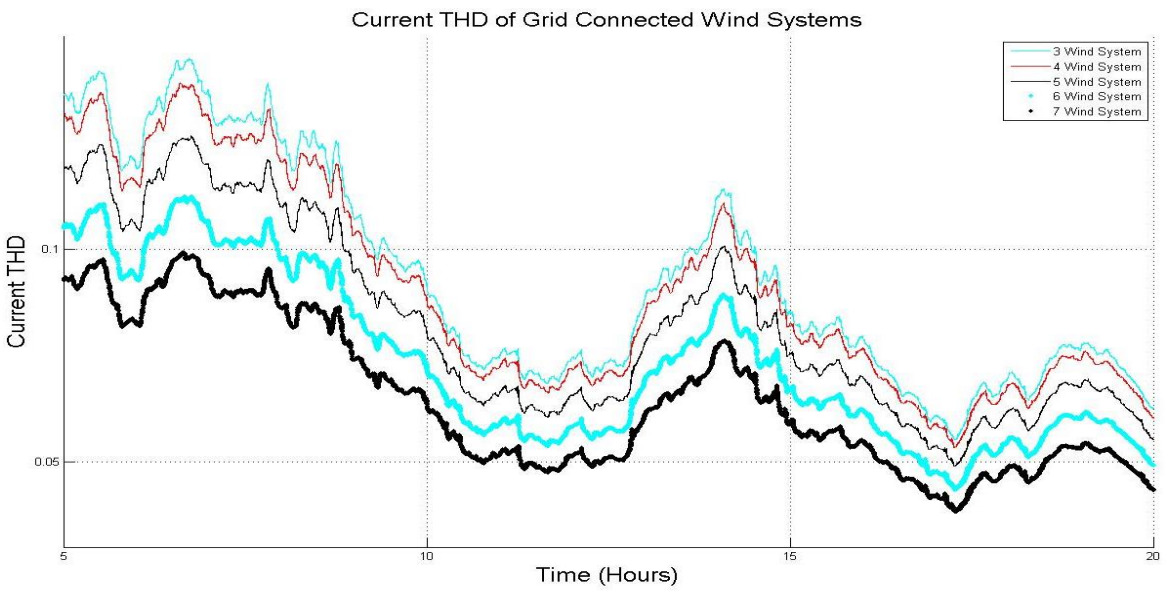


Figure 5-10 Relation between number of wind systems and current THD

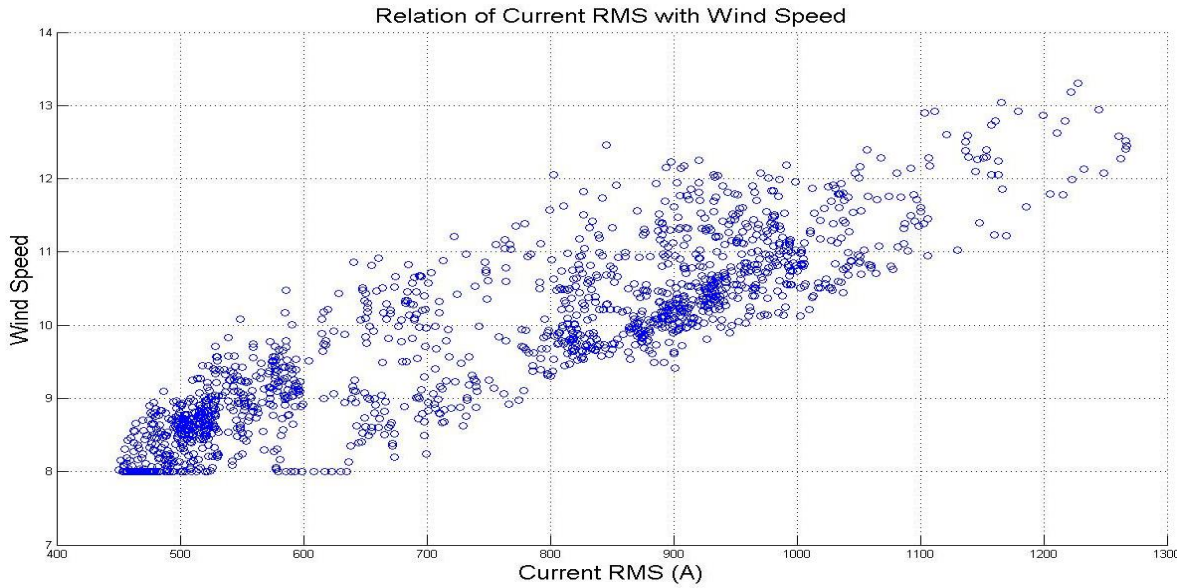


Figure 5-11 Relation between Current RMS and Wind Speed

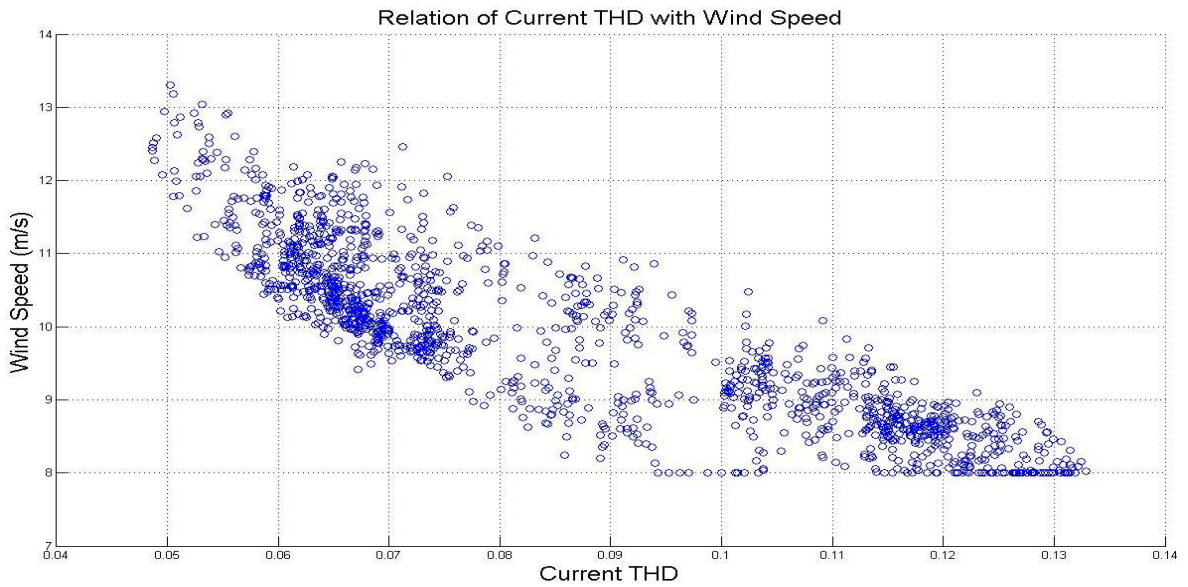


Figure 5-12 Relation between Current THD and Wind Speed

The relation of current RMS distribution with wind speed is shown in figure 5.11 while the relation of current THD distribution with wind speed is shown in figure 5.12. It

is clear that the trend of current RMS and THD in case of wind system is not exactly the same as was found in PV system. If wind speed changes, then change in voltage and current would not only depend on the previous value of voltage and current but also on the previous state of wind turbine. This is because of inertia of PMSG and delay in response time of wind turbine.

Individual voltage harmonics of different grid connected wind systems are shown in figure 5.13, while individual current harmonics of different grid connected wind systems are shown in figure 5.14. As the number of wind system increases, individual voltage harmonics also increase except 5th harmonic while individual current harmonic do not show any clear pattern.

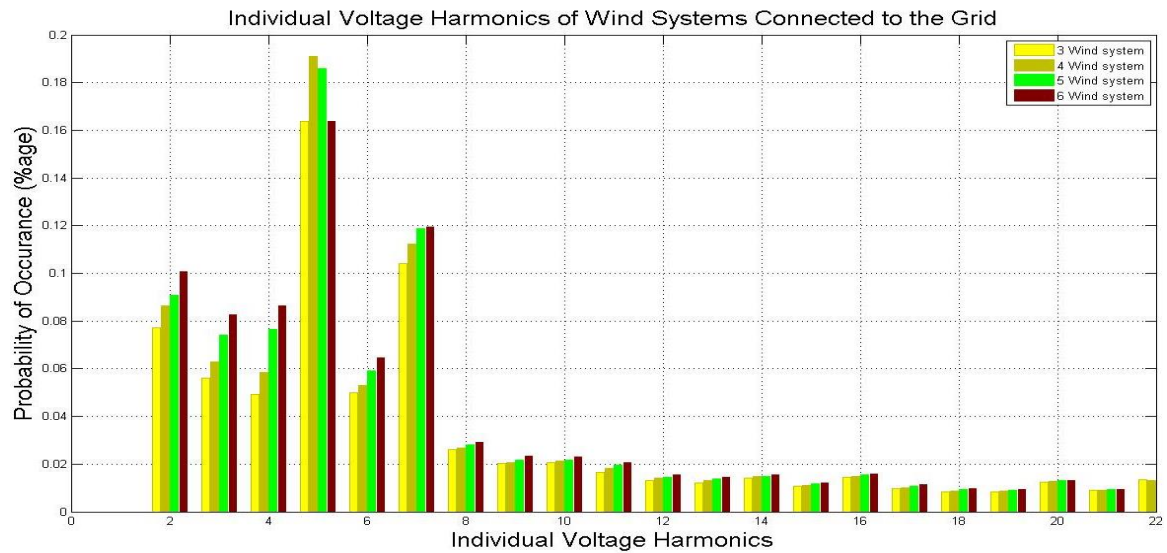


Figure 5-13 Individual voltage harmonics of grid connected wind systems

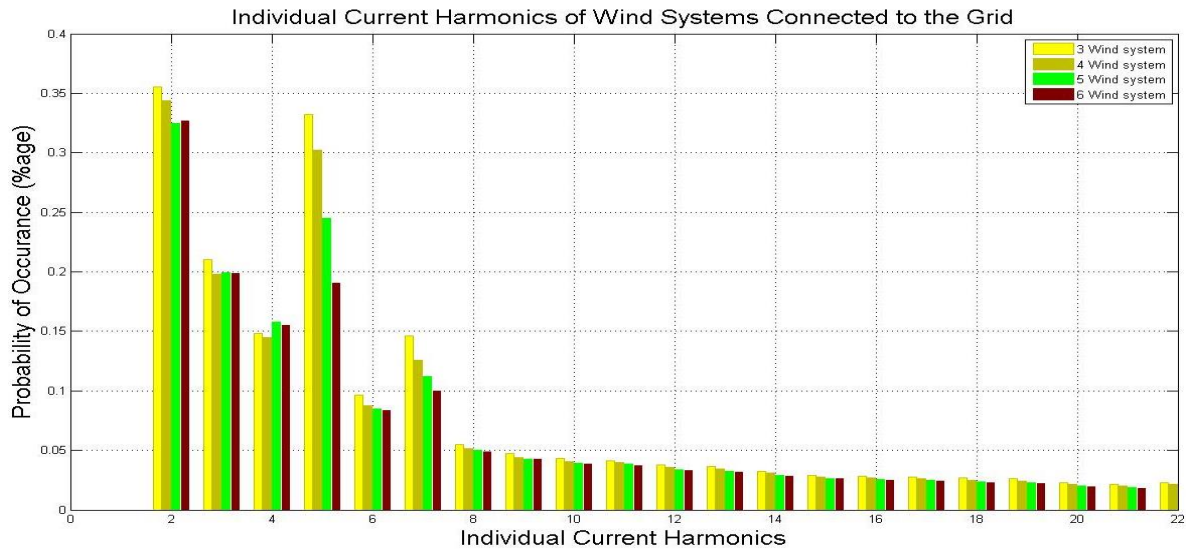


Figure 5-14 Individual current harmonics of grid connected wind systems

According to figure 5.10, the worst case for current harmonics is when only one wind system is connected to the grid. Now individual voltage & current harmonics before and after the filter for a wind system are shown in figure 5.14 and 5.15. Harmonics are reduced considerably after applying the filter.

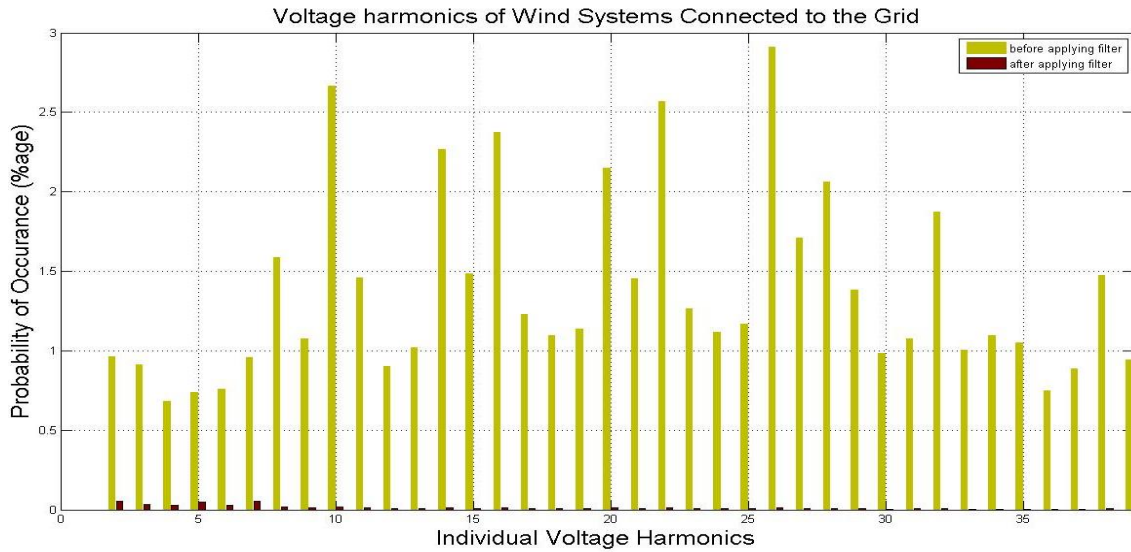


Figure 5-15 Individual voltage harmonics before and after the filter

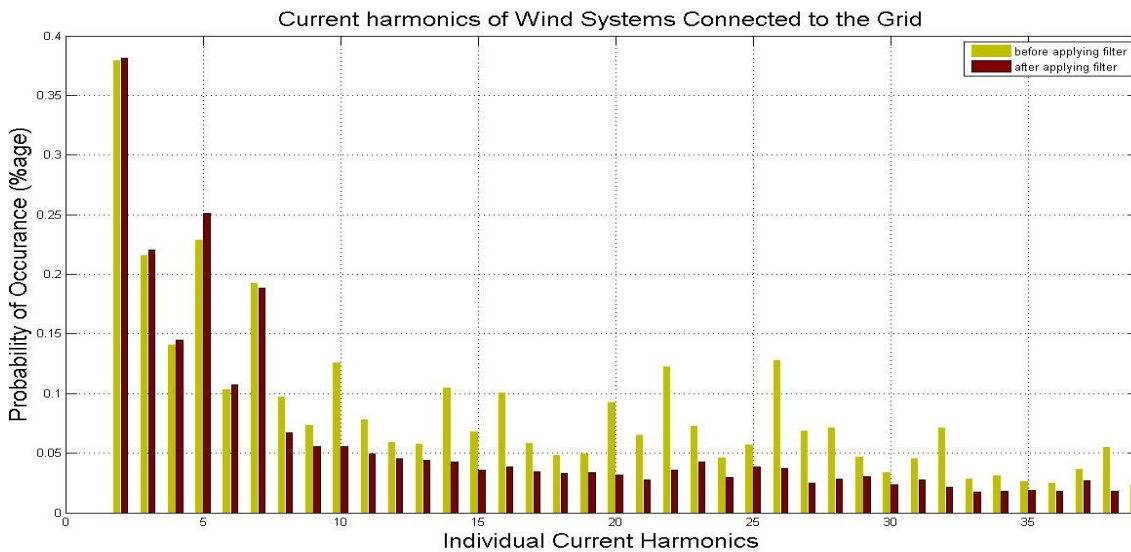


Figure 5-16 Individual current harmonics before and after the filter

5.3 Correlation functions for wind system

Results for wind systems show similar behavior as PV system but with an error value. Results of THD show that wind speed plays the main role in distorting the current waveform. These results clearly show that both voltage & current THD are strongly related to wind speed in case of grid connected wind system.

The results show that as the wind systems are increased the voltage RMS, Current RMS and voltage THD increase while current THD decreases.

Using curve-fitting tool in Matlab the following correlation function are obtained between current, voltage and wind speed for one wind system:

$$I_{rms_w} = k_{i_rms_w} W_{speed} + I_{rms_w0} + \mathcal{E}_{i_rms_w} \quad (5.1)$$

$$V_{rms_w} = k_{v_rms_w} W_{speed} + V_{rms_w0} + \mathcal{E}_{v_rms_w} \quad (5.2)$$

$$V_{thd_w} = k_{v_thd_w} W_{speed} + V_{thd_w0} + \mathcal{E}_{v_thd_w} \quad (5.3)$$

$$I_{thd_w} = k_{i_thd_w} W_{speed}^{b_{i_thd_w}} + I_{thd_w0} + \mathcal{E}_{i_thd_w} \quad (5.4)$$

Where

W_{speed} = Wind Speed (m/s)

I_{rms_w} = RMS Current at grid side of inverter (A)

I_{rms_w0} = RMS Current constant for given wind system (A)

$k_{i_rms_w}$ = Scalar Multiple for RMS Current

V_{rms_w} = RMS Voltage at grid side of inverter (V)

V_{rms_w0} = RMS Voltage constant for given wind system (V)

$k_{v_rms_w}$ = Scalar Multiple for RMS Voltage

V_{thd_w} = THD Voltage at grid side of inverter

V_{thd_w0} = THD Voltage constant for given wind system

$k_{v_thd_w}$ = Scalar Multiple for THD Voltage

I_{thd_w} = THD Current at grid side of inverter

$I_{thd_w0}, k_{i_thd_w}, b_{i_thd_w}$ = THD Current constants for given wind system

$\mathcal{E}_{i_rms_w}, \mathcal{E}_{v_rms_w}, \mathcal{E}_{v_thd_w}, \mathcal{E}_{i_thd_w}$ = Errors Values for wind system

Using equation 5.1 in curve-fitting tool in Matlab the relation between current RMS and wind speed is shown in figure 4.17.

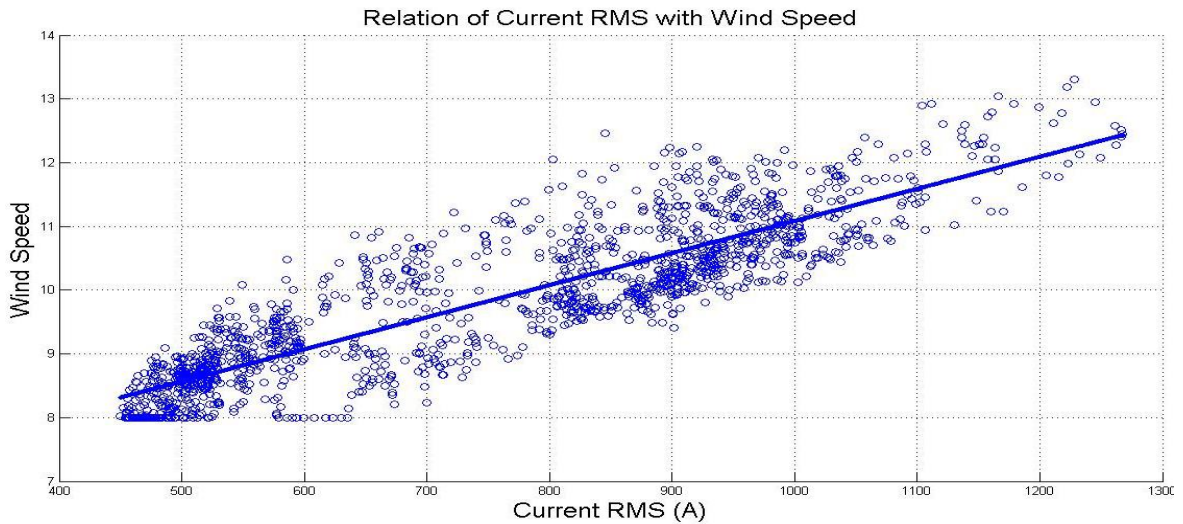


Figure 5-17 Applying Curve fitting Tool on Current RMS and Wind Speed

Following values are used for different parameters

$$8 \text{ m/s} < W_{speed} < 13.5 \text{ m/s}$$

$$I_{rms_w0} = 6.05 \text{ A}$$

$$k_{i_rms_w} = 0.005037$$

$$\mathcal{E}_{i_rms_w} = k_e W_{speed} + I_{e0}$$

Where $I_{e0} = \pm 0.021$ & $k_e = \pm 0.000027$

SIMULATION RESULTS OF GRID CONNECTED PV AND WIND SYSTEMS COMBINED

6.1 Design of PV and Wind System Combined

The block diagram of the grid connected PV and wind system combined is shown in figure 6.1. Here also a step up transformer is used for grid integration. Voltage and current measurement blocks are located between wind system and transformer.

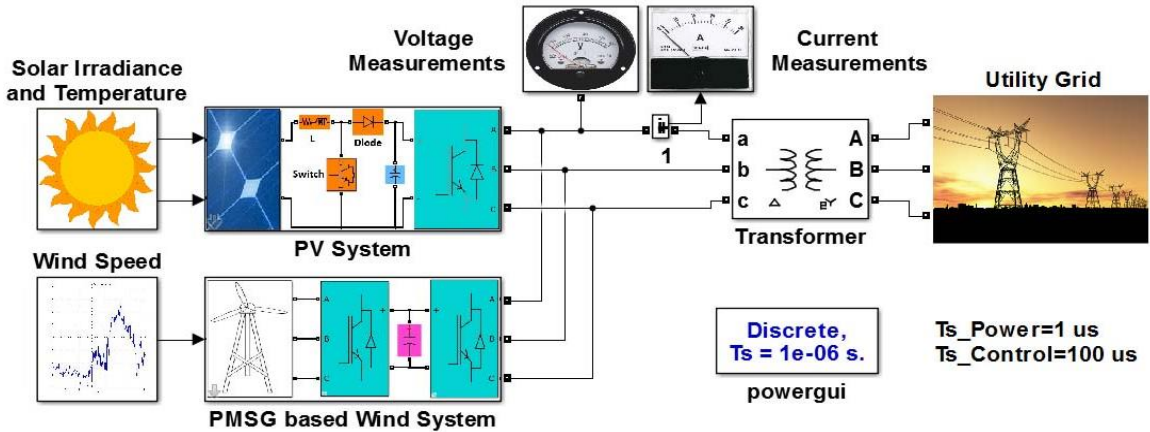


Figure 6-1 Grid Connected Renewable System

6.2 Simulation Results of PV and Wind System Combined

In simulations grid connected PV and wind systems are used to verify the relation between renewable resource parameters and power quality indices. The same irradiance, temperature and wind speed curves are used as before. The relations for voltage & current RMS from 5 AM to 8 PM are shown in figure 6.2 and 6.3. This shows that a

direct relation exists between voltage THD and number of renewable systems while inverse relation exists between current THD and number of renewable systems.

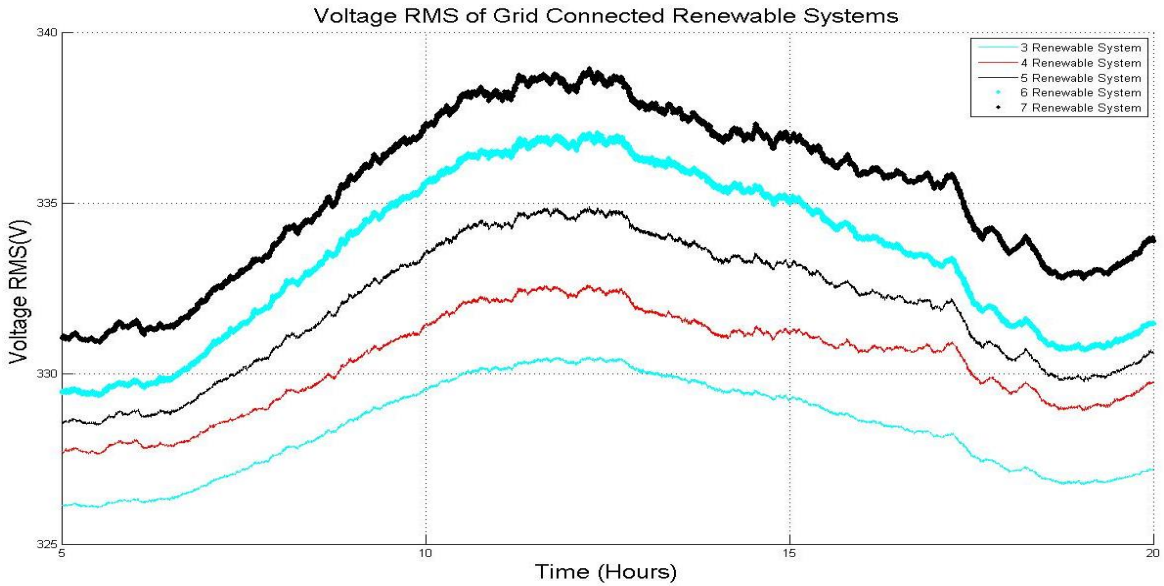


Figure 6-2 Relation between number of renewable systems and voltage RMS

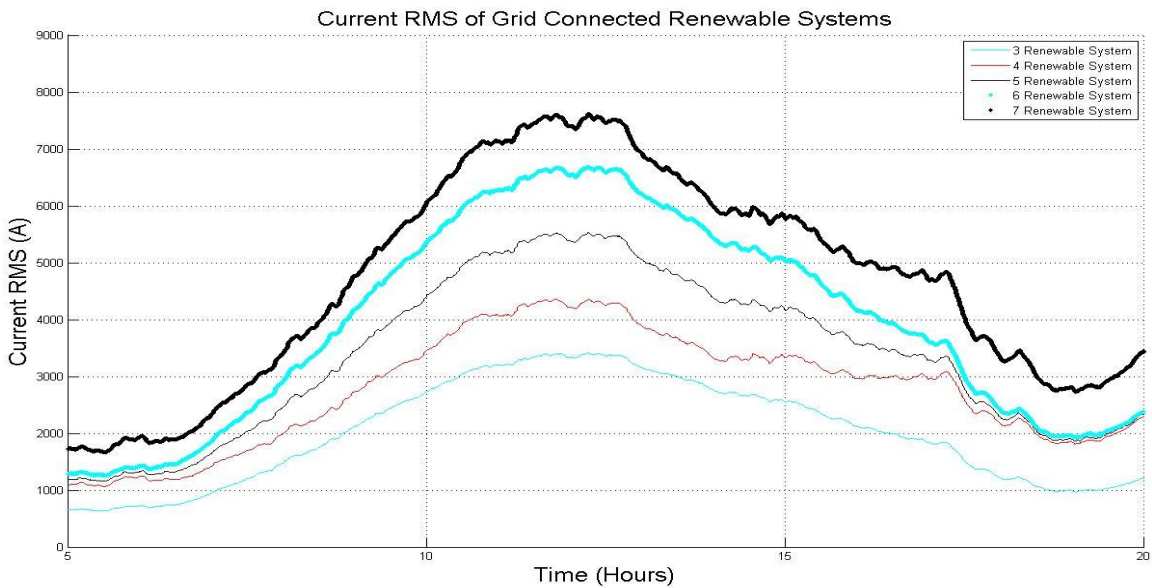


Figure 6-3 Relation between number of renewable systems and current RMS

The relation between number of renewable systems and voltage THD is shown in figure 5.9 while the relation between the number of renewable system and current THD is shown in figure 5.10.

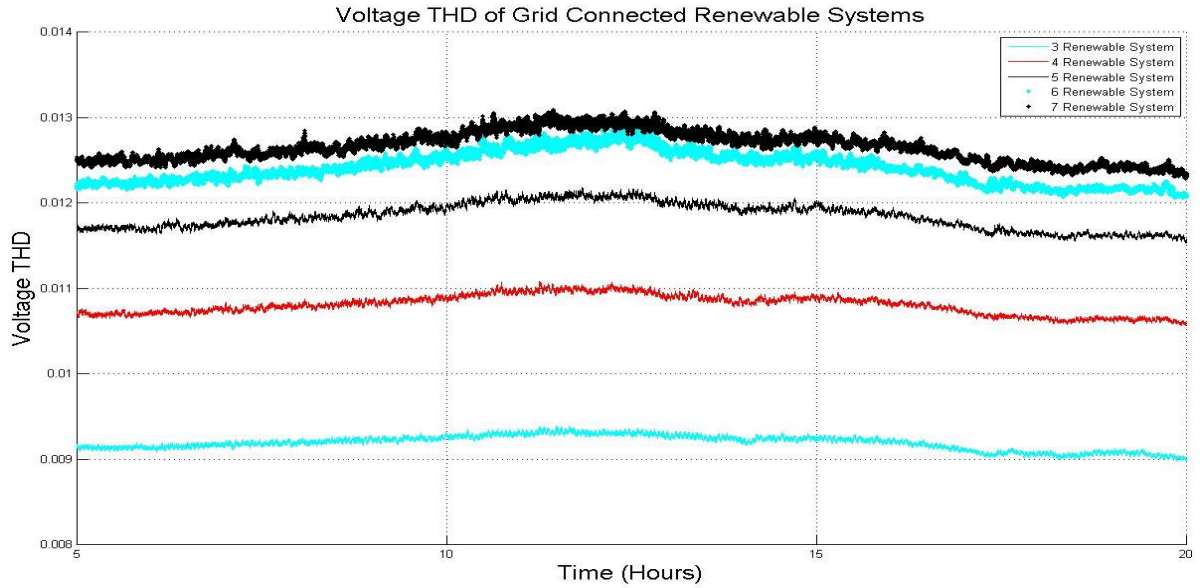


Figure 6-4 Relation between number of renewable systems and voltage THD

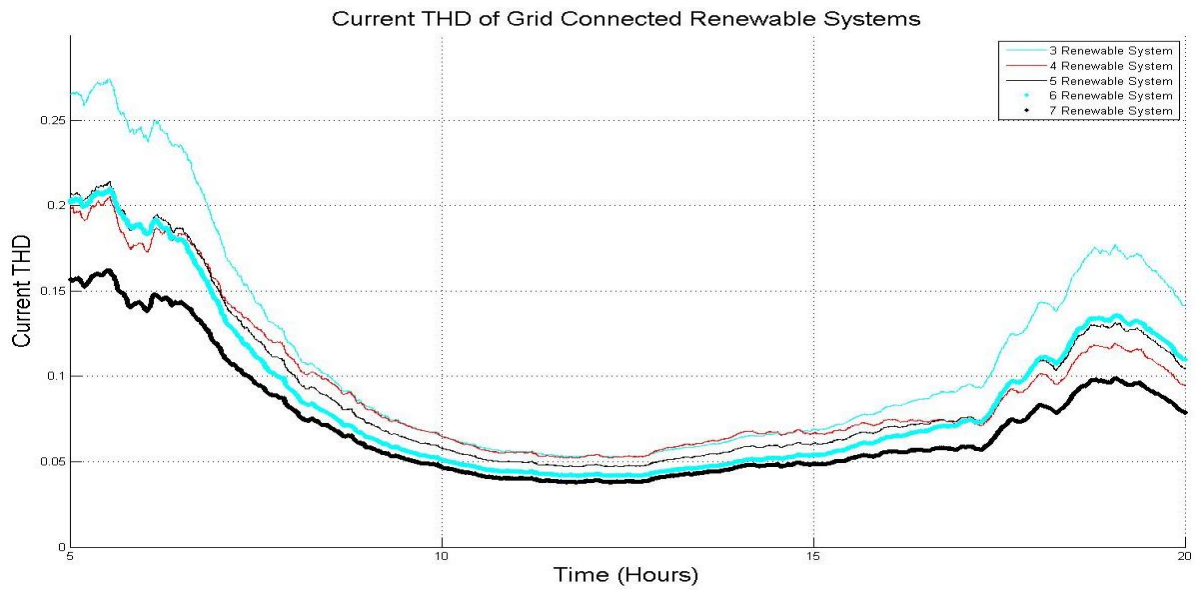


Figure 6-5 Relation between number of renewable systems and current THD

These results show that voltage THD increase while current THD decrease as the number of grid connected renewable system is increased. It means that current THD curve would be at highest level when only one renewable system is connected to the grid.

Similarly all other result would have the same behaviors as was found in previous chapters. The above results, after putting into curve-fitting tool, show the following correlation function between RES parameters and power quality indices.

$$I_{rms_res} = k_{i_rms_pv} S_{Ir} + I_{rms_pv0} + k_{i_rms_w} W_{speed} + I_{rms_w0} + \mathcal{E}_{i_rms_w} \quad (6.1)$$

$$I_{thd_res} = k_{i_thd_pv} S_{Ir}^{b_{i_thd_pv}} + I_{thd_pv0} + k_{v_rms_w} W_{speed} + V_{rms_w0} + \mathcal{E}_{v_rms_w} \quad (6.2)$$

$$V_{rms_res} = k_{v_rms_pv} S_{Ir} + V_{rms_pv0} + k_{v_thd_w} W_{speed} + V_{thd_w0} + \mathcal{E}_{v_thd_w} \quad (6.3)$$

$$V_{thd_res} = k_{v_thd_pv} S_{Ir} + V_{thd_pv0} + k_{i_thd_w} W_{speed}^{b_{i_thd_w}} + I_{thd_w0} + \mathcal{E}_{i_thd_w} \quad (6.4)$$

Where

I_{rms_res} = RMS Current at grid side of inverter (A)

I_{thd_res} = THD Current at grid side of inverter

V_{rms_res} = RMS Voltage at grid side of inverter (V)

V_{thd_res} = THD Voltage at grid side of inverter

This phenomenon of increasing voltage RMS, as the number of RES increases, can also be used to improve the voltage profile but voltage THD would be degraded. The buses which are far away from distribution transformer and are located at the end of radial network have less immunity as compared to those located close to the distribution transformer. Violation of power quality standards are a serious thread for distribution network and limit the unconditional installation of RES. Installing RES on grid is inevitable but if proper planning is not done or proactive actions are not taken, then problem of power quality will become worse. Simulation methods should be used for

evaluating the power quality indices of grid connected renewable systems. Forecasted data of solar irradiance, temperature and wind speed could be used for evaluating the power quality indices for future planning. Active power filter should be used for eliminating the harmonics to improve the power quality.

CHAPTER 7

CONCLUSION AND FUTURE WORK

7.1 Conclusion

In this study a comprehensive design of grid connected PV and wind systems are presented along with active power filters. Simulations results of grid connected PV system, and grid connected wind system show that active power filter play an important role in minimizing the harmonics at the PCC. The results show that there is strong relation between solar irradiance and power quality indices of a grid connected PV system. The results also show that there is strong relation between wind speed and power quality indices of a grid connected wind system. The results also show that there is strong relation between number of renewable systems and power quality indices of a grid connected renewable systems. The results also show that the behavior of grid connected wind system is not exactly the same as of grid connected PV system because of the inertia of wind turbine. Thus there is an error factor involve in relations of wind speed with power quality indices.

In simulations the power quality indices of grid connected renewable system are measured using different combinations of renewable systems. The relations of power quality indices especially harmonic distortion using solar irradiance or wind speed and number of grid connected systems were find using different combinations of renewable systems. The results show a strong relation of harmonic distortion with number of renewable system and solar irradiance or wind speed. Measurement from different combinations of grid connected solar and wind systems are taken and then

recommendations are given at the end. The objective of trying different combinations was to find the extreme case where the power quality standards might be violated.

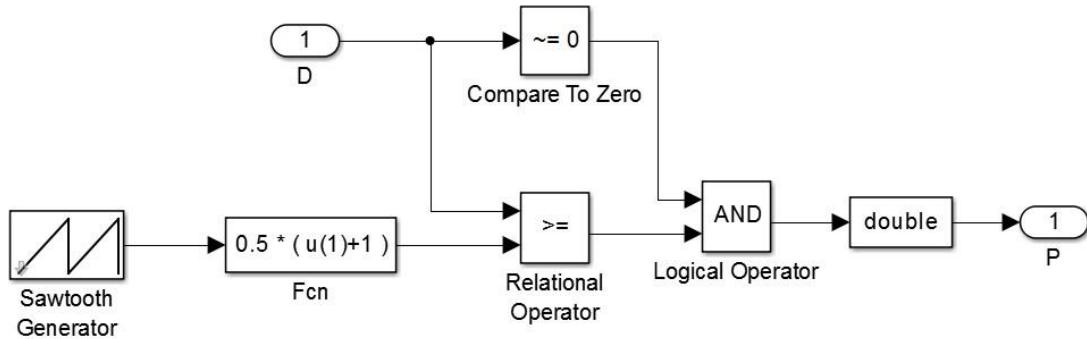
7.2 Future Work

Throughout the thesis, only solar PV and wind energy system have been used. These energy sources have intermittent nature e.g. solar PV is available only at day time. Power quality can be studied after installing Non-RES in DG to make it more reliable and more independent from grid power. Power quality can be studied after installing finite energy storage device such as superconducting magnetic energy storage devices, supercapacitors, batteries etc. This will improve the power quality and will make the system more reliable.

APPENDIX A

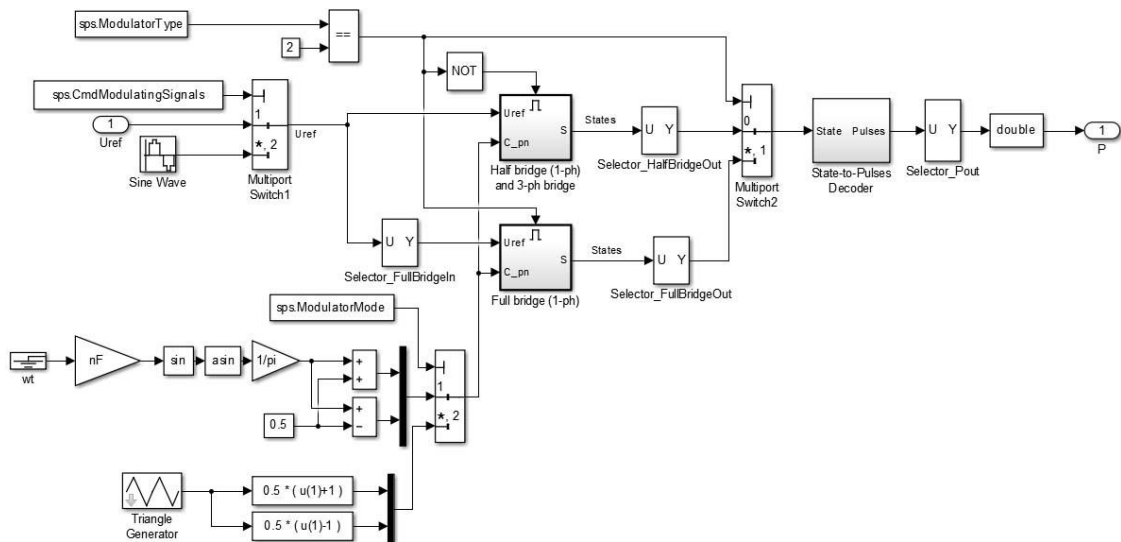
PWM generator block

This block is present inside the MPPT block and output of this block is the output of MPPT block which is used to control the switch of DC-DC converter.



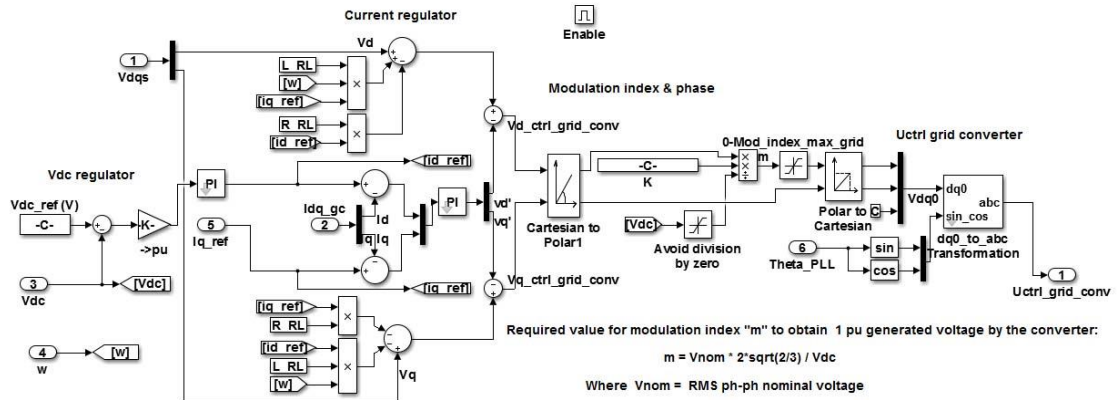
PWM (3 phase)

This block is present inside the inverter control block. Output of this block is the output of inverter control block which is used to control the inverter.



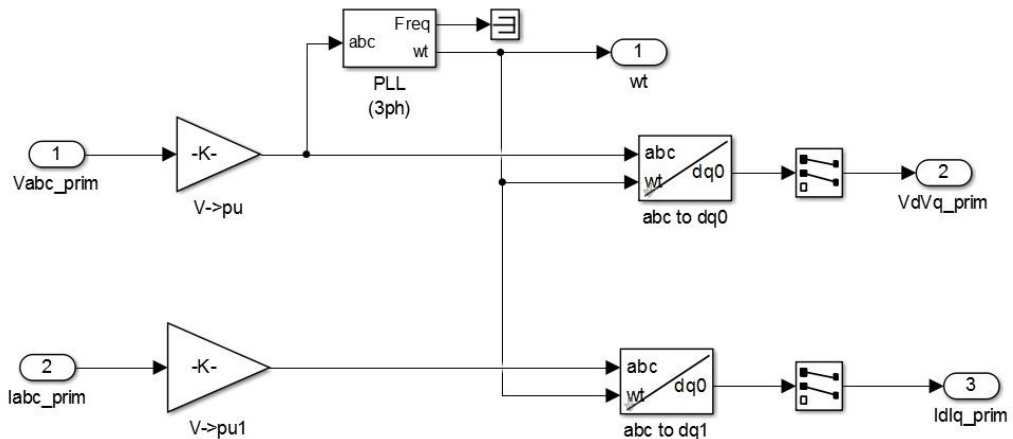
Grid side inverter control

This block is present inside inverter control block. This block comes after “measurement and transformation” and before “3-phase PWM generator” block as shown in figure 3.12



PLL and Measurements

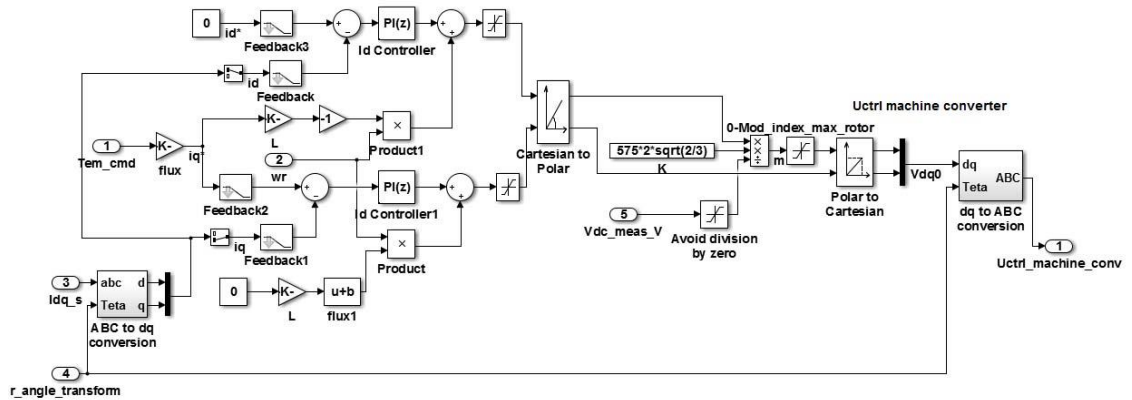
This block is present inside the “measurement and transformation” block. This block comes after “filter” block and before “abc to dq0” block as shown in figure 3.13



APPENDIX B

Rotor side converters control

This block is present inside inverter control block. This block is after “measurement and transformation “block and before “3-phase PMW generator” block as shown in figure 3.21



Grid side converters control

The grid side converters control is same as grid side inverter control given in appendix A.

REFERENCES

- [1] B. Stuart, "Saudi Arabia targets 41 GW of solar by 2032," *pv-magazine*.
- [2] A. News, "Saudi Arabia aims to be world's largest renewable energy market," *www.arabnews.com*.
- [3] R. Hudson, "PV Inverters with VAR Control, LVRT, and Dynamic Control," *High Penetration Photovoltaic Workshop, Denver, CO, 2010*.
- [4] E. Demirok and D. Sera, "Clustered PV inverters in LV networks: An overview of impacts and comparison of voltage control strategies," *Electrical Power & ,* pp. 1–6, 2009.
- [5] G. Peek, C. Hanley, and J. Boyes, "Solar Energy Grid Integration Systems–Energy Storage (SEGIS-ES)," *Dan Ton, US Department of Energy*, no. July, 2008.
- [6] S.-I. Inage, "Prospects for Large-Scale Energy Storage in Decarbonized Power Grids," 2009.
- [7] T. Ehara, "Overcoming PV grid issues in urban areas," *International Energy Agency, Photovoltaic Power* , 2009.
- [8] H. Asano, K. Yajima, and Y. Kaya, "Influence of photovoltaic power generation on required capacity for load frequency control," *Energy Conversion, IEEE* , vol. 11, no. 1, pp. 1–6, 1996.
- [9] C. Whitaker, J. Newmiller, M. Ropp, and B. Norris, "Renewable Systems Interconnection Study: Distributed Photovoltaic Systems Design and Technology Requirements," 2008.
- [10] M. Patsalides, A. Stavrou, V. Efthymiou, and G. E. Georghiou, "Towards the establishment of maximum PV generation limits due to power quality constraints," *International Journal of Electrical Power & Energy Systems*, vol. 42, no. 1, pp. 285–298, Nov. 2012.
- [11] Roger C. Dugan, M. F. McGranaghan, S. Santoso, and H. W. Beaty, *Electrical power systems quality*, Second. New York: McGraw-Hill, 2002.
- [12] R. Erickson and D. Maksimovic, *Fundamentals of power electronics*. Springer Science & Business Media Inc., 1997.

- [13] K. Fekete, Z. Klaic, and L. Majdandzic, "Expansion of the residential photovoltaic systems and its harmonic impact on the distribution grid," *Renewable Energy*, vol. 43, pp. 140–148, Jul. 2012.
- [14] D. Infield and P. Onions, "Power quality from multiple grid-connected single-phase inverters," *Power Delivery, IEEE*, vol. 19, no. 4, pp. 1983–1989, 2004.
- [15] A. Latheef, V. Gosbell, and V. Smith, "Harmonic Impact of Residential Type Photovoltaic Inverters on 11kV Distribution System," *Australian Universities*, 2006.
- [16] Y. Miyamoto and H. Sugihara, "Demonstrative research on clustered PV systems," *Photovoltaic Specialists Conference*, 2009.
- [17] V. Hengsritawat, T. Tayjasanant, and N. Nimpitiwan, "Optimal sizing of photovoltaic distributed generators in a distribution system with consideration of solar radiation and harmonic distortion," *International Journal of Electrical Power & Energy Systems*, vol. 39, no. 1, pp. 36–47, Jul. 2012.
- [18] S. Bhattacharyya, J. M. a. Myrzik, and W. L. Kling, "Consequences of poor power quality - an overview," *42nd International Universities Power Engineering Conference*, no. 1, pp. 651–656, Sep. 2007.
- [19] R. Targosz and J. Manson, "Pan-European power quality survey," *9th International Conference on Electrical Power Quality and Utilisation*, pp. 1–6, Oct. 2007.
- [20] M. Patsalides, "Assessing the level of harmonic distortion due to PV generation in mini grids," *hybrid and mini-grid*, 2008.
- [21] E. Standard, "50160: Voltage Characteristics of Electricity Supplied by Public Distribution Systems," *European Standard, CLC, BTTF*, no. March, 1994.
- [22] IEC Standards, "IEC 61000-4-30: Testing and Measurement Techniques - Power Quality Measurement Methods," 2003.
- [23] IEC Standards, "IEC 61727: Photovoltaic systems - Characteristics of the utility interface," 2004.
- [24] I. Standards, "IEC 61400-21: Measurement and Assessment of Power Quality Characteristics of Grid Connected Wind Turbines," *LEC Std*, vol. 2001, 2008.
- [25] A. Baghini, "Handbook of power quality," Wiley, pp. 525–526.

- [26] A. Broshi, "Monitoring power quality beyond EN 50160 and IEC 61000-4-30," *Electrical Power Quality and Utilisation, EPQU*, no. July, pp. 16–20, 2007.
- [27] B. Franken, V. Ajodhia, and K. Petrov, "Creating a regulatory framework for voltage quality," *electrical power quality*, 2007.
- [28] ERGEG, "European regulators' group for electricity and gas (ERGEG): Towards Voltage Quality Regulation In Europe: An ERGEG Public Consultation Paper," 2006.
- [29] M. Aiello, a. Cataliotti, S. Favuzza, and G. Graditi, "Theoretical and Experimental Comparison of Total Harmonic Distortion Factors for the Evaluation of Harmonic and Interharmonic Pollution of Grid-Connected Photovoltaic Systems," *IEEE Transactions on Power Delivery*, vol. 21, no. 3, pp. 1390–1397, Jul. 2006.
- [30] S. Ong and Y. Cheng, "An overview of international harmonics standards and guidelines (IEEE, IEC, EN, ER and STC) for low voltage system," , *IPEC International*, vol. 1, pp. 602–607, 2007.
- [31] J. Wong, P. Baroutis, R. Chadha, R. Iravani, M. Graovac, and X. Wang, "A methodology for evaluation of permissible depth of penetration of distributed generation in urban distribution systems," *IEEE Power and Energy Society General Meeting - Conversion and Delivery of Electrical Energy in the 21st Century*, pp. 1–8, Jul. 2008.
- [32] A. Canova and L. Giaccone, "Electrical impact of photovoltaic plant in distributed network," , *IEEE Transactions on*, vol. 45, no. 1, pp. 341–347, 2009.
- [33] J. C. Hernández, a. Medina, and F. Jurado, "Impact comparison of PV system integration into rural and urban feeders," *Energy Conversion and Management*, vol. 49, no. 6, pp. 1747–1765, Jun. 2008.
- [34] F. Blaabjerg, K. Ma, and D. Zhou, "Power electronics and reliability in renewable energy systems," *IEEE International Symposium on Industrial Electronics*, pp. 19–30, May 2012.
- [35] M. H. Moradi and M. Abedinie, "A combination of Genetic Algorithm and Particle Swarm Optimization for optimal DG location and sizing in distribution systems," *2010 Conference Proceedings IPEC*, pp. 858–862, Oct. 2010.
- [36] S. Ghosh, S. P. Ghoshal, and S. Ghosh, "Optimal sizing and placement of distributed generation in a network system," *International Journal of Electrical Power & Energy Systems*, vol. 32, no. 8, pp. 849–856, Oct. 2010.

- [37] R. K. Singh and S. K. Goswami, "Optimum allocation of distributed generations based on nodal pricing for profit, loss reduction, and voltage improvement including voltage rise issue," *International Journal of Electrical Power & Energy Systems*, vol. 32, no. 6, pp. 637–644, Jul. 2010.
- [38] M. Oshiro, K. Tanaka, T. Senjyu, S. Toma, A. Yona, A. Y. Saber, T. Funabashi, and C.-H. Kim, "Optimal voltage control in distribution systems using PV generators," *International Journal of Electrical Power & Energy Systems*, vol. 33, no. 3, pp. 485–492, Mar. 2011.
- [39] J. Thongpron, "Study of a PV–Grid Connected System on its Output Harmonics and Voltage Variation," *Asian J. Energy*, vol. 5, pp. 59–73, 2004.
- [40] A. Woyte and V. Van Thong, "Voltage fluctuations on distribution level introduced by photovoltaic systems," *IEEE Transactions on*, vol. 21, no. 1, pp. 202–209, 2006.
- [41] P. Chen, Z. Chen, B. Bak-Jensen, R. Villafafila, and S. Sorensen, "Study of power fluctuation from dispersed generations and loads and its impact on a distribution network through a probabilistic approach," *9th International Conference on Electrical Power Quality and Utilisation*, pp. 1–5, Oct. 2007.
- [42] F. Viawan, "Probabilistic approach to the design of photovoltaic distributed generation in low voltage feeder," *Probabilistic Methods*, 2006.
- [43] M. Benhabib, "Harmonic effects caused by large scale PV installations in LV network," *Electrical Power Quality*, 2007.
- [44] E. Vasanasong and E. Spooner, "The effect of net harmonic currents produced by numbers of the Sydney Olympic Village's PV systems on the power quality of local electrical network," *Power System Technology*, vol. 00, pp. 1001–1006, 2000.
- [45] W. Yan, M. Braun, and J. Von Appen, "Operation strategies in distribution systems with high level PV Penetration," *Solar world*, pp. 2–6, 2011.
- [46] P. Kirawanich and R. M. O'Connell, "Potential harmonic impact of a residential utility-interactive photovoltaic system," *Ninth International Conference on Harmonics and Quality of Power. Proceedings (Cat. No.00EX441)*, vol. 3, pp. 983–987.
- [47] M. Bollen and C. Schwaegerl, "Distributed energy resources and waveform distortion," *power [kW]*, no. 0369, pp. 21–24, 2007.

- [48] D. Parmar and L. Yao, "Impact of unbalanced penetration of single phase grid connected photovoltaic generators on distribution network," *Universities' Power Engineering Conference*, p. 201, 2011.
- [49] S. Cobben, B. Gaidon, and H. Laukamp, "Impact of Photovoltaic Generation on Power Quality in Urban areas with High PV Population: Results from Monitoring Campaigns," 2008.
- [50] M. Patsalides and D. Evagorou, "The effect of solar irradiance on the power quality behaviour of grid connected photovoltaic systems," *and Power Quality*, 2007.
- [51] M.-C. Alvarez-Herault, R. Caire, B. Raison, N. HadjSaid, and W. Bienia, "Optimizing traditional urban network architectures to increase distributed generation connection," *International Journal of Electrical Power & Energy Systems*, vol. 35, no. 1, pp. 148–157, Feb. 2012.
- [52] R. P. S. Leão, G. C. Barroso, R. F. Sampaio, J. B. Almada, C. F. P. Lima, M. C. O. Rego, and F. L. M. Antunes, "The future of low voltage networks: Moving from passive to active," *International Journal of Electrical Power & Energy Systems*, vol. 33, no. 8, pp. 1506–1512, Oct. 2011.
- [53] J. Enslin, "Harmonic interaction between large numbers of photovoltaic inverters and the distribution network," *, IEEE Bologna*, pp. 3–8, 2003.
- [54] S. Kjaer, "A review of single-phase grid-connected inverters for photovoltaic modules," *Industry Applications, IEEE*, vol. 41, no. 5, pp. 1292–1306, 2005.
- [55] B. Li, X. Tian, and H. Zeng, "A grid-connection control scheme of PV system with fluctuant reactive load," *Electric Utility Deregulation and*, pp. 786–790, 2011.
- [56] Z. Xiangyang and L. Shiyang, "A Research of Harmonics for Multiple PV Inverters in Grid-Connected," *Power and Energy Engineering*, 2012.
- [57] S. Kouro and M. Malinowski, "Recent advances and industrial applications of multilevel converters," *Industrial Electronics*, vol. 57, no. 8, pp. 2553–2580, 2010.
- [58] K. K. Gupta and S. Jain, "A multilevel Voltage Source Inverter (VSI) to maximize the number of levels in output waveform," *International Journal of Electrical Power & Energy Systems*, vol. 44, no. 1, pp. 25–36, Jan. 2013.
- [59] J. Rodriguez, J. Lai, and F. Peng, "Multilevel inverters: a survey of topologies, controls, and applications," *Industrial Electronics, IEEE*, vol. 49, no. 4, pp. 724–738, 2002.

- [60] R. Portillo and M. Prats, "Modeling strategy for back-to-back three-level converters applied to high-power wind turbines," *Industrial Electronics*, vol. 53, no. 5, pp. 1483–1491, 2006.
- [61] R. Melício, V. M. F. Mendes, and J. P. S. Catalão, "Harmonic assessment of variable-speed wind turbines considering a converter control malfunction," *IET Renewable Power Generation*, vol. 4, no. 2, p. 139, 2010.
- [62] A. Nabae, I. Takahashi, and H. Akagi, "A new neutral-point-clamped PWM inverter," *Industry Applications, IEEE*, vol. I, no. 5, 1981.
- [63] E. Babaei, S. H. Hosseini, G. B. Gharehpetian, M. T. Haque, and M. Sabahi, "Reduction of dc voltage sources and switches in asymmetrical multilevel converters using a novel topology," *Electric Power Systems Research*, vol. 77, no. 8, pp. 1073–1085, Jun. 2007.
- [64] S. Badkubi, D. Nazarpour, J. Khazaie, and M. Khalilian, "Reducing the current harmonics of a wind farm generation based on VSC-HVDC transmission line by shunt active power filters," *Energy Procedia*, vol. 14, p. 1, Jan. 2012.
- [65] F. Smits, "History of silicon solar cells," *Electron Devices, IEEE Transactions on*, no. 7, pp. 640–643, 1976.
- [66] H. Tsai, C. Tu, and Y. Su, "Development of generalized photovoltaic model using MATLAB/SIMULINK," *Proceedings of the world congress on*, pp. 0–5, 2008.
- [67] J. J. Wysocki and P. Rappaport, "Effect of Temperature on Photovoltaic Solar Energy Conversion," *Journal of Applied Physics*, vol. 31, no. 3, p. 571, 1960.
- [68] J. Suganya and M. Carolin Mabel, "Maximum power point tracker for a photovoltaic system," *International Conference on Computing, Electronics and Electrical Technologies (ICCEET)*, no. 3, pp. 463–465, Mar. 2012.
- [69] W. Knaupp, "Evaluation of PV module designs at irregular operation conditions," *Photovoltaic Specialists Conference*, pp. 1213–1216, 1997.
- [70] X. Ruan, "Isolated Buck-Boost DC/DC converter for PV grid-connected system," *2010 IEEE International Symposium on Industrial Electronics*, pp. 889–894, Jul. 2010.
- [71] D. P. Hohm and M. E. Ropp, "Comparative study of maximum power point tracking algorithms," *Progress in Photovoltaics: Research and Applications*, vol. 11, no. 1, pp. 47–62, Jan. 2003.

- [72] Z. Xuesong, S. Daichun, M. Youjie, and C. Deshu, "The simulation and design for MPPT of PV system Based on Incremental Conductance Method," *WASE International Conference on Information Engineering*, no. 50877053, pp. 314–317, Aug. 2010.
- [73] B. Gu and K. Nam, "A DC-link capacitor minimization method through direct capacitor current control," *IEEE Transactions on Industry Applications*, vol. 42, no. 2, pp. 573–581, Mar. 2006.
- [74] N. Mahamad, C. M. Hadzer, and S. Masri, "Application of LC filter in harmonics reduction," *PECon Proceedings. National Power and Energy Conference*, pp. 268–271, 2004.
- [75] B. Wu, Y. Lang, N. Zargari, and S. Kouro, *Power conversion and control of wind energy systems*, p. 59365, August, 2011.
- [76] Y. Ditkovich, a. Kuperman, a. Yahalom, and M. Byalsky, "A Generalized Approach to Estimating Capacity Factor of Fixed Speed Wind Turbines," *IEEE Transactions on Sustainable Energy*, vol. 3, no. 3, pp. 607–608, Jul. 2012.
- [77] E. Koutroulis and K. Kalaitzakis, "Design of a maximum power tracking system for wind-energy-conversion applications," *Industrial Electronics, IEEE*, vol. 53, no. 2, pp. 486–494, 2006.
- [78] M. E. Haque, M. Negnevitsky, and K. M. Muttaqi, "A Novel Control Strategy for a Variable Speed Wind Turbine with a Permanent Magnet Synchronous Generator," *IEEE Industry Applications Society Annual Meeting*, pp. 1–8, Oct. 2008.
- [79] D. Qiu-ling, L. I. U. Gou-rong, and X. Feng, "Control of Variable-speed Permanent Magnet Synchronous Generators Wind Generation System," in *International Conference on Electrical Machines and Systems*, pp. 2454–2458, 2008
- [80] C. Busca, A.-I. Stan, T. Stanciu, and D. I. Stroe, "Control of Permanent Magnet Synchronous Generator for large wind turbines," *IEEE International Symposium on Industrial Electronics*, pp. 3871–3876, 2010.
- [81] T. Murata, J. Tamura, and T. Tsuchiya, "Modeling and simulation of wind turbine -fed Interior Permanent Magnet Synchronous Generator," *18th International Conference on Electrical Machines*, no. 4, pp. 1–6, Sep. 2008.
- [82] M. Yin, G. Li, M. Zhou, and C. Zhao, "Modeling of the wind turbine with a permanent magnet synchronous generator for integration," *Power Engineering Society*, pp. 1–6, 2007.

- [83] M. Molina, "Dynamic modeling of wind farms with variable-speed direct-driven PMSG wind turbines," *and Exposition: Latin*, pp. 816–823, 2010.
- [84] I. Margaritis and N. Hatziaargyriou, "Direct drive synchronous generator wind turbine models for power system studies," no. November, pp. 1–7, 2010.
- [85] L. Yang, Z. Chen, P. Yuan, and Z. Chang, "A novel fuzzy logic and anti-windup PI controller for a rectifier with direct driven permanent magnet synchronous generator," *2nd International Conference on Power Electronics and Intelligent Transportation System (PEITS)*, pp. 422–426, Dec. 2009.
- [86] F. Deng and Z. Chen, "Low-voltage ride-through of variable speed wind turbines with permanent magnet synchronous generator," *35th Annual Conference of IEEE Industrial Electronics*, no. 2, pp. 621–626, Nov. 2009.
- [87] R. Mittal, K. S. Sandhu, and D. K. Jain, "Fault ride-through capability of grid connected variable speed permanent magnet synchronous generator for wind energy conversion system," *IEEE Electrical Power & Energy Conference (EPEC)*, pp. 1–6, Oct. 2009.
- [88] M. G. Molina and P. E. Mercado, *Wind Power in Power Systems*. Chichester, UK: John Wiley & Sons, 2005.
- [89] L. Holdsworth, X. Wu, J. Ekanayake, and N. Jenkins, "Comparison of fixed speed and doubly-fed induction wind turbines during power system disturbances," *IEE Proceedings-Generation*, pp. 343–352, 2003.
- [90] a. H. M. a. Rahim and I. O. Habiballah, "DFIG rotor voltage control for system dynamic performance enhancement," *Electric Power Systems Research*, vol. 81, no. 2, pp. 503–509, Feb. 2011.
- [91] X. Yao, C. Guo, and Z. Xing, "Pitch regulated LQG controller design for variable speed wind turbine," *International Conference on Mechatronics and Automation*, pp. 845–849, Aug. 2009.
- [92] W. Li and G. Joós, "Comparison of energy storage system technologies and configurations in a wind farm," *Specialists Conference, PESC IEEE*, pp. 1280–1285, 2007
- [93] A. Mohd and E. Ortjohann, "Challenges in integrating distributed energy storage systems into future smart grid," *ISIE*, pp. 1627–1632, 2008.
- [94] L. Xu and Y. Wang, "Dynamic modeling and control of DFIG-based wind turbines under unbalanced network conditions," *Power Systems, IEEE Transactions on*, vol. 22, no. 1, pp. 314–323, 2007.

- [95] A. Garcia, D. Holmes, and T. Lipo, "Reduction of bearing currents in doubly fed induction generators," *Conference, 2006. 41st IAS*, vol. 00, no. c, pp. 84–89
- [96] D. Vilathgamuwa, "Space vector modulated cascade multi-level inverter for PMSG wind generation systems," , *IECON'09*. pp. 4600–4605, 2009.
- [97] L. M. Gong and Z. Q. Zhu, "A Novel Method for Compensating Inverter Nonlinearity Effects in Carrier Signal Injection-Based Sensorless Control From Positive-Sequence Carrier Current Distortion," *IEEE Transactions on Industry Applications*, vol. 47, no. 3, pp. 1283–1292, May 2011.

Vitae

- Atta Ur Rahman.
- Born in April 12, 1985 in PAKISTAN.
- Received Bachelor of Science (B.S) degree in Telecom Engineering from National University of Computer and Emerging Sciences (NUCES) Islamabad, PAKISTAN in June 2010.
- Joined the Department of Electrical Engineering at King Fahd University of Petroleum and Minerals (KFUPM), Dhahran, Saudi Arabia as Full Time Student in January 2012.
- Received Master of Science (M.S) degree in Electrical Engineering from KFUPM, Saudi Arabia in July 2014.